

Republic of Iraq  
Ministry of Higher Education and  
Scientific Research  
University of Misan /College of  
Engineering  
Department of Civil Engineering



# **BEHAVIOR OF LIGHTWEIGHT REINFORCED CONCRETE SLAB EXPOSED TO FIRE**

By

Noor kadm Hmod

B.Sc. civil engineering, 2009

A THESIS

Submitted in Partial Fulfillment of the

Requirements for the Degree of

Master of Science/Master of Structural Engineering

(in Civil Engineering)

Thesis Supervisor: Prof. Dr. Samir Mohammed Chassib

April 2026

بِسْمِ اللَّهِ الرَّحْمَنِ الرَّحِيمِ

الحمد لله رب العالمين ۞ الرحمن الرحيم ۞ مالك يوم الدين

۞ اياك نعبد و اياك نستعين ۞ اهدنا الصراط المستقيم ۞ صراط

الذين انعمت عليهم غير المغضوب عليهم ولا الضالين ۞

صدق الله العظيم

سورة الفاتحة

## EXAMINING COMMITTEE'S REPORT

We certify that we, the examining committee, have read the thesis titled (**Behavior of Light Weight Reinforced Concrete Slab Exposed to Fire**) Which is being submitted by (**Noor kadm Hmod**), and examined the student in its content and in what is concerned with it, and that in our opinion, it meets the standard of a thesis for the degree of Master of Science in Civil Engineering (Structures).

Signature:

Name: **Prof. Dr. Samir M. Chassib**

(Supervisor)

Date: / /2026

Signature:

Name: **Prof. Dr. Rafid Saeed Atea**

(Member)

Date: / /2026

Signature:

Name: **Assist Prof. Dr. Murtada Abass Abd Ali**

(Member)

Date: / /2026

Signature:

Name: **Prof. Dr. Abbas Oda Dawood**

(Chairman)

Date: / /2026

Approval of the College of Engineering:

Signature:

Name: **Prof. Dr. Abbas Oda Dawood**

Dean, College of Engineering

Date: / /2026

## **SUPERVISOR CERTIFICATION**

I certify that the preparation of this thesis entitled "**Behavior of Light Weight Reinforced Concrete Slab Exposed to Fire**" was presented by "**Noor Kadm Hmod**", and prepared under my supervision at The University of Misan, Department of Civil Engineering, College of Engineering, as a partial fulfillment of the requirements for the degree of Master of Science in Civil Engineering (Structural Engineering).

Signature:

**Prof. Dr. Samir Mohammed Chassib**

Date: \ \2026

In view of the available recommendations, I forward this thesis for discussion by the examining committee.

Signature:

Name: **Assist Prof. Dr. Murtada Abass Abd Ali**

Head of Civil Eng. Department

Date:

## ACKNOWLEDGMENTS

First and Foremost, We Offer Our Thanks and Praise to God for His Abundant Blessings.

I Extend My Deepest Gratitude and Appreciation to My Revered Imam, the Awaited Mahdi (May God Hasten His Reappearance).

I Also Express My Sincere Thanks and Gratitude to My Supervisor, **Prof. Dr. Samer Mohammed Jassim**. I Further Thank **Prof. Dr. Abbas Awda Dawood**, Dean of the College of Engineering, **Assist. Dr. Murtadha Abbas**, Head of The Department of Civil Engineering, and **Prof. Dr. Abdulkhaliq A. Jaafer** for Their Guidance, Assistance, and Support in Completing the Research Requirements.

Finally, I Would Like to Express My Profound Gratitude and Appreciation to My Parents, My Husband, My Children, and All My Family Members for Their Immense Love and Support; They Have Been a Source of Strength and Motivation for Me.

# TABLE OF CONTENTS

<b>Abstract.....</b>	<b>I</b>
<b>Supervisor Certification.....</b>	<b>III</b>
<b>EXAMINING COMMITTEE’S REPORT .....</b>	<b>IV</b>
<b>ACKNOWLEDGEMENTS .....</b>	<b>VI</b>
<b>TABLE OF CONTENTS .....</b>	<b>VII</b>
<b>LIST OF TABLES .....</b>	<b>XI</b>
<b>LIST OF FIGURES .....</b>	<b>XIII</b>
<b>CHAPTER One:Introudction .....</b>	<b>1</b>
1.1 General.....	1
1.2 Lightweight Concrete.....	2
1.3 General Applications of Lightweight Concrete in Structural Systems.....	3
1.4 Advantages and Disadvantages of Lightweight Concrete.....	3
1.5 Slab Definition.....	4
1.5.1 Solid Slab Types.....	5
1.2.1.1 Slab in One Way.....	5
1.6 The Properties of Normal Concrete are Affected by Fire.. ....	6
1.7 The Properties of Lightweight Concrete Under Fire are Affected.....	6
1.8 Factors Influencing the Fire Resistance of Concrete.....	7

1.9	LECA Concrete (Lightweight Concrete).	9
1.10	Problem Statement	11
1.11	Study Objective	12
1.12	Aim of Study	12
1.13	Thesis Layout.	13
<b>CHAPTER Two: LITERATUREREVIEW</b>		<b>14</b>
2.1	Introduction	14
2.2	Role in a Fire Condition	14
2.3	Fire scenario used in concrete studies.	15
2.3.1	ISO834	18
2.3.2	The United States' ASTM E119	18
2.3.4	Flame Fire.	19
2.4	Effect of Fire on Normal Reinforced Concrete Slab.	20
2.5	Effect of Fire on A light- weight Reinforced Concrete Slab.	28
2.6	Concluding Remarks	35
<b>Chapter Three: Experimantal Program</b>		<b>36</b>
3.1	Introduction	36
3.1	Specimens Symbol	38
3.3	Test Program	38
3.4	Materials	39
3.4.1	Cement	41

3.4.2	Fine aggregate (Sand)	43
3.4.3	Coarse aggregate (Gravel)	44
3.4.4	Coarse aggregate(LECA)	46
3.4.5	Water	43
3.4.6	Superplasticizer	43
3.4.7	Steel Reinforcement	45
3.8	Mix Concrete Mix Design and Mixing Procedures	46
3.9	Fresh Concrete Tests	47
3.9.1	Slump Flow Test	48
3.10	Hardening Test	49
3.10.1	Tests for Concrete Properties	49
3.10.1	Compressive Strength Test	50
3.10.2	Splitting Tensile Strength Test	52
3.10.3	Flexural Strength Test	54
3.10.4	Slab Details	55
3.11	Prosses	63
3.13	Burning Methods and Fire Exposure	67
3.13.A	Thermal and Loading Test of Specimens	67
3.13. B	Direct Flame Exposure Method	73
<b>Chapter Four:Result and Discussion</b>		<b>78</b>
4.1	General	78

4.2 Study of the Properties of Concrete .....	78
4.2.1 Changes in Temperature During the Burning Stage.....	78
4.2.2 Fire Load Test Results .....	84
4.2.2.1 Load Capacity and Failure Mode .....	85
4.2.2.2 Load and Deflection Behavior .....	88
4.2.2.3 Load Versus Steel Ratio .....	93
4.2.2.4 Ductility Factor .....	95
4.2.2.5 Stiffness .....	96
4.2.2.6 Absorption Energy.....	97
4.3 Study of the Properties of Concrete .....	98
4.3.1 Changes in Temperature During the Burning Stage .....	98
4.3.2 Fire Load Test Results .....	103
4.3.2.1 Load Capacity and Failure Mode. ....	108
4.3.2.2 Load and Deflection Behavior.....	99
4.3.3.3 Load and Deflection Behavior.....	99
4.3.3.4 varying Reinforcement Ratios and Loading Conditions.	113
4.3.3.5 Ductility.....	112
4.3.3.6 Stiffness .....	115
4.3.3.7 Energy Absorption.....	117
<b>Chapter Five:Conclusions and Recommendations .....</b>	<b>120</b>
5.1 Introduction.....	120
5.2 Conclusions.....	120
5.3 Flexural Behavior of Concrete Slabs at Exposed Fire.....	122

5.4 Recommendations..... 123  
References ..... 125

## LIST OF FIGURES

Figure 1.1 Examples of structures subject to fire..	9
Figure 1.2 Shape the LECA Aggregate.....	11
Figure 2.1 Fire Tetrahedron [7]..	13
Figure 2.2 ISO 834 and ASTM E119 Time-Temperature Curves.....	15
Figure 2.3 Fire Development Curve [11].	17
Figure 2.4 Shows the Comparative for to Temperature and Strength [12] .....	19
Figure 2.5 Shows The Comparative for to Temperature and Time [13].	20
Fi Figure 2.6 Show the relationship between emotion and stress according to the source [14].....	21
Figure 2.7 Show The Curve Between Temperature and Time [15 ] .	22
Figure 2.8 Show the Curve Between load and deflection [16].....	23
Figure 2.9 Show the Curve Between load and deflection [18 ].....	24
Figure 2.10 show the relationship between the temperature and stress according to ACI and EURP [21].....	27
Figure 2.11 Image containing details of the search form[25].	29
F Figure 2.12 Relation Between Time and Deflection [28].	32
Figure 3.1 Flow chart of experimental work	37
Figure 3.2 Grading graph of fine Aggregate. ....	42
Figure 3.3 Grading graph of coarse Aggregate. ....	43
Figure 3.4 Lightweight aggregate (LECA).....	45
Figure 3.5 Shows the Details and Properties of Admixture. ....	47

Figure 3.6 Showing the Testing Device. ....	48
Figure 3.7 Slump test of fresh concrete. ....	52
Figure 3.8 compressive test of concrete. ....	54
Figure 3.9: Splitting Tensile Test. ....	56
Figure 3.10 :Flexural strength test prism test Sof LWC, (b) prism test of NRC .....	58
Figure 3.11: Slab Details. ....	60
Figure 3.12: Datils of slab.....	59
Figure 3.13: fabrication, moulds, and casting of the specimens for group 1. ....	65
Figure 3.14 : fabrication, moulds, and casting of the specimens for group 2.....	66
Figure 3.15: Curve of ISO-834.....	67
Figure 3.15: Firebricks for the oven, laser thermometer, and gas supply for the burners inside the oven. ....	68
Figure 3.16: The outer iron structure of the furnace.....	65
Figure 3.17: Thermocouples and the device LVDT .....	70
Figure 3.18: Input device for connecting thermocouples .....	71
Figure 3.19: Testing and burning process. [ 50 ].....	72
Figure 3.20 : Testing Process.....	73
Figure 3.21 a-Gaseous heat source b-laser thermometer.....	74
Figure 3.22 : Second series tesing at university of Misan.....	75
Figure 3.23: A clip illustrating the loading and mechanical LVDT device. ....	76
Figure 3.24 : Sample inspection device with cross-sectional diagram...	77

Figure 4.1 The Temperature Distribution on a Sample .....	79
Figure 4.1 The Temperature Distribution on a Sample Slab of normal Reinforced Concrete .....	75
Figure 4.2 The Temperature Distribution on a Sample Slab of normal Reinforced Concrete .....	80
Figure 4.3 The Temperature Distribution on a Sample Slab (SNA $\rho$ -800) of normal Reinforced Concrete.....	80
Figure 4.4 The Temperature Distribution on a Sample Slab (SNA $\rho^{\wedge}$ -800) of normal Reinforced Concrete .....	81
Figure 4.5 The Temperature Distribution on a Sample Slab (SLA $\rho$ -400) of lightweight Reinforced Concrete .....	82
Figure 4.6 The Temperature Distribution on a Sample Slab (SLA $\rho^{\wedge}$ -400). .....	82
Figure 4.7 The Temperature Distribution on a Sample Slab (SLA $\rho$ -800). .....	79
Figure 4.8 The Temperature Distribution on a Sample Slab (SLA $\rho^{\wedge}$ -800) .....	84
Figure 4.9 Models After Burning, Loading, and Failure Status.....	84
Figure 4.10 Load Deflection Curve for Lightweight Specimens. ....	89
Figure 4.11 Load Deflection Curve for Normal Concrete Specimens. ...	89
Figure 4.12 Different patterns and load conditions resulting from heat.	92
Figure 4.13 The Different Models and Load.....	94
Figure 4.14 The Resulting Patterns and Ductility. ....	95
Figure 4.15 Specimen and Stiffness Resulting from Thermal Effect.....	97
Figure 4.16 The Energy Absorption. ....	98
Figure 4.17 show the temperature distribution at SN4D $\rho$ - 300C° .....	100

Figure 4.18 show the temperature distribution at SN3D $\rho^{\wedge}$ -300C° .....	101
Figure 4.19 show the temperature distribution at SN5D $\rho^{\wedge}$ -400C° .....	100
Figure 4.20 Show the Temperature Distribution at 400C° .....	102
Figure 4.21 Show the Temperature Distribution at SL3D $\rho^{\wedge}$ -300C° .....	102
Figure 4.22 show the temperature distribution at SL4D $\rho^{\wedge}$ -300C° .....	103
Figure 4.23 show the temperature distribution at SL1D $\rho^{\wedge}$ -400C° .....	103
Figure 2.24 The Failure Pattern in Normal and Lightweight Concrete.	108
Figure 4.25 Load And Deflection Curve for normal .....	110
Figure 2.26 Load and deflection curve .....	111
Figure 4.27 The effect of temperature on load. ....	112
Figure 4.28 The effect of temperature .....	114
Figure 4.29 Pregnancy Projection Chart for Calculating the Ductility.	116
Figure 4.30 Ductility for Specimen. ....	117
Figure 4.31 The Stiffness of the Working Models .....	119

## LIST OF SYMBOLES AND ABRVATION

$f'_c$	Cylinder concrete compressive strength in MPa
$f_{cu}$	Cube Compressive Strength in MPa
$\emptyset$	Diameter of Reinforcement mm
$DI$	Ductility Index
$f_r$	Modulus of Rupture in MPa
$f_t$	Tensile Strength in MPa
$f_y$	Yield Strength in MPa
$\Delta_y$	Yield Deflection in mm
$\Delta_u$	Ultimate Deflection in mm
LWC	Lightweight Concrete
NWC	Normal Aggregate Concrete
LECA	Lightweight Expanded Aggregate Concrete
ASTM	American Society of Testing Materials
RC	Reinforced Concrete
ACI	American Concrete Institute
K	Stiffness kN/mm

## LIST OF TABLES

Table 2-1 ISO834 and ASTM-E119 Time curves at various poin.....	19
Table 3-1: Parameters of the study. ....	36
Table 3-2: Physicals properties of ordinary Portland cement [33].....	40
Table 3-3 : Chemical composition of cement [34]. ....	41
Table 3-4: Grading of the fine aggregate.....	42
Table 3-5: Physical properties of the fine aggregate. ....	42
Table 3-6 Grading of the coarse Aggregate. ....	43
Table 3-7 Typical properties for LECA [3].....	45
Table 3-8 Grading of Coarse Aggregate for LECA.....	45
Table 3-9 Types, Appearances and Relative Density of Superplasticizers.. .....	47
Table 3-10 Steel Rebars Properties. ....	48
Table 3-11 Proportions of constituent materials mixes.....	50
Table 3-12 Slump Test Results.....	51
Table 3-13 Compressive strength test .....	54
Table 3-14 Results of splitting tensile strength .....	56
Table 3-15 Flexural strength result.....	57

Table 3-16 First Series Models.....	59
Table 3-17 Second Series Models.....	61
Table 4-1 Deflections of Specimens.....	90
Table 4-2 Percentage Decreasing in Ultimate Load. .....	92
Table 4-3 Ductility Index for Specimens under load.....	95
Table 4-4 Stiffness of the Specimens .....	97
Table 4-5 Table Represent the Absorption Energy.....	98
Table 4-6 Ultimate load and service load.....	105
Table 4-8 Shows the service and Ultimate Load Results.....	110
Table 4-9 Service Load And Ultimate Deflection.....	111
Table 4-10 The Effect of Temperature on Load.....	113
Table 4-11 Steel Reinforcement Ratio and Ultimate Load .....	114
Table 4-12 Ductility Index. ....	115
Table 4.13 The Stiffness Values.....	117
Table 4.14 Energy Absorption Data .....	118

## LIST OF EQUATION

(2.1) Temperature-Time ISO-834.....	14
(1.2) Temperature-Time ASTM-E119.....	15
(3.1) Splitting Tensile Strength.....	47
(3.2) The modulus of rupture .....	54

## CHAPTER ONE: INTRODUCTION

### 1.1 General

Concrete is regarded as the most widely utilized construction material globally, owing to its cost-effectiveness and ease of application, which have contributed to its widespread use in the construction sector. One of the most important factors in favoring this material is its compressive strength. Because heavy structures and conventional materials have numerous negative effects on the structure, lightweight concrete (LWC) has become more popular in recent years. This is the type of concrete employed in this study [1]. In the field of civil engineering, concrete that is lightweight is crucial. It is utilized in structural components like beams, slabs, and walls. In addition, it is utilized to create lightweight building blocks that serve as thermal insulation in contrast to conventional building blocks. Because concrete is lightweight and can be used effectively in structural components like walls, slabs, and beams, it lowers loads in contrast to conventional building blocks, it also creates lightweight blocks that serve as thermal insulation. In addition, insulation and low weight lower heating and cooling energy consumption. Additionally, because of their lightweight, structural parts may be made smaller, which lowers installation costs. The slabs are thought of as one of the structural components that use lightweight concrete slabs, which greatly reduces the structure's overall weight. When compared to wood and iron, typical concrete's primary drawback as a building material is its relative weight (2200 to 2500 kg/m<sup>3</sup>) [2]. In all circumstances, the building components weigh a lot in relation to the

loads. Since light concrete weighs less than 2000 kg/m<sup>3</sup>, it should be the preferred option. Additionally, structural concrete weighing 1400 to 1900 kg/m<sup>3</sup> can be produced at a slightly higher cost, and semi-structural concrete for internal blocks weighing 900 kg/m<sup>3</sup> can be produced and effectively utilized as interior walls. In general, light concrete weighs less than 2,000 kilograms per cubic meter. Their use is intended to lessen the foundations by lowering the self-weight. Much focus has been paid to the necessity of creating cost-effective and efficient ways to strengthen, repair, or improve existing structures. Wang (2007) [3], design modifications, increased loads, and the desire to fix deterioration brought on by years of usage are usually the driving forces behind strengthening an existing building. Concrete can be significantly affected by fire exposure, which can compromise the structural integrity and safety of buildings. Exposed concrete can be severely damaged by fire, endangering a building's safety and structural soundness. Several variables, including the type of concrete used, the presence of reinforcing materials, and the fire's strength and duration, affect how a fire affects concrete [4].

## 1.2 Lightweight Concrete.

Lightweight concrete is considered one of the modern construction materials that has received considerable attention in civil engineering due to its reduced density compared to normal-weight concrete. This type of concrete is produced by using lightweight aggregates or by introducing air voids into the concrete mix, resulting in a lower overall structural weight. Lightweight concrete helps reduce the dead load on structures, which improves structural efficiency and can lead to more

economical foundation designs. It also offers better thermal and sound insulation properties compared to conventional concrete. However, its mechanical strength is generally lower than that of normal-weight concrete, which requires careful consideration in structural applications and design [5].

### **1.3 General Applications of Lightweight Concrete in Structural Systems.**

The general applications of lightweight concrete in structural systems are mainly based on its primary advantage, which is reducing self-weight while maintaining an acceptable level of strength. Therefore, it is used in the following cases:

a-Structural slabs :It is used in floor and roof slabs to reduce dead loads on beams, columns, and foundations, especially in multi-storey buildings.

b- Bridges: It is applied in bridge decks and pavement components to reduce the load on supporting elements and improve structural efficiency.

Precast elements: This includes precast walls, façade panels, and concrete units, where the reduced weight facilitates transportation and installation.

c-High-rise buildings: It helps reduce the overall load on columns and foundations, leading to smaller structural member sizes and lower construction costs.

## 1.4 Advantages and Disadvantages of Lightweight Concrete.

### Advantages:

1. **Reduced self-weight:** Low density decreases dead loads on structural members, leading to smaller sections for beams, columns, and foundations.
2. **Improved structural efficiency:** Reduces overall load demand, which is especially beneficial in high-rise buildings and long-span structures.
3. **Thermal insulation:** Provides better heat resistance compared to normal-weight concrete, improving energy efficiency in buildings.
4. **Sound insulation:** Offers improved acoustic performance, making it suitable for residential and commercial buildings.
5. **Ease of handling and construction:** Lighter elements are easier to transport, lift, and install, especially in precast systems.

### Disadvantages :

1. **Lower compressive strength:** Generally weaker than normal-weight concrete, limiting its use in heavily loaded structural elements.
2. **Higher material cost:** Production materials and lightweight aggregates can be pricier.
3. **Higher creep and shrinkage:** May experience greater long-term deformations compared to normal concrete.
4. **Durability concerns:** In some cases, it may be more sensitive to environmental effects if not properly designed or cured, leading to potential issues such as reduced lifespan or increased maintenance needs over time.

5. **Workability issues:** Some mixes may require special handling and mix design control to achieve desired performance, particularly in terms of consistency and ease of placement, which can affect the overall quality of the concrete structure.

### **1.5 Slab Definition.**

A roof slab is a horizontal structural element, usually made of reinforced concrete, placed at the top of a building as part of its load-bearing system. It supports vertical loads such as the roof's own weight, equipment, and thermal effects, transferring these loads to supporting structural members such as beams, columns, or load-bearing walls [6].

Roof slabs play a crucial role in the structural integrity of buildings by evenly distributing both dead loads (self-weight and permanent fixtures) and live loads (maintenance workers, occasional usage) to the structural supports [7]. They can function as either flexible or rigid diaphragms, influencing how lateral loads from wind or seismic forces are distributed, in addition to slabs supported on beams ,the common types include:

- Flat Slab / Flat Plate: Supported directly on columns or walls, often used in commercial and residential buildings.
- Waffle Slab: Contains a ribbed grid structure to reduce weight and increase load capacity, suitable for large-span areas.

Roof slabs also offer added benefits such as fire resistance, acoustic insulation, and flexibility in installing services and insulation systems Kreo.net [8].

## **1.5.1 Solid Slab Types**

### **1.5.1.1 Slab in One Way**

The slab can only be supported on opposing sides, loads are carried perpendicular to the supporting beams, resulting in a mostly unidirectional structural action of the slab. However, as Fig.1-1 illustrates, the introduction of intermediate beams may result in a one-way slab. Perpendicular to the support beam, this form of slab only sustains loads in one direction [9] .

## **1.6 Properties of Normal Concrete Under Fire Conditions.**

When ordinary concrete is exposed to high temperatures, its main components cement, water, and aggregates undergo significant physical and chemical changes that impact its structural performance. Once the temperature exceeds about 100 °C, the bound water within the cement paste begins to evaporate, weakening the bond that holds the aggregates together and reducing mechanical strength. As the temperature continues to rise, structural degradation accelerates, further diminishing the concrete's load-bearing capacity and overall integrity Cavill (2004) [10].

## **1.7 Properties of Lightweight Concrete Under Fire Conditions.**

The growing demand for lightweight structural concrete is due to its numerous benefits, making it an important material in construction. Lightweight concrete LWC is commonly used in various types of structures, especially tall buildings, where it is crucial to reduce the overall mass. LWC can improve the structural response and meet design specifications. A notable example of the advantages of LWC is

the Southwestern Bell building in Kansas City. The building's designers opted for lightweight expanded shale concrete instead of traditional sand and gravel concrete. This change allowed them to safely add 14 levels, effectively doubling the building's height to 28 stories. During the construction of the Southwestern Bell building, ready-mix concrete factories were not widely available, so concrete was mixed on-site. This presented technical challenges in creating a consistent and workable mix and in setting the concrete in column and beam forms, especially with the limited mixing equipment available. However, these challenges were overcome by utilizing technical expertise developed at the University of Kansas. In addition to its use in tall buildings, LWC was also applied to construct garden walls, windows, and stairs. LWC is particularly suitable for small homes with load-bearing walls and roof and panel construction due to its lower strength. It is also used in the production of prestressed and precast structural components, where panels serve as internal thermal insulators [11].

### **1.8 Factors Influencing the Fire Resistance of Concrete**

Fire resistance is a critical property in the structural design of buildings, particularly those exposed to high thermal or environmental hazards. Several interrelated factors affect the fire performance of concrete, each contributing to the material's ability to maintain structural integrity under fire conditions. The main influencing factors can be outlined as follows:

#### **A- Concrete Mix Design**

The composition of the concrete mix plays a vital role in determining its fire resistance. Concrete with higher density and a lower water-to-

cement ratio generally exhibits better performance under fire exposure. Such mixes are less prone to spalling a phenomenon where surface layers of concrete break off due to internal pressure caused by heat and moisture. The quality of materials and the homogeneity of the mix are also essential for enhancing thermal resistance.

#### B-Type of Aggregate Used

The type of aggregate incorporated into the mix significantly influences concrete's behavior under elevated temperatures. Natural aggregates, such as sand and gravel, tend to offer better fire resistance compared to lightweight aggregates, which may be more susceptible to degradation when exposed to intense heat [12].

#### C-Steel Reinforcement

The presence of steel reinforcement within concrete has a notable impact on its performance during a fire. As temperatures rise, steel begins to lose its mechanical properties, reducing the load-bearing capacity of the structure. This can lead to partial or total failure of structural elements if not properly addressed in the design phase. In this context, the current study examines the behavior of a reinforced concrete slab exposed to uniform fire exposure. Figure 1.2 shows the effect of fire on the building and the resulting damage to the concrete [13].

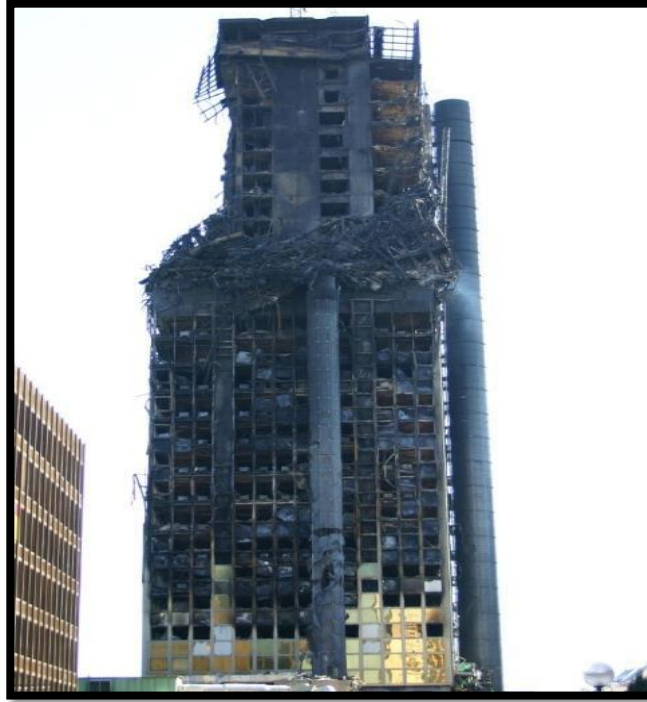


Figure 1.1 Examples of Structures Subject to Fire.

### **1.9 LECA Concrete (Lightweight Concrete).**

Lightweight Expanded Clay Aggregate (LECA) is produced by firing natural clay in a rotary kiln at temperatures between 1100 °C and 1200 °C, resulting in lightweight, porous, ceramic pellets with a hard outer shell and honeycombed interior structure [14]. When used as a substitute for conventional coarse aggregates in concrete, LECA significantly alters the concrete density, thermal performance, and handling characteristics. One of the most notable properties of LECA is its low bulk density, typically in the range of 300–800 kg/m<sup>3</sup>, which is substantially lower than crushed stone or gravel. This reduced density directly translates into lighter structural elements and can lower the overall dead load of buildings by up to 40%, which is particularly beneficial in high-rise and seismically active regions. Despite its

lightweight nature, LECA demonstrates sufficient mechanical stability; structural lightweight concretes containing LECA commonly achieve 28-day compressive strengths between 20–32 MPa, in compliance with ASTM C330 specifications. The aggregate's porous internal structure offers excellent thermal insulation (thermal conductivity as low as 0.097 W/m·k) and acoustic dampening capabilities. This property makes LECA-based concrete an attractive choice for energy-efficient construction, as it can reduce HVAC energy demands by approximately 15%. Additionally, LECA is chemically inert, highly durable in aggressive environments, and resistant to freeze–thaw cycles and chloride penetration, making it suitable for marine and chemically exposed structures [15]. Furthermore, LECA's rounded particle shape improves the workability of fresh concrete, facilitating easier placement and compaction. Its ceramic composition renders it non-combustible, maintaining structural integrity even under prolonged high-temperature exposure. From a sustainability perspective, LECA is produced from abundant natural raw materials, is recyclable, and contributes to green building certification credits due to its role in reducing energy consumption and structural material usage. These combined properties make LECA-based concrete highly versatile, suitable for structural and non-structural applications such as precast panels, lightweight slabs, bridge decks, wall elements, and insulating screeds, shows Fig. 1.3.



Figure 1.2: Shape the LECA Aggregate.

### 1.10 Problem Statement

When concrete slabs are exposed to fire while under structural load, their resistance gradually decreases, potentially leading to loss of stability and collapse. Hence, it is important to study the behavior of slabs during fire to understand their performance and ensure the structural safety of buildings. This study focuses on comparing the mechanical and thermal properties of both ordinary concrete and lightweight concrete when exposed to high temperatures. This includes evaluating residual mechanical strength and flexural strength, as well as studying thermal behavior and its impact on structural performance.

The objective is to investigate whether lightweight concrete, which uses lightweight aggregates made from LECA as an alternative to coarse aggregate, exhibits better or different performance compared to conventional concrete when exposed to fire.

### **1.11 Study Objective**

This study aimed to investigate what happens to lightweight concrete when heated. This was done by testing its mechanical properties and flexural strength using LECA lightweight aggregate. It is known that the presence of steel reinforcement significantly affects the flexural resistance of a component to fire. Therefore, the effects were studied by controlling the proportion of steel reinforcement to increase its resistance.

### **1.12 Aim of Study**

1- Study the flexural behavior of concrete slabs prepared from conventional concrete and lightweight concrete, and conduct a comparative study to demonstrate the effect of high temperatures on the flexural performance of concrete slabs.

2- Conduct an experimental study on the effect of temperature variations on the structural performance of conventional and lightweight reinforced concrete slabs, using two stages: direct exposure to an uncontrolled flame, followed by exposure to a controlled fire, according to the standard temperature-time curve (ASTM-E119, 2020) under 50% of the maximum load.

### 1.13 Thesis Layout.

The current thesis is structured as follows:

**Chapter 1:** provides a general overview of concrete slabs, including their classification and the behavior of lightweight concrete slabs under fire conditions.

**Chapter 2:** This section provides a comprehensive review of previous studies related to concrete slabs, encompassing their classification and the behavior of lightweight concrete slabs under fire exposure, along with a comparative analysis between earlier findings and the results of the current research.

**Chapter 3:** This chapter presents the experimental program adopted in this study, including the materials used, specimen preparation, and testing procedures. It also describes the methodology employed to investigate the behavior of lightweight concrete slabs under fire conditions, along with the parameters considered in the experimental work.

**Chapter 4:** This chapter presents the results obtained from the experimental program and provides a detailed discussion of the observed behavior of lightweight concrete slabs under fire conditions. The results are analyzed in terms of the selected parameters, and compared with relevant previous studies to highlight similarities and differences in behavior.

**Chapter 5:** This chapter presents the main conclusions drawn from the experimental program and the results analysis of lightweight concrete slabs under fire conditions.

## **CHAPTER TWO: LITERATURE REVIEW**

### **2.1 Introduction**

The impact of fire on concrete structures and the creation of a trustworthy algorithm to forecast the true thermal and structural reaction of any structural element have been the subjects of countless studies throughout the evolution of fire safety engineering. The main goal of this chapter is to provide an overview of the state of the science and literature on reinforced concrete slabs made of regular concrete and lightweight reinforced concrete and the impact of fire and temperature on the structural behavior of reinforced concrete slabs, this review focuses on a comprehensive assessment of concrete behaviour under fire exposure, with particular emphasis on reinforced concrete slabs' thermal and structural responses. The main topics addressed are as follows:

- 1-Role of Fire Condition on Concrete.
- 2-Fire Loading Scenarios and Heating Regimes in Concrete Research
- 3-Structural and Material Response of Normal-Weight Reinforced Concrete Slabs under Elevated Temperatures
- 4-Thermo-Mechanical Performance of Lightweight Reinforced Concrete Slabs under Fire Conditions

### **2.2 Role of Fire Condition on Concrete.**

Despite significant progress in fire research, there is still no widely agreed-upon definition of fire since the definitions of the primary international standards currently in use are ambiguous. Heat, oxidizer (oxygen), and fuel were the three fundamental elements of the Fire

Triangle hypothesis, which was first proposed Seito et al. (2008) [16], According to this theory, removing any one of these elements from the triangle will directly put out the fire. But the notion was reworked after the halon extinguishing agent, now called the Fire Tetrahedron Fig. 2-1 was discovered. The Fire Tetrahedron, on the other hand, is composed of heat, oxidizer, fuel, and chain reaction. Heat is the element that ignites, maintains, and facilitates the propagation of a fire. The oxygen in the air, also known as an oxidizer, is essential for burning. Fuel is what spreads fire and can be solid, liquid, or gaseous. The chain reaction allows the burning process to continue on its own. The flames radiate heat which is transferred to the fuel. By breaking it up into smaller pieces, it produces a continuous (self-sustaining) cycle in which the particles burn and combine with oxygen to radiate heat back into the fuel, as shows in Fig. 2-1.

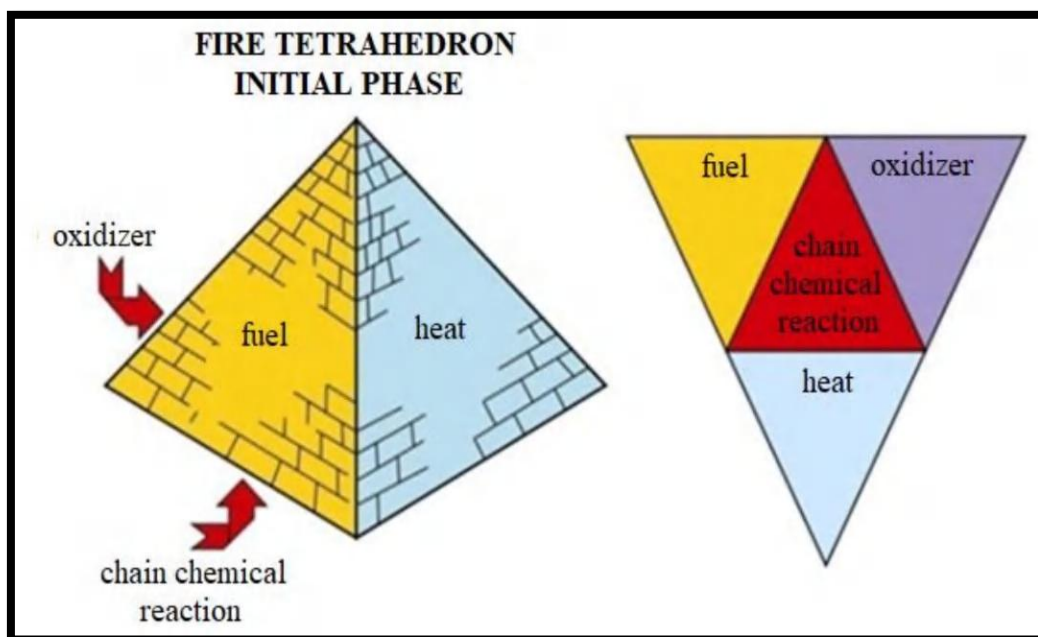


Figure 2-1 Fire Tetrahedron [16].

Concrete is well-known for its good performance at high temperatures because it has thermal properties that make it low in thermal conductivity and not flammable. Concrete's parts are denser and bigger than those of other materials, such as metal and wood, which means they may survive longer. Also, concrete doesn't let out any harmful fumes when it gets hot. So, some people would say that concrete is not a basic part of the fire tetrahedron because it is not a solid fuel. Flammable materials that are solid, liquid, or gas and burn in a fire affect concrete.

This flammable charge usually originates from solid cellulose-based materials including doors, furniture, office supplies, carpeting, draperies, etc. in both residential and commercial structures. According to multiple studies, a more exposed portion of concrete typically loses around 25% of its initial compressive strength when heated to temperatures around 300°C and roughly 75% when heated to 600°C. Fire-exposed concrete undergoes significant temperature changes.

A more exposed section of the concrete loses its initial compressive strength, since hot surface layers have a significant tendency to separate from the cooler layers within the element, according to multiple studies. Across the globe, this kind of detachment is known as spalling. The first object to catch fire, the fire performance characteristics of objects nearby, and the item's distribution across the environment all influence the spread of small amounts of fire Neville, (1981) [17].

### 2.3 Fire Loading Scenarios and Heating Regimes in Concrete Research.

To investigate the effects of heat exposure and confirm the structure's resistance, the simulation of the real fire action needs to be schematically depicted. As a result, a simulation of the temperature-time connection is used. All of the adopted fire curves are expressed using the temperature-time(T-t) link. Time-temperature curves, which are idealized models of "standard fires," or flames in rooms, are the foundation of most fire resistance tests. Because the tests follow pre-established time-temperature curves, it is easy to calculate the heat load imparted to a test specimen at any given time during testing Lie, (1992) [18]. The typical fire test time-temperature curves for several countries are displayed in Fig. 2-2.

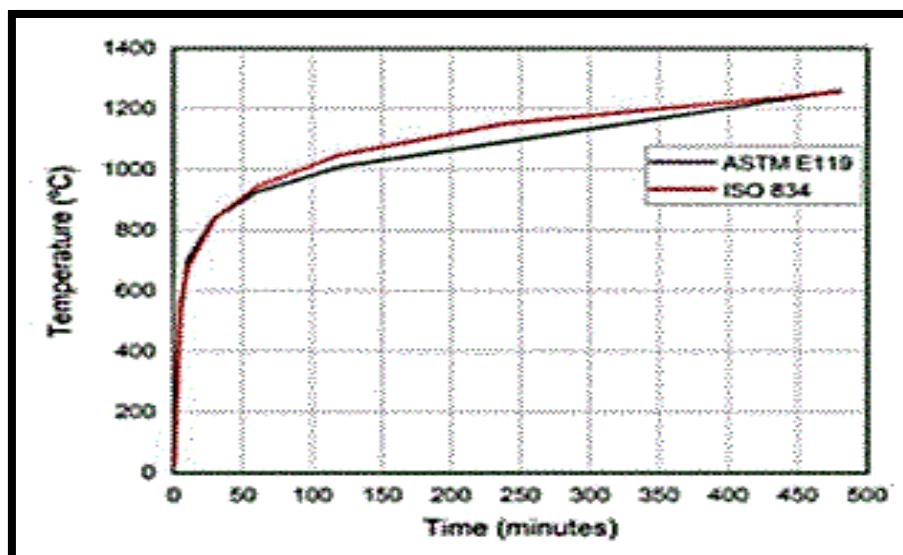


Figure 2-2: ISO 834 and ASTM E119 Time-Temperature Curves [18].

### 2.3.1 ISO834

The most used curve for planning and analyzing structural components and structures is the ISO834 standard curve. Since paper, wood, fabric, etc. are thought to be the primary fire source, it is also known as the cellulosic curve. In the first ten minutes, the temperature rises from 20 to 671°C, which is an extremely high slope. The temperature reaches 945°C after an hour ISO-834, 1975. The following equation represents the temperature-time increase T(1) (in. °C):-

$$(T) = T_0 + 345 \log^{10}(8t + 1) \dots \dots \dots (2 - 1)$$

where t is the time in minutes and T<sub>0</sub> is the ambient temperature, which is typically taken to be equal to 20 °C.

### 2.3.2 Fire Resistance Testing According to ASTM E119

Together with the corresponding ISO 834 temperatures, the ASTM E119 curve, which depicts the fire-time connection, is specified by distinct points, as indicated in Table 2-1. The following simplified formula generally matches the ASTM Ellingwood & Shaver, (1979) [19] :-

In hours

$$T = 20 + 750(1 - e^{-3.7955th}) + 170.41\sqrt{th} \dots \dots \dots \text{th in hours. (2-2)}$$

**Table 2-1 ISO834 and ASTM-E119 Time curves at various point**

<b>Time</b>	<b>ASTME119 Temperature</b>	<b>ISO 834 Temperature</b>
0	20	20
5	538	568
10	704	671
30	843	842
60	927	945
120	1010	1049
240	1093	1153

### 2.3.4 Flame Fire

The heating stage at the start of a fire, known as ignition, is characterized by a slow increase in temperature, no impact on the chamber's characteristics, and no risk of property or human life being destroyed by structural collapse. This stage, which is often referred to as the pre-ignition phase Costa (2003) [20] as shown in Fig. 2-3, concludes at the ignition moment.

- The phase marked by a sharp shift in temperature rise is called ignition.

All of the flammable items in the chamber burn at this stage.

The hot gases' temperature stays over 300°C until it reaches the curve's apex, which is usually higher than 1000°C.

- Following the complete extinguishment of the flammable elements in the chamber, the cooling phase is the one that represents the slow drop in the temperature of the gases in the surrounding environment.
- When there are no fresh firewood loads to fuel the flame, heat loss, or the fire's slow cooling, starts.

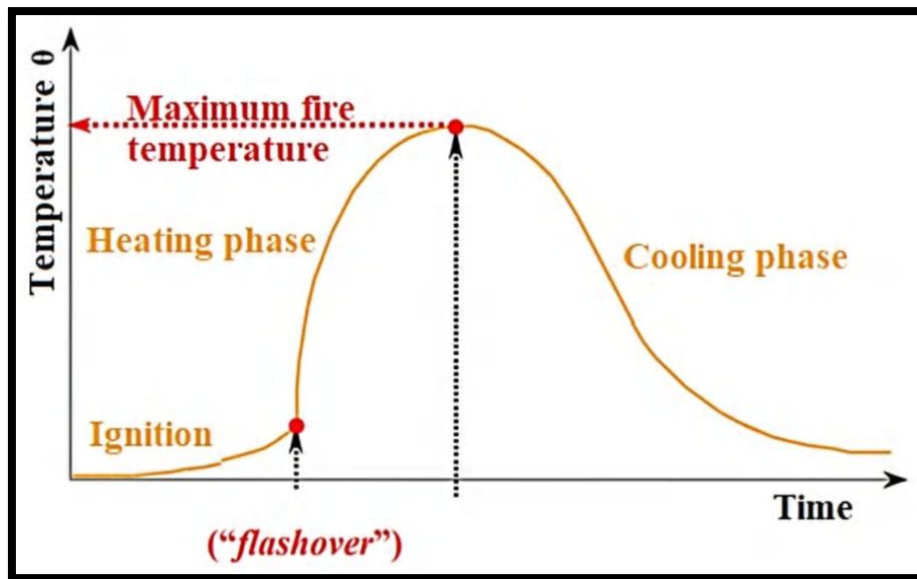


Figure 2-3 Fire Development Curve [20].

## 2.4 Structural and Material Response of Normal-Weight Reinforced Concrete Slabs under Elevated Temperatures.

Fire is a critical factor in the safety and durability of civil engineering structures. Reinforced concrete slabs, commonly used in floor and ceiling construction, are designed to withstand loads and environmental conditions. However, when exposed to fire their performance can be significantly degraded.

In his study Gabriel [21] looked at how fire affected reinforced concrete slabs and showed how intricate physicochemical changes controlled by the mix proportions and composition of the concrete determine its thermal reactivity. Ultra-high-performance concrete reacts differently to heat than normal-strength and high-performance, concrete. Transient creep is a crucial component of concrete's fire performance that, if ignored, could result in erroneous structural analysis, especially in columns. Spalling, a decrease in compressive strength, and a weaker link with reinforcement are typical failure

processes. The basic goals of fire-resistance design are to minimize heat transmission to allowable levels and maintain an efficient concrete cover. Spalling is a concern that is made worse by limited concrete permeability, and recent developments in thermo-hydro-mechanical finite element models (THM-FEM) have greatly improved the predicted outcome.

This can be mitigated by incorporating polypropylene fibers or applying thermal barriers to exposed surfaces. Concrete fire resistance is assessed through three primary methods: direct fire testing, prescriptive approaches, and performance-based methods, the latter including advanced finite element analyses. While performance-based design is still emerging in some countries, it represents a growing shift toward enhanced fire safety in structural engineering, as shown in Fig. 2-4.

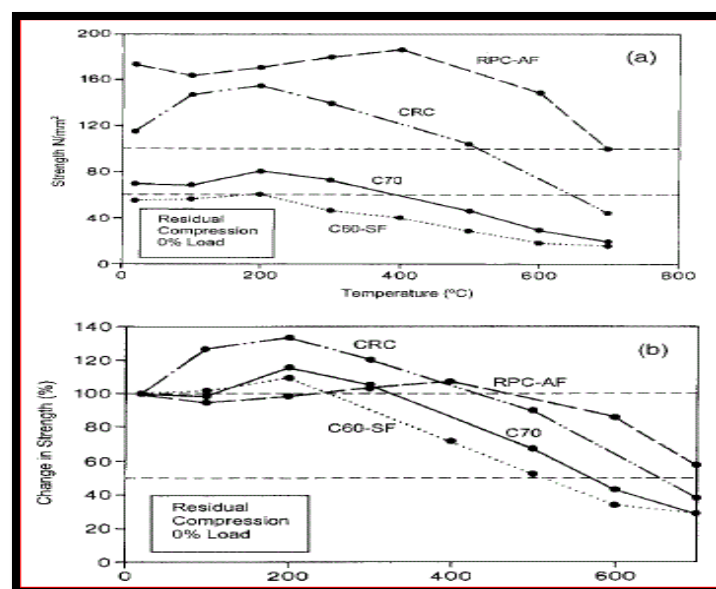


Figure 2-4 Shows the Comparative for to Temperature and Strength [21].

Zhaohui Huang [22] presented a sophisticated computational model to evaluate how concrete spalling affects the structural and

thermal behavior of fire-exposed reinforced concrete slabs. In order to accurately simulate spalling effects, the model expands upon a tiered approach in which spalled layers are represented as elements without thermal or mechanical resistance. In a 10-story structural model, the study examined 16 scenarios with differing levels of spalling and fire compartment locations. The impact of spalling in central sections is considerably lessened by thermal restraint from nearby cooler structures, according to the results. On the other hand, because of their restricted heat confinement, corner slabs are more susceptible additionally, the study highlighted the role of compressive membrane action, which helps mitigate the structural impact of spalling. This research provided one of the first numerical demonstrations of how concrete spalling critically influences slab performance under fire conditions, as shown in Figure. 2-5.

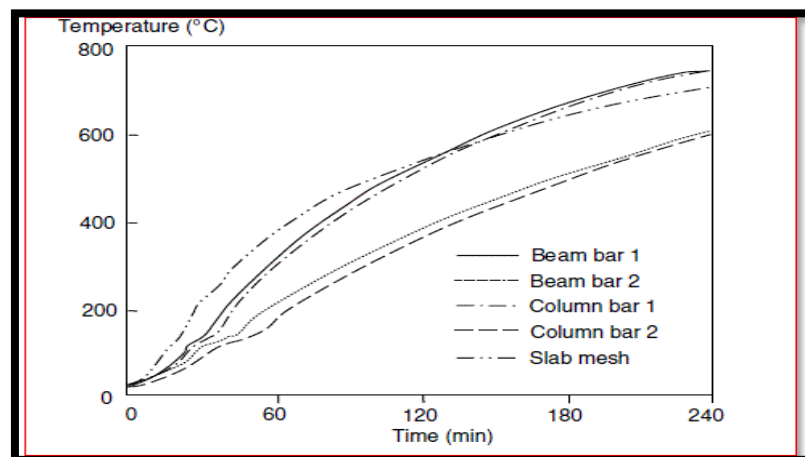


Figure 2.5 Shows The Comparative for to Temperature and Time [22].

The impact of moisture accumulation in cooler areas of the concrete cross-section was highlighted, Yong Wang [23] that looked at the thermal behavior of reinforced concrete (RC)

slabs under fire circumstances. Based on a thorough analysis of current constitutive laws and design guidelines, the study presented a numerical model to evaluate the thermal performance of RC slabs at high temperatures. The study suggested new constitutive models for concrete that account for the material's thermal and mechanical reactions to fire exposure. Both large-scale and small-scale fire tests on easily supported RC slabs were used to validate these models. The effects of concrete material laws, size effect, moisture content, and transient strain on slab performance during fire were investigated using parametric analysis. Findings revealed that moisture content significantly affects temperature distribution and structural response. The proposed models demonstrated reasonable accuracy in predicting fire resistance times, albeit with conservative estimations compared to experimental data. Moreover, the study found that existing standards, such as ASCE, tend to underestimate mid-span deflection and overestimate fire resistance duration, as shown in Fig.2-6.

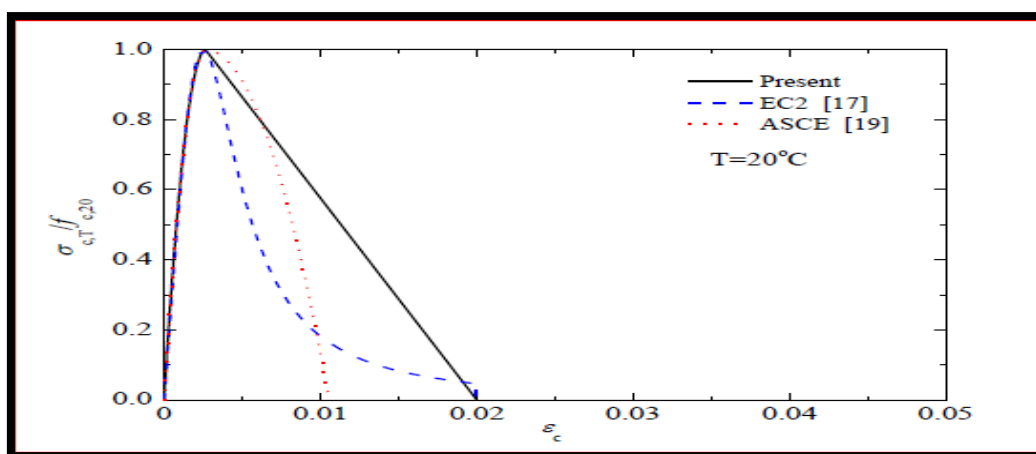


Figure 2-6 Shows the Relationship Between Emotion and Stress According to the Source [23].

Saeed [24] also studied the fire behavior of one-way reinforced concrete slabs, focusing on fire resistance and structural post-fire hazards during the cooling phase. Using standard (ISO 834) and parametric fire tests, the study determined the "maximum risk time" the period between fire extinguishment and potential collapse.

Sixteen reinforced concrete slabs were analyzed using the finite difference method to evaluate the effects of grout, concrete cover thickness, and live load ratio. The results showed that fire resistance increased with concrete cover thickness, and that unstacked slabs often performed better during the heating phase. However, grout improved resistance during the cooling phase by providing additional thermal insulation, increasing the cover thickness from 15 mm to 30 mm improved fire resistance by up to 120%, while grout added up to a 162% improvement for thinner covers. Despite these improvements, the slabs remained vulnerable after cooling, with internal temperatures sometimes exceeding surface temperatures. Overall, the study confirmed that the thickness of the cover and plaster significantly affected fire performance, while the live load ratio consistently reduced fire resistance by approximately 28% ,as shown in Fig. 2-7.

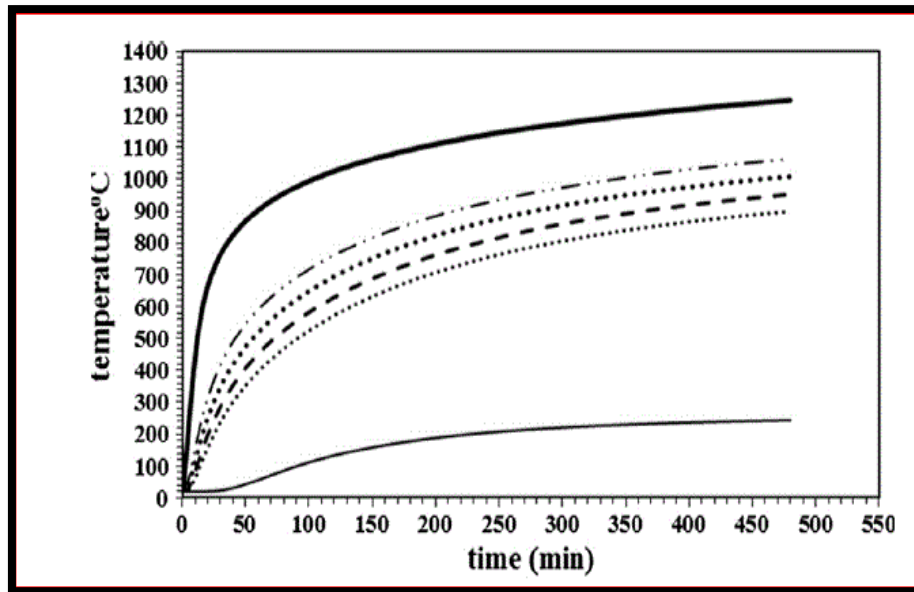


Figure 2-7 Shows the Curve Between Temperature and Time [24] .

Wang Yong [25] a numerical model for analyzing the thermal behavior of reinforced concrete (RC) slabs exposed to high temperatures, incorporating the effects of moisture accumulation in cooler regions of the concrete, known as "moisture clog." The study introduced enhanced concrete constitutive laws, based on a detailed review of existing literature and design standards, to better predict mechanical and thermal behavior during fire exposure.

These proposed laws were validated through full-scale and small-scale fire tests on simply supported RC slabs. Parametric analyses examined the influence of moisture content, transient strain, concrete material properties, and slab size on fire performance. Results confirmed the potential of the suggested models for predicting RC slab behavior under fire conditions, as shown in Figure 2-8.

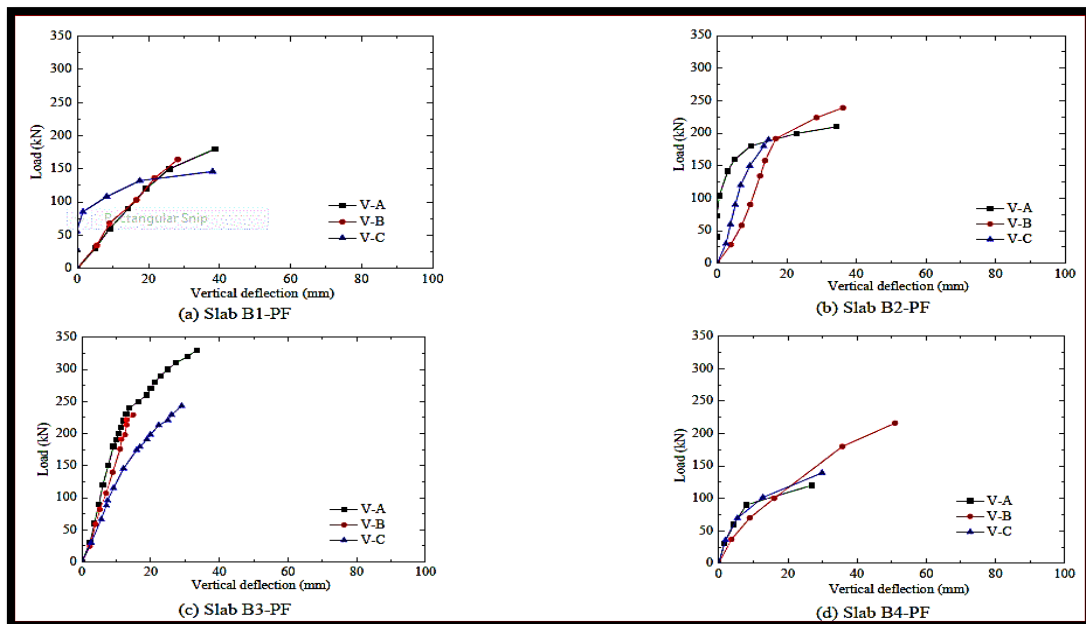


Figure 2-8 Shows the Curve Between load and deflection [25]

prolonged exposure to high temperatures on concrete with various aggregate morphologies. A study by Shyamala et al. [26] summarized the results, showing a continuous decrease in compressive, tensile, and flexural strength, with rapid deterioration above  $500^{\circ}\text{C}$  due to water loss, quartz transformation, and expansion. Factors such as aggregate morphology, age, heating duration, load, cooling method, and water-to-carbon ratio affected performance. The study emphasized the need for further research on the thermos plasticity of concrete to select safer materials for fire-exposed structures.

Wang. Y.[27] investigated twelve continuous RC slabs under different fire scenarios to evaluate post-fire behavior. The study found that traveling fires caused more severe cracking and increased the risk of sudden punching shear failures, while higher reinforcement ratios enhanced residual stiffness and load capacity.

Overall, the post-fire strength could be effectively predicted using punching shear theory, emphasizing the importance of reinforcement detailing and accurate fire scenario modeling in resilient slab design, as shown in Figure.2-9.

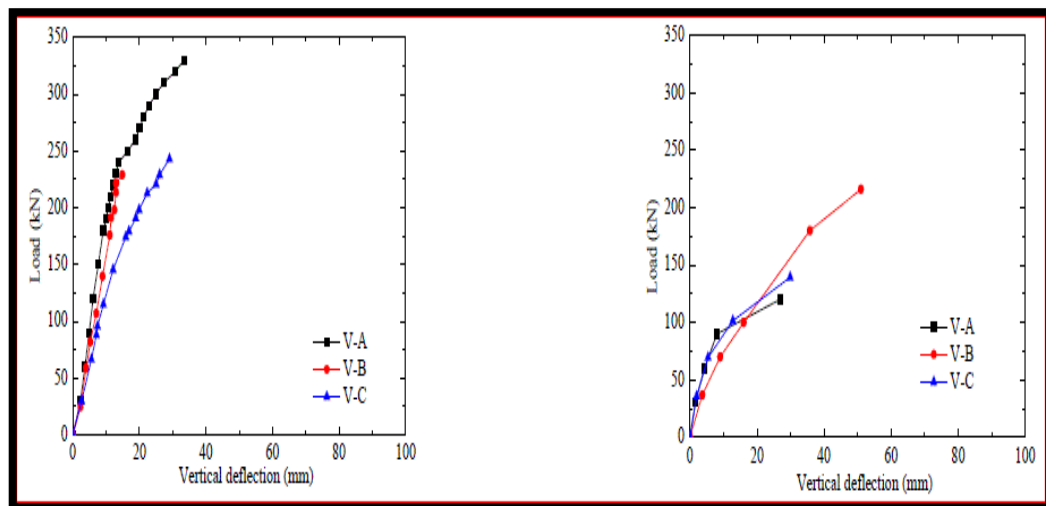


Figure 2-9 Show the Curve Between load and deflection [27 ]

Wang [28], studied twelve reinforced concrete slabs under different fire scenarios to assess post-fire behavior. They examined the effects of reinforcement detailing, steel ratio, and fire type on deflection, load capacity, cracking, and failure. Results showed that traveling fires caused earlier and more severe cracking, often leading to punching shear failures, while higher reinforcement ratios improved stiffness but increased brittle failure risks. The study compared prediction methods, finding that slab geometry and reinforcement had greater impact than fire direction. Traditional models were less accurate for moving fires but remained valid for uniform exposure. Overall, combining ACI 318-08 with deflection criteria was recommended as a practical approach for estimating

residual slab capacity, emphasizing the need for scenario-specific fire design.

The impact of fire exposure on the mechanical characteristics of concrete was examined by Ali [29] 800 °C was reached during the two and six hours that the specimens were exposed to fire. 150 mm cubes' compressive strength and 100 x 100 x 400 mm prisms' flexural strength were measured. The compressive strength of the concrete dropped by 38% more after 6 hours of burning than it did after 2 hours. After burning, the concrete's density decreased by 8%, and its elastic modulus and rupture also decreased.

#### **2.4 Thermo-Mechanical Performance of Lightweight Reinforced Concrete Slabs under Fire Conditions.**

The Effect of Fire on a Lightweight Reinforced Concrete Slab. Fire resistance primarily refers to the performance of structural elements in buildings, rather than the materials themselves. However, the properties of a material significantly influence how well it performs within a structural element. This section will discuss how fire affects concrete. First, it is non-combustible, unlike materials such as wood. Second, it acts as a good insulator due to its low thermal diffusion rate, especially when compared to steel. However, there are two major challenges associated with concrete at high temperatures. The first is the deterioration of mechanical properties at high temperatures, which can be exacerbated by explosive scaling. This phenomenon results in material loss, a reduction in the concrete cross-section, and exposure of the reinforcing steel to high temperatures. The second challenge relates to the physical and

chemical changes in the material due to heating. These factors can negatively impact a concrete element's ability to effectively isolate, separate, and support loads.

A research study on methods for assessing the residual strength of reinforced concrete structures after fire exposure, focusing on nondestructive and semi destructive testing techniques, was conducted by Wroblewska [30]. The study demonstrated that concrete deterioration at high temperatures especially near the surface is often underestimated by conventional core-based destructive testing methods, which do not take into account the heterogeneous distribution of damage within the cross-section.

The study highlighted the importance of determining the depth of the severely damaged surface layer, as this area may not contribute to structural integrity. Standard compressive strength testing of extracted cores is limited by its inability to capture strength changes along the specimen axis. Alternatively, laboratory methods such as the air permeability index, dynamic elastic modulus, and layered compressive strength tests have been proposed to more accurately assess thermal damage. Advanced techniques such as X-ray diffraction and scanning electron microscopy can also be used to estimate temperature exposure across a structural element. For on-site assessment, semi-destructive methods, such as pull-out, discontinuity, fracture, internal fracture, and probe penetration tests, offer faster and more cost-effective alternatives [31]. Although these methods are limited in depth and accuracy, they provide valuable insights into the surface condition of fire-damaged concrete when full laboratory testing is impractical, as shown in Figure 2-10.

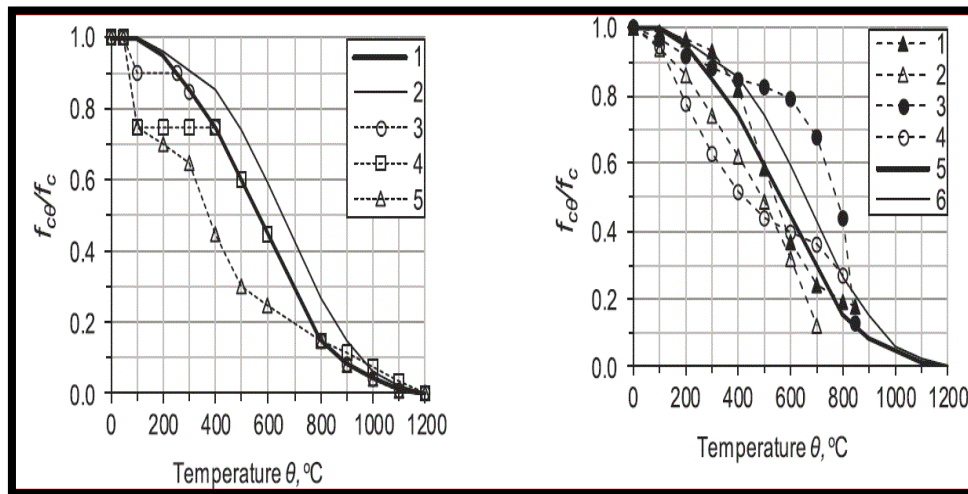


Figure 2-10 show the relationship between the temperature and stress according to ACI and EURP [31]

Lightweight reinforced concrete (LWRC) slabs are widely used in civil engineering for floor and ceiling construction due to their advantages in reducing dead weight, improving seismic performance, and enhancing thermal insulation properties Shbeeb [32], A two-way slab, characterized by its load distribution in both directions, is often utilized in buildings and structures where large spans are required Abdullah [33] the behavior of lightweight concrete, especially when exposed to fire, can differ significantly from normal-weight concrete. This report discusses the effects of fire on lightweight reinforced concrete two-way slabs, including the impact on the material properties, structural performance, and potential failure mechanisms [34].

Altalib [35] studied the properties of lightweight concrete composed of LECA as a substitute for conventional aggregates under the influence of high temperatures. During this study, the mechanical

properties of concrete were analyzed, as well as the residual characteristics of tensile and flexural strengths. Four samples were prepared using mix designs without fibers and Nano-SiO<sub>2</sub>, samples with different proportions of Nano-SiO<sub>2</sub>, samples with different proportions of fibers, and samples containing both fibers and Nano-SiO<sub>2</sub>. The results showed damage to the samples without Nano-SiO<sub>2</sub> and fibers, discoloration, reduced strength, and reduced weight. However, adding Nano-SiO<sub>2</sub> fibers, or using them together, improved the properties of concrete at all temperatures. Due to Nano-SiO<sub>2</sub>, its pozzolanic interactions improve the microstructure, and the fibers prevent cracks in the concrete. This study summarized the effect of changing the size of the samples on compressive strength. The results showed an increase in the strength of samples with smaller sizes, resulting in conversion factors for non-standard samples to standard ones, as Shon in Figure. 2-11.

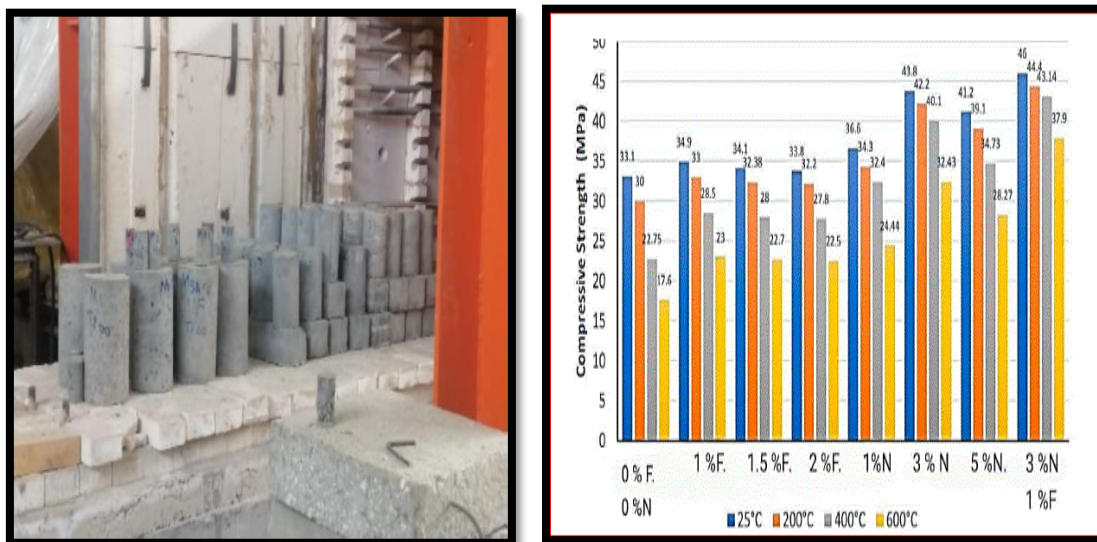


Figure 2-11 Image containing details of the search form[35].

In the construction industry, lightweight concrete is an innovative material that offers reduced weight without compromising essential mechanical and structural qualities. This paper provides a comprehensive analysis of lightweight concrete slabs, addressing their characteristics, applications, challenges, and recent advancements. Their performance in various structural scenarios is evaluated through experimental data analysis and a review of existing scientific literature. Because of its strength and adaptability, concrete is frequently utilized in building. Conventional concrete's substantial weight, however, might provide difficulties, especially in situations with strict load constraints or lightweight structural designs. In order to overcome these difficulties, lightweight concrete has been created by using lightweight aggregates or air-entraining methods to lower density. Lightweight concrete has a density of less than  $2000 \text{ kg/m}^3$ , which is lower than that of conventional concrete, which normally weighs between  $2200$  and  $2500 \text{ kg/m}^3$ . By adding air spaces or lightweight particles to the mixture, this decreased density is accomplished. Lightweight Concrete Slab Features being lightweight reduces the dead load on buildings because of its high porosity, thermal and acoustic insulation provides exceptional insulation qualities lightweight slabs are easy to handle and install to move and set up. Mechanical Properties: They offer enough compressive strength, depending on the kind of aggregate utilized.

Alaa Fahd [36] investigated the mechanical deterioration of lightweight concrete (LWC) after fire exposure, focusing on the use of steel fibers and nano silica as reinforcement additives. With the increasing demand for sustainable and fire-resistant building

materials, four concrete mix designs were tested: plain LWC, LWC with steel fibers, LWC with Nano silica, and LWC with both. After heating the samples to 200°C, 400°C, and 600°C, the results showed that while all samples lost strength, those containing steel fibers and/or Nano silica retained significantly better compressive and tensile properties and exhibited less damage.

The study concluded that the addition of steel fibers and Nanosilica improves the fire resistance of LWC by reducing cracking, enhancing bonding, and increasing peak stress. These materials offer a promising solution for developing more durable and resilient concrete structures.

Huang Zhuhai [37] This study presented a comprehensive model that integrates the effects of concrete spalling on the behavior of reinforced concrete slabs during fires. The model is based on the author's previous layering technique. The research begins with a detailed analysis of uniformly loaded reinforced concrete slabs subjected to varying degrees of concrete spalling under a standard fire regime. In addition, a conventional reinforced concrete building was examined through a series of analyses of its floor slabs, which were subjected to varying levels of concrete spalling.

Mona [38] summarized an experimental study on the behavior of 21 self-compacting concrete (SCC) reinforced concrete slabs and their ability to withstand maximum loads in buildings by testing the concrete's mechanical properties and flexural strength using steel, polypropylene, and fiberglass (2250 × 1000 × 100 mm). The tested slabs were exposed to two controlled elevated temperatures (400 and 800°C) in addition to the ambient temperature. The slab samples

were loaded to 50% of the maximum load before combustion; these loads were assumed to be equivalent to the service load during fire exposure. The fire exposure tests lasted for 120 minutes. At 400°C and 800°C, the deflections increased after 120 minutes of fire exposure to 50% of the maximum load. When a plaster layer was added to the panels, the deflections after 120 minutes of fire exposure were reduced for panels with 10 mm and 20 mm plaster layers at 400°C and 800°C compared to SSC panels without a plaster layer under the same load conditions. For the plaster-coated slabs, the temperature decreased. The residual strength of the slabs exposed to temperatures of 400°C and 800°C for the thermally insulated plaster slabs remained high, as shown in Figure. 2-12.

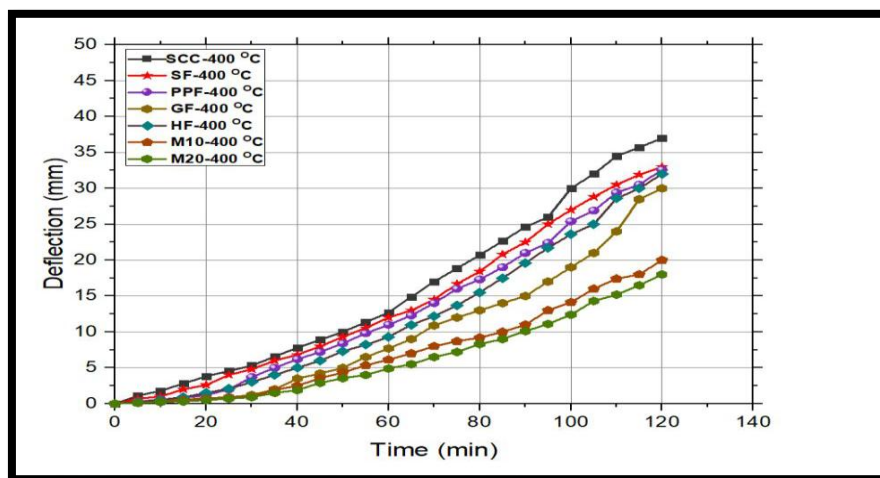


Figure 2-12 Relation Between Time and Deflection [38].

Klak and Jomaa'h [39] investigated the flexural behavior of one-way reinforced lightweight aggregate concrete slabs exposed to elevated temperatures. The study found that higher LECA content and increased temperature reduced flexural strength, stiffness, and

load-bearing capacity, while deflections increased. Incorporating LECA affected the structural performance under fire condition.

## **2.6 Concluding Remarks**

This chapter provides an overview of research related to fire exposure and its effects on concrete, reinforcing steel, and reinforced concrete slabs. Observations from previous research indicate the following:

1. In the reviewed research, only one fire mode was used.
2. Reduction in the strength of reinforcing steel and concrete under hot conditions.

The main objective of this chapter is to identify knowledge gaps to demonstrate the uniqueness of the study, which can be summarized as follows:

A review of the literature reveals a paucity of information on how high temperatures affect lightweight concrete slabs.

Comparing specimen firing methods (exposing them to high temperatures), no comparative research has been conducted between the current method (direct flame method) and the American Code 119 and ISO 834 methods.

## CHAPTER THREE: EXPERIMENTAL PROGRAM

### 3.1 Introduction

Laboratory tests of the materials, casting and testing of models, were conducted in the laboratories of the university of Misan and university Tikrit. This was part of an experimental work aimed studying the structural behavior of RC slabs exposed to high temperatures. The experimental program included testing twenty models of steel-reinforced NRC and LWC slabs. The study focused primarily on analyzing the flexural behavior of reinforced concrete slabs with regular steel reinforcement when exposed to fire, with careful monitoring of the effects of various factors on the flexural resistance, loss of stiffness, and deterioration of the mechanical properties of concrete under the influence of heat. The main variables affecting the structural performance of the models were also identified, such as the type of concrete, the longitudinal reinforcement ratio, method of burning, duration of burning as detailed in Table 3-1 which shows the model design and the variation in their properties & Fig. 3.1, which shows flow chart. This study aims to provide a deeper understanding of how high temperatures affect the structural behavior of LWC slabs, thus contributing to the development of safer and more efficient fire-resistance designs for concrete structures.

**Table 3.1: Parameters of the Study.**

Seq.	Slab Variables	Details
1	Concrete type	NRC and LWC were used
2	Burning periods	Variable fire exposure periods
3	Method of Burning	Using two methods such as direct burning and ISO834 and ASTM-E119
4	Reinforcement ratio	Variable ratio of steel rebar

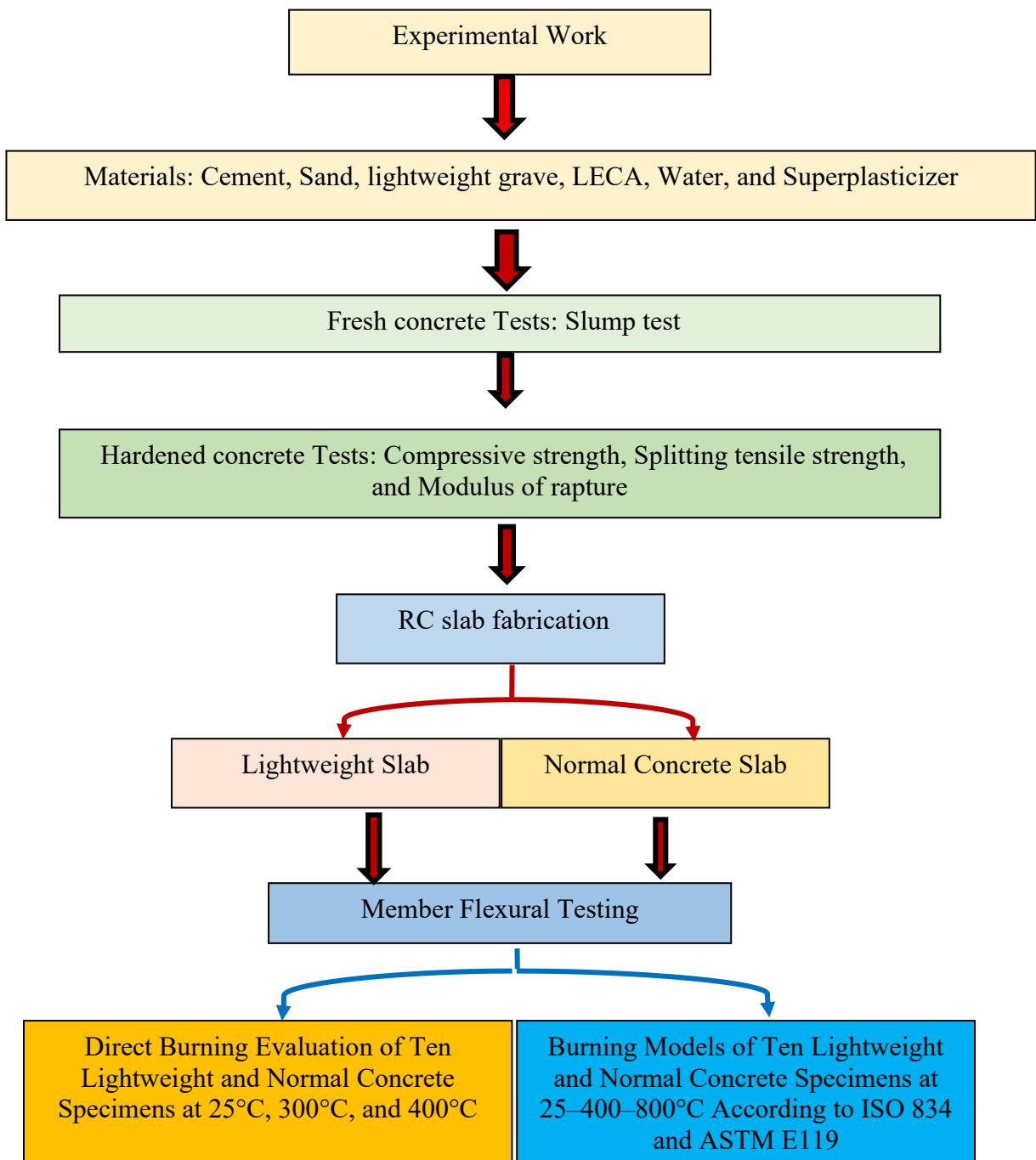


Figure 3.1 Flow Chart of Experimental Work.

### 3.2 Specimens Symbol.

The naming and coding of the experimental work models were adopted as follows:

#### SN1D $\rho$ -25

S=Slab

$\rho$ =Steel Reinforcement Ratio

N=Normal Concrete

D=Direct Flare

25=Temperature

#### SL1A $\rho^{\wedge}$ -800

S=Slab

$\rho^{\wedge}$ = Denies Steel Reinforcement Ratio

L=Lightweight Concrete

A=ASTM-E119

800=Temperature.

### 3.3 Testing Program

The first stage of the research process involves selecting the construction materials used and conducting physical and chemical tests on them. This aims to determine the basic properties of each material and study its suitability for use in concrete mixes. These tests help determine the optimal and most compatible proportions of cement, aggregate, water, and additives, ensuring high mechanical properties and consistent quality of the concrete produced. The second stage involves preparing and testing experimental models to determine the mechanical properties of the proposed concrete mixes, such as compressive, tensile, and flexural strength, as well as studying workability and density. By analyzing the results of these tests, the best concrete mix that achieves the desired performance is selected. Following this, the final models of reinforced concrete slabs are cast according to the selected proportions and then subjected to burning with two methods and then testing until failure to

study their behavior. This procedure enables a comprehensive assessment of the performance of slabs in terms of their load-bearing capacity, resistance to deformation, and the nature of ultimate fracture. These results also contribute to understanding the structural properties of reinforced concrete and developing design methods that enhance efficiency and safety in future engineering applications.

### **3.4 Materials**

The sample selection process was carried out with utmost care in terms of quantity, type, and quality, based on an extensive study aimed at ensuring an accurate representation of realistic construction conditions. This step was carefully implemented before the concrete slab pouring process began, ensuring that the mix components were compatible with the research objectives and experimental requirements. The materials used in this research included cement, natural aggregate, natural sand, water, and a superplasticizer, all of which are commercially available in local markets. These materials were carefully selected to be representative of the materials actually used in typical construction projects, with the goal of achieving realistic results and enabling their field applicability in engineering projects.

#### **3.4.1 Cement**

This study used exclusively Iraqi Portland cement produced at the Cresta plant to ensure uniformity of the material used and to obtain accurate and comparable results. Tests on the study materials were conducted in the laboratories of the University of Misan, following precise methodological procedures, to evaluate the chemical and physical properties of the cement used before it was used in the mixing and casting of concrete forms. The cement was transported and stored with utmost care to preserve its properties. It was stored in a dry environment at a moderate temperature to prevent moisture

absorption or any undesirable chemical reactions that might affect the quality of the results. A comprehensive set of chemical and physical laboratory tests was also conducted according to the American standard [40]. These tests included determining the initial and final setting time, sulphate content, and volume stability, in addition to testing the fineness and specific gravity. The results of these tests showed complete compliance with the requirements of Iraqi Specification [41], confirming the quality of the cement and its suitability for use in this research. The selection of this type of cement was based on the results of these precise tests, which demonstrated its high efficiency and stability in various environmental conditions, making it suitable for lightweight reinforced concrete applications within the framework of the current study. Details of the tests and results are presented in Tables 3-2 & 3-3, which illustrate the chemical and physical properties used in the evaluation.

**Table 3-2 : Physicals Properties of Ordinary Portland Cement [41].**

<b>Physical Properties</b>	<b>Test Results</b>	<b>Limit of Iraqi specification</b>
Vicat time of Setting		
Early:	Two Hours	More than forty-five
Ultimate:	Less than Four	Less than ten
strength of mortars		
3 day (Mpa)	Twenty-One	More than fifteen
7day (Mpa)	Twenty-eight	More than twenty-three
28day (Mpa)	Thirty-five	

**Table 3-3 : Chemical Composition of Cement [41].**

Compound Composite	Weight	Limits
Limes	64%	N-A
Silicas	21%	N-A
Alumina's	4.6%	N-A
Iron oxidizes	3.3%	N-A
Magnesians	2.4%	≤5%
Sulphates	2.3%	≤2.8%
ignitions	3.6%	≤4%
Insolubles residuals	1.2%	≤1.5%
Limes fullness issue	0.750%	(0.66-1.02) %
T. silicates	50.7%	N-A
D. silicates	18.3%	N-A
T. aluminates	8.1%	N-A
Tetracalcw alumminoferites	9.9%	N-A

### 3.4.2 Aggregate

#### A. Fine aggregate (Sand):

In this investigation, it was brought from Basra in southern Iraq. The maximum grain size is 4.75 mm. To evaluate the particle size distribution of the sand, the sieve analysis test was performed according to [42]. This test method involves passing the sand through a series of sieves with different mesh sizes to separate and measure the different particle sizes present in the sample. The results of the sieve analysis help determine the gradation and suitability of the sand for use in concrete. Tables 3-4 & 3-5 and Fig. 3.2 show case the sand grading used for normal concrete in the study. These tables provide detailed information about the particle sizes and their corresponding percentages within the sand sample.

**Table 3-4: Grading of the Fine Aggregate.**

	size of Sieves	% Passing percentages	
		Fines aggregates	No.5/1984Limits(Zone 2)
1	10	100	100
2	4.75	99	90-100
3	2.36	90	75-100
4	1.18	75	55-90
5	0.60	53	35-59
6	0.30	17	8-30
7	0.15	2	0-10

**Table 3-5: Physical Properties of the Fine Aggregate.**

Physical Properties	Tests	No.5/1984Limits
Specific gravities $Kn/m^3$	2.65	-
$SO^3$	0.33	Less than half
Preoccupation %	1.10	-
bulk density Slack $Kg/m^3$	1646	-

It is worth noting that the sand used in this investigation complies with Iraqi Specifications [43], indicating that it meets the required standards and specifications outlined by the Iraqi authorities. By conducting these tests and ensuring compliance with relevant standards, the study authors aimed to ensure the quality and appropriateness of the sand as a crucial component in the concrete mixture. This meticulous approach enhances the reliability and validity of the research findings and supports the overall integrity of the study.

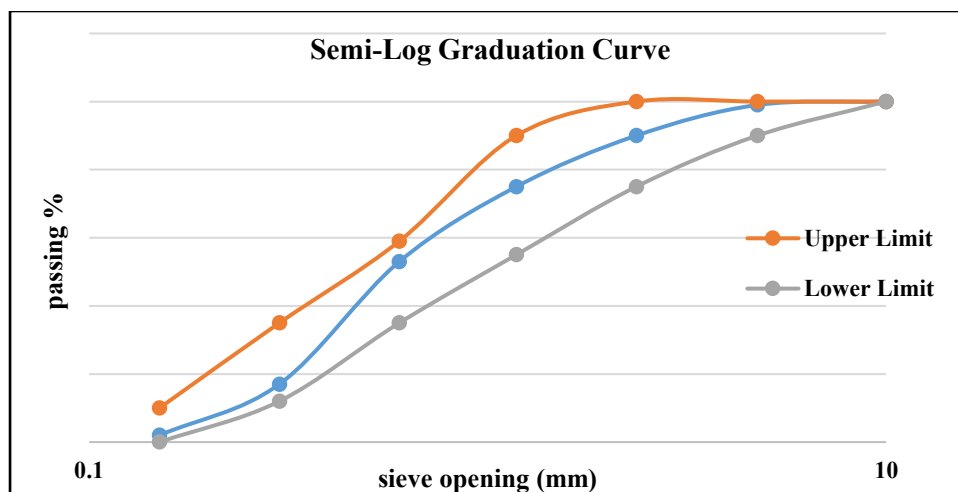


Figure 3.2 Grading Graph of Fine Aggregate.

### **B. Coarse aggregate (Gravel):**

The coarse aggregate used in this study has rounded particles with a maximum nominal size of 19 mm. It was obtained from the Amarah. This particular source was chosen for its high purity and homogeneity of physical properties, as well as its local availability and common use in construction work, making it suitable for research applications aimed at stimulating the realistic conditions of concrete structures in Iraq. The aggregate was subjected to a series of standard laboratory tests to determine its physical properties, such as specific gravity, water absorption, sintering resistance, and particle gradation, to ensure its compliance with the quality requirements of the Iraqi specifications. The detailed results of these tests are presented in Table 3-6 , which shows a precise comparison between the aggregate gradation used and Iraqi Standard Specification [44]. Test results showed that the aggregate used met the Iraqi standard specifications, demonstrating its high quality and suitability for use in reinforced concrete production. The rounded shape of the aggregate particles also helped improve concrete workability and reduce interparticle friction, which positively impacts the consistency and mechanical performance of the concrete mix under various loading conditions.

**Table 3.6 Grading of the Coarse Aggregate.**

<b>No.</b>	<b>Sieve size</b>	<b>Cumulative passing%</b>	<b>Limits according to IQS 45/1984</b>	<b>Iraqi specification lower limit</b>	<b>Iraqi specification upper limit</b>
1	37.5	100	100	100	100
2	20	100	97.5	95	100
3	14	84.63	85	80	90
4	10	46.64	45	30	60
5	5	2.92	5	0	10

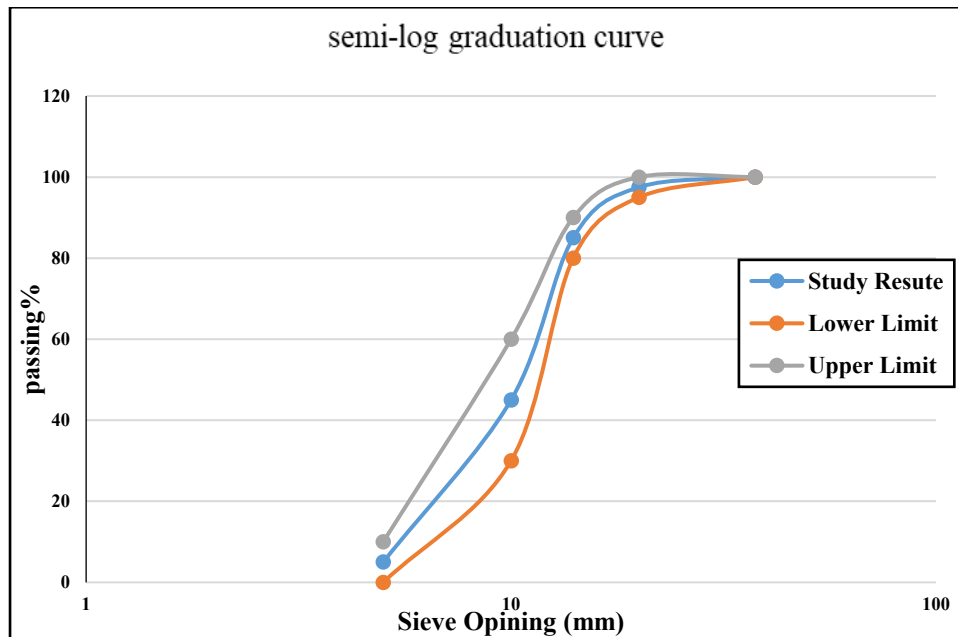


Figure 3.3 Grading Graph of Coarse Aggregate.

### C. Coarse Aggregate (LECA)

The coarse aggregate used in this study is lightweight, consisting of 10 mm spherical particles. It was carefully selected to meet the research objectives of studying the properties of reinforced lightweight concrete. This aggregate has a bulk density nearly two to three times lower than that of natural gravel, which significantly contributes to reducing the overall concrete density and improving thermal insulation while maintaining adequate mechanical strength. The physical and engineering properties of this lightweight aggregate were studied through a series of laboratory tests, including specific gravity, water absorption, slump resistance, and particle gradation, to ensure its compliance with the requirements of the Iraqi standard specifications. The detailed results of these tests are included in Tables 3-7 and 3-8 in addition to Fig. 3.4, which provide a precise comparison between the gradation of the lightweight aggregate used and Iraqi Standard Specification [45]. Test results showed that the aggregate used falls within the permissible limits according to Iraqi specifications, confirming its suitability for use in the production of high-performance lightweight concrete. Its regular spherical shape also helped

improve concrete workability and reduce water consumption, which contributes to improving the quality of the concrete mixes used in the study and achieving higher cohesion between its components.



Figure 3.4 Lightweight aggregate (LECA)

**Table 3-7: Typical properties for LECA [46].**

Properties	LECA Aggregate
Density (Kg/m <sup>3</sup> )	650
Bulk density (kg/m <sup>3</sup> )	450
Grain size (mm)	10
H <sub>2</sub> O absorption 24 h (%)	0
Fineness modulus (FM)	---
Shape	round

**Table 3.8 Grading of Coarse Aggregate for LECA.**

Sieve size	Cumulative passing%	Limits according to IQS 45/1984[46]
20	100	100
12	92	100-90
9.5	55	70-40
4.75	14	15-0
2.33	2	5-0

### 3.4.3 Water

In this investigation, R.O. water was utilized for both the Preparation and curing of the specimens. R.O. water is a purified form of Water obtained through the reverse osmosis process, which removes impurities and contaminants from the Water. The use of R.O. water in concrete specimen

preparation ensures that the Water does not introduce any unwanted impurities or chemicals that could potentially affect the properties or performance of the specimens. It helps maintain the purity and consistency of the Water used in the concrete mixture. Additionally, R.O. water was employed to cure the specimens [46].

#### **3.4.4 Superplasticizer**

Chemical admixtures play an important and fundamental role in controlling the mechanical properties of concrete, in addition to their direct impact on workability and other structural characteristics. Among the most important of these admixtures are water reducers, which are the primary factor in improving the workability of concrete mixes. They make the mixture more fluid and easier to pour while reducing the amount of water required to achieve optimal workability [47].

Among the most prominent chemical additives that have witnessed rapid development and widespread adoption in the building materials market are superplasticizers, also known as high-range water-reducing agents. These additives are used in the production of highly fluid concrete or self-compacting concrete, as they contribute to achieving a mixture with good segregation resistance while maintaining the required cohesion and homogeneity. In this study, Viscocrete 180 GS, a superplastic admixture [48]. It was selected for its high water-reducing capacity and improved concrete mix homogeneity without adversely affecting setting time or concrete compressive strength. Table 3-9& Fig. 3.5 shows the detailed properties and test results of Viscocrete 180 GS, including density, viscosity, water-reducing ratio, and effect on setting time. The results demonstrate that the use of this admixture significantly improved the overall performance of concrete mixes and achieved advanced mechanical properties that meet the requirements of experimental research.

**Table 3-9: Types Appearances and Relative Density of Superplasticizers.**

Superplasticizer	Chloride content	Relative density	Appearance
Sika ® Viscocrete 180 GS	NIL	1.095 kg/lt	dark blue liquid



Figure 3.5 Shows the Details and Properties of Admixture.

### 3.4.6 Steel Reinforcement.

In this study, 8 mm and 10 mm diameter reinforcing steel bars were used to strengthen concrete specimens. The reinforcing steel underwent tensile testing to determine its mechanical properties, such as yield strength, ultimate tensile strength, and elongation, according to the American [49],[50] specification for carbon steel reinforcement used in reinforced concrete. The test results showed that the bars used had mechanical properties that met the standard criteria, confirming their suitability for use in experimental models. This adherence to specifications contributes to ensuring the accuracy of the results and achieving a realistic representation of the structural behavior of the reinforced concrete elements under different loads, see the Table 3-10 showing the test results, and see the Fig .3.6 showing the testing device.

**Table 3-10: Steel Rebars Properties.**

Bar size (mm)	Test results		
	Yield stress (N/mm <sup>2</sup> )	Ultimate Strength (N/mm <sup>2</sup> )	Elongation (%)
10	512	601	18.1
8	445.5	603	21.2



Figure 3.6 Showing the Testing Device.

### 3.5 Mix Concrete Mix Design and Mixing Procedures

- All materials and equipment required for the casting process must be prepared in advance to ensure accuracy, consistency, and safety during testing.
- The preparation process involves several precise stages. First, the wooden molds, made of high-quality plywood, are thoroughly cleaned to remove any dust, impurities, or residues that could affect the surface finish of the specimens.
- These molds are then coated with a thin layer of oil or a suitable anti-adhesive to prevent the concrete from sticking to the mold surfaces. The prepared molds are designed in two sets: the first set consists of ten panels manufactured at the University of Maysan, as shown in Table 3.17.
- The second set also consists of ten panels, manufactured at the University of Tikrit, as detailed in Table 3.18. The dimensions

of the first set of panels are 1000 mm in length, 400 mm in width, and 80 mm in depth, respectively, according to the required specimen thickness.

- The second set of molds measures 2250 x 1000 x 100 mm. In addition to wooden molds, steel molds of various standard dimensions are used for casting control samples. These include cubic molds with internal dimensions of 150 x 150 x 150 mm, cylindrical molds of 150 x 300 mm, and prismatic molds measuring 100 x 100 x 500 mm. All steel molds are similarly oiled to facilitate mold removal and maintain sample dimensional accuracy. Equipment for measuring the workability of fresh concrete, including the standard shrinkage cone, must also be cleaned and prepared for use.
- Steel reinforcing bars are then prepared according to the design and dimensions specified in the experimental design table, ensuring correct cutting, bending, and positioning. Furthermore, the chemical admixture, particularly the superplasticizer, is prepared according to the manufacturer's instructions to achieve the required workability without excessive water addition. The raw materials for concrete production are then systematically arranged. For ordinary concrete, these materials include ordinary Portland cement (OPC), natural sand, crushed gravel, and reverse osmosis (RO) water. For lightweight concrete, lightweight expanded clay aggregate (LECA) is used instead of gravel, while maintaining the consistency of the other components. The concrete mix is formulated according to American standards. A hand trowel must be provided to level the surfaces of the freshly cast

samples and ensure uniformity across all samples. design and mixing procedure for Concrete Mixtures as shown Table 3-11.

**Table 3.11 Proportions of constituent materials mixes.**

Type of Concrete	NRC	LWC
Cement (kg/m <sup>3</sup> )	400	400
Sand (kg/m <sup>3</sup> )	820	850
Gravel (kg/m <sup>3</sup> )	1100	----
LECA (kg/m <sup>3</sup> )	----	350
W/C (kg/m <sup>3</sup> )	180	115
Superplasticizer %	1	2
f <sub>c</sub> (MPa)	30	30
Density( kg/m <sup>3</sup> )	2322	1870
Specified Concrete Mix Design	ACI-211.1-91[52]	ACI-211.2[53]

### 3.6 Fresh Concrete Tests

In the experimental program, an important aspect was the selection of appropriate concrete mixtures to achieve the desired concrete properties. This involved carefully choosing the proportions of various ingredients, such as cement, aggregates, Water, and any additional admixtures or fillers, based on the specific objectives of the study. The fresh concrete mixtures investigate the consistency of concrete during the casting. Once the concrete mixtures were prepared, then the hardened tests were performed such as casting cubes and cylinders Etc.

#### 3.6.1 Slump Test

Slumps test is used to evaluate the workability and consistency of fresh concrete. It is one of the most common tests used to assess the properties of fresh concrete. The purpose of the test is to determine the fluidity of the concrete mix and its ability to flow and compact without segregation. To perform the test, all required materials and tools are prepared, including a sample of fresh concrete, a slump

mold in the shape of a cone with a height of 305 mm, a bottom diameter of 200 mm, and a top diameter of 100 mm. A metal stamping rod 400 mm in length and 13 mm in diameter, as well as a flat metal base plate, are also required. The surface of both the base plate and the mold is cleaned to ensure it is free from impurities or excess moisture. The mold is then placed firmly on the flat base. It is filled with concrete in three equal layers, each representing approximately one-third of the mold's height. After placing each layer, the concrete is compacted using the metal rod by applying 25 vertical strokes, ensuring uniform distribution of the mix without disturbing the previous layers. Once the final layer is placed, the concrete surface is leveled using the rod to remove excess material and ensure it is flush with the mold's edge. The mold is then lifted slowly and vertically, without any tilting or lateral movement, to avoid disturbing the concrete sample show Table 3-12& Fig. 3.7.

**Table 3.12 Results of the Concrete Slump Test**

<b>Mix No.</b>	<b>Concrete type</b>	<b>Slump Value (mm) of First group</b>	<b>Slump Value (mm) of Second group</b>
1	LWC	92	90
2	NRC	95	87

The concrete is observed after settling, and the amount of settling is measured as the vertical difference between the mold height and the highest point of the concrete mass after settling. This value is usually expressed in millimeters or inches. The amount of settling is recorded and interpreted based on the desired degree of workability of the concrete mix. A higher settling value indicates a higher fluidity, while a lower settling value indicates a more cohesive and solid mix. The settling test results are presented in the following

table and figure, which illustrate the measured values for the concrete mixes used in this study and their compliance with the design requirements [52].



Figure 3.7 Slump Test of Fresh Concrete.

### 3.7 Hardening Test.

In the laboratory, most specimens for hardened concrete testing are cast into metal or plastic molds according to predetermined dimensions and standards. After casting, the specimens are left undisturbed for approximately 24 hours. This is the period during which the concrete undergoes initial setting and early strength development due to the hydration reaction between water and cement. After 24 hours, the molds are carefully demoulded to ensure that no damage or cracking occurs during the demoulding process. The specimens are then transferred to water curing tanks, where they are fully immersed in clean water to maintain a humid, homogeneous environment that allows the hydration process to continue. Water curing is one of the most common and effective curing methods. It maintains the moisture and temperature of the concrete, which helps continue the chemical reactions within the cement paste and improves the strength and durability of the concrete over time. Specimens remain in water for the specified curing period until they reach the required testing age, whether 7 days, 28 days, or another period depending on the test

type. Following these precise steps ensures that concrete specimens have reached the required level of hydration and structural maturity before being subjected to hardened state tests, enhancing the accuracy and scientific comparability of results.

### **3.7.1 Tests for Concrete Properties**

#### **3.7.1.1 Compressive Strength Test**

In this study, concrete cubes with dimensions of (150 x 150 x 150) mm were cast for both normal concrete (NRC) and lightweight concrete (LWC) to determine the compressive strength. The casting process was carried out according to standard procedures to ensure accurate results representing the actual behavior of concrete under loads [53]. After casting, all specimens were cured in water tanks for the standard curing period of (28 days) to ensure continuous hydration and full development of the concrete's mechanical strength. See the Table3 -13 and Fig.3 .8 showing the results of the 7-28-day examination, and see the figure showing the testing device for the models prepared for operation.

Multiple concrete mixes of lightweight concrete were created to achieve the required strength through trial and error; however, even after achieving this strength, conventional concrete still provides a higher load-bearing capacity compared to lightweight concrete.

**Table 3-13: Compressive strength test at 7-28 days.**

Compressive strength (MPa)				
Age	Lightweight concrete Group 1 (laboratory Misan)	Lightweight concrete Group2 (laboratory Tikrit)	Normal concrete Group1 (laboratory Misan)	Normal concrete Group 2 (laboratory Tikrit)
7 days	22.6	23	30.668	30.7
	25.927	24.5	30.353	31.353
	25.286	25.2	33.54	33.54
Average of 7 days	24.457	24.23	31.5	31.8
28 days	32.4	33.1	40.5	40.5
	30.5	30.5	40.8	40.8
	29.7	29.7	39.8	42.1
Average of 28 days	30.87	31.1	40.4	41.13



Figure 3.8 Compressive Test of Concrete.

This curing method is one of the most effective methods for maintaining the moisture necessary for cementitious crystal growth, which improves concrete durability and increases its compressive strength. The specimens were gradually loaded until failure to determine the maximum load the specimen could withstand.

### 3.7.1.2 Splitting Tensile Strength

For the lightweight concrete (LWC) specimens and cylindrical samples measuring 150 mm in diameter and 300 mm in height, the splitting tensile strength test was performed in accordance with the procedures outlined [56]. This standardized test method is designed to determine the tensile strength of cylindrical concrete specimens by subjecting them to a diametral compressive force that induces tension within the specimen. The test was conducted using a universal testing machine (UTM) with a maximum load capacity of 2000 kN, as illustrated in Fig. 3.9. Prior to testing, all specimens were inspected to ensure that their surfaces were smooth, clean, and free from visible defects or irregularities that could influence the accuracy of the results. During testing, each cylindrical specimen was carefully positioned horizontally between the compression platens of the machine, ensuring that the longitudinal axis of the cylinder was perpendicular to the applied load. To achieve uniform load distribution and to minimize stress concentrations at the points of contact, two thin wooden strips or layers of soft padding were placed along the top and bottom generatrices of the cylinder. The loading process was initiated gradually to prevent impact or shock loading, and a continuous, steady vertical pressure was applied until visible cracking and ultimate failure occurred. Unlike conventional compressive strength testing [57], the applied load in this test acts perpendicular to the cylinder's axis, inducing tensile stresses along the vertical plane that ultimately lead to specimen splitting show Table 3-14 and Fig. 3.9 .

Splitting tensile strength is determined using Eq. (3-1):

$$f_t = 2P / \pi ld \dots \dots \dots (3-1)$$

where:

$f_t$  = Splitting tensile strength (MPa).

$P$  = Maximum applied load (N).

$d$  = Diameter of the specimen (mm).

$l$  = Length of the specimen (mm).

**Table 3.14 Results of Splitting Tensile Strength**

Type of concrete	Splitting Tensile Strength (N/mm <sup>2</sup> ) 28-Day			
	Cylinder 1	Cylinder 2	Cylinder 3	Average
LWC	2.7	2.3	2.3	2.4
	2.9	2.4	2	2.43
NRC	3.4	3.51	4	3.63
	3.3	3.8	4	3.7



Figure 3.9: Splitting Tensile Test.

### 3.7.1.3 Flexural Strength

In the study, the flexural strength of the concrete specimens for each replacement ratio was evaluated using the results obtained from testing prisms. The flexural strength testing followed the [55] standard, which provides guidelines for conducting third-point loading tests on concrete slabs. Test prisms with dimensions of (100 x 100 x 500) mm was cast and cured under the same conditions as the specimens used for the compressive strength tests. The

curing conditions typically involve maintaining a specified temperature and moisture level to promote proper hydration and the development of strength in the concrete. For the flexural strength testing, a testing machine with a capacity of 2000 kN (kilonewtons) was used. This loading configuration induces bending stresses within the slab, allowing for the determination of its flexural strength. Flexural strength (*MPa*) is obtained by Three simply supported prisms with dimensions of (100x100x500) mm tested as revealed in Fig. 3.10. The prism specimen was fabricated and tested after 28 days. The flexural tests were carried out according to the American specification [56] . The modulus of rupture was calculated using Eq. (3-2):

$$f_r = \frac{3pL}{2bd^2} \dots \dots \dots (3 - 2)$$

where:

$f_r$  = Modulus of rupture (MPa)

$p$  = Maximum applied load (N)

$L$  = Span length (mm)

$b$  = Width of the specimen (mm)

$d$  = Depth of the specimen (mm)

**Table 3.15 Flexural Strength Result.**

Type of concrete	Average Flexural Strength (N/mm <sup>2</sup> ) 28 Day		
	prismatic 1	prismatic 2	prismatic 3
LWC	4.85	5.34	4.51
	5.15	5.01	4.6
NRC	3.6	3.51	3.4
	3.25	3.62	3.84



Figure 3.10 :Flexural Strength Test Prism Test Sof LWC, (b) Prism Test of NRC.

### 3.8 Slab Details.

The study involved the preparation and testing of a set of RC concrete slabs specifically designed to investigate the effects of fire and high temperatures on the behavior of both types of reinforced concrete: normal concrete and lightweight concrete. The experimental work was divided into two main methods for testing the fire resistance of concrete: the direct flame method and the ASTM-E119 method, based on ISO 834 show Table 3-18 and Fig. 3.11. This was done to accurately compare the two methods in terms of the structural and thermal performance of the concrete elements.

In the first method (ASTM-E119/ISO 834), larger models measuring  $2250 \times 1000 \times 100$  mm were prepared to simulate the behavior of real-world structural slabs. This method followed American standards for testing concrete's fire resistance, exposing the models to standard temperatures according to the ISO 834 curve for a fixed duration of 120 minutes. This method was characterized by precise control of the heat-up curve over time to ensure the consistency and comparability of the experimental conditions. Three

main temperatures were used in the experiments: 25°C, 400°C, and 800°C, designated as T25, T400, and T800, respectively.

**Table 3.16: First Series Models.**

<b>ISO834&amp; ASTM-E119</b>					
<b>Slab Dimension (2250*1000*100) mm</b>					
<b>Seq.</b>	<b>ID</b>	<b>Thickness</b>	<b>Burning Period minute</b>	<b>Degree of temperate C°</b>	<b>Concrete Type</b>
1	SN1 A <sub>p</sub> -25	100	120	25	Normal concrete
2	SN 2A <sub>p</sub> -400	100	120	400	Normal concrete
3	SN 3A <sub>p</sub> -800	100	120	800	Normal concrete
4	SN4A <sub>p</sub> <sup>^</sup> -400	100	120	400	Normal concrete
6	SN5A <sub>p</sub> <sup>^</sup> -800	100	120	800	Normal concrete
1	SL1A <sub>p</sub> -25	100	120	25	Lightweight concrete
2	SL2A <sub>p</sub> -400	100	120	400	Lightweight concrete
4	SL3A <sub>p</sub> -800	100	120	800	Lightweight concrete
5	SL4A <sub>p</sub> <sup>^</sup> -400	100	120	400	Lightweight concrete
6	SL5A <sub>p</sub> <sup>^</sup> -800	100	120	800	Lightweight concrete

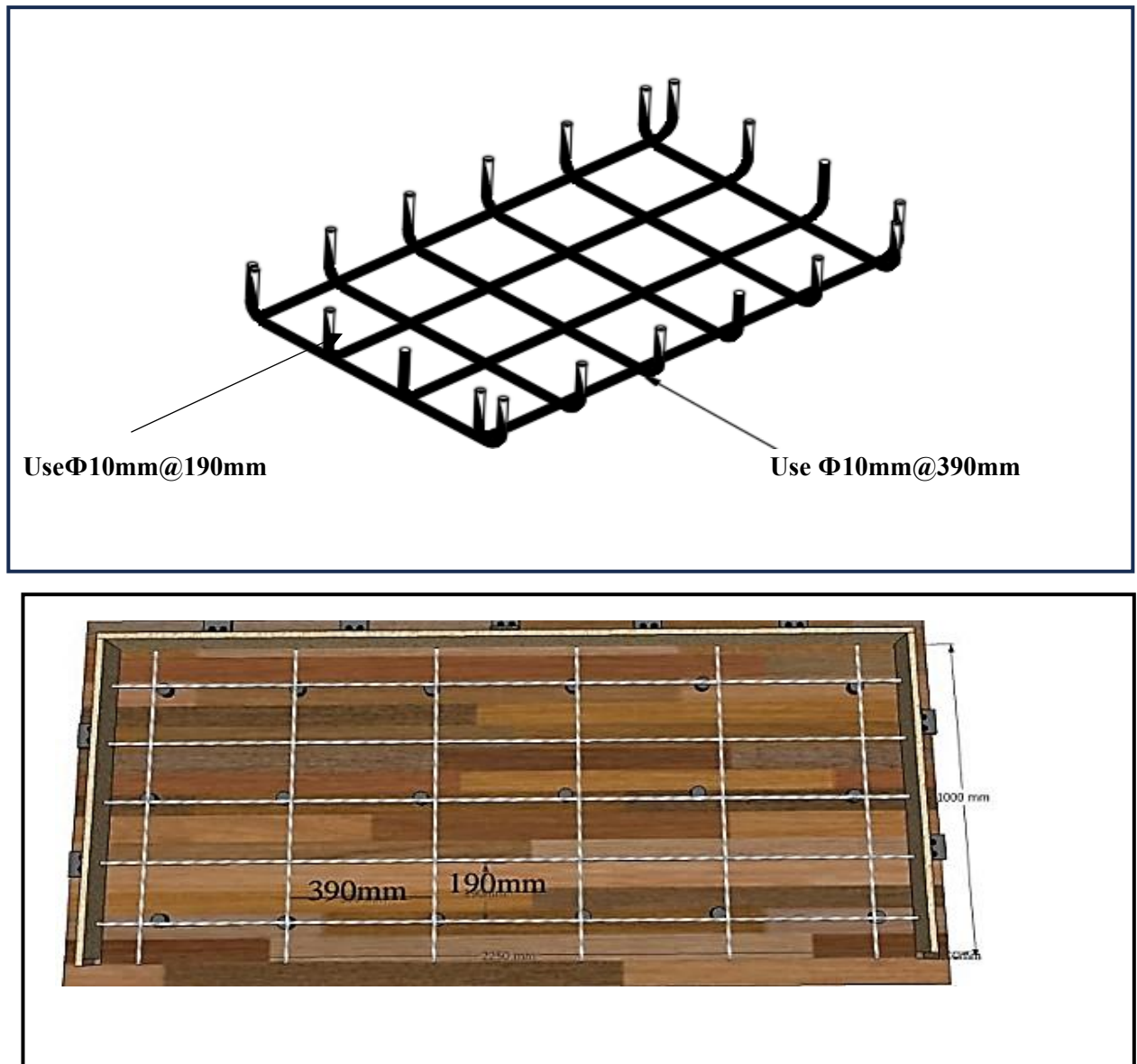


Figure 3.11: Slab Details.

In the Second method (Random exposure), models with relatively small dimensions ( $1000 \times 400 \times 80\text{mm}$ ).

**Table 3.17: Second Series Models.**

<b>Direct Burning method (Random Exposure of fire)</b>					
<b>Slab Dimension (1000 x 400) Thickness (80) mm</b>					
<b>Seq.</b>	<b>ID</b>	<b>Concrete Type</b>	<b>Thickness (mm)</b>	<b>Burning Period minute</b>	<b>Degree of Temperature C°</b>
1	SN1D $\rho$ -400	Normal concrete	80	75	400
2	SN5D $\rho^{\wedge}$ -400	Normal concrete	80	75	400
3	SN4D $\rho$ -300	Normal concrete	80	75	300
4	SN3D $\rho^{\wedge}$ -300	Normal concrete	80	75	300
5	SN2D $\rho$ -25	Normal concrete	80	75	25
6	SL1D $\rho$ -400	Lightweight concrete	80	75	400
7	SL2D $\rho^{\wedge}$ -400	Lightweight concrete	80	75	400
8	SL4D $\rho$ -300	Lightweight concrete	80	75	300
9	SL5D $\rho$ -25	Lightweight concrete	80	75	25
10	SL3D $\rho^{\wedge}$ -300	Lightweight concrete	80	75	300

These models in Table 3-17 and Fig .3.12 were directly exposed to flame in a special fire furnace, with one surface of the model exposed to the direct flame without any additional protection, to simulate the conditions of a direct fire in buildings. This method included several key variables, most importantly the type of concrete, the reinforcement ratio, and the flame exposure time, which 75 minutes, in addition to the slab thickness and the direct firing method. Symbols such as ( $\rho$ ) indicated a standard reinforcement ratio, and ( $\rho^{\wedge}$ ) indicated an increase in reinforcement [57] .

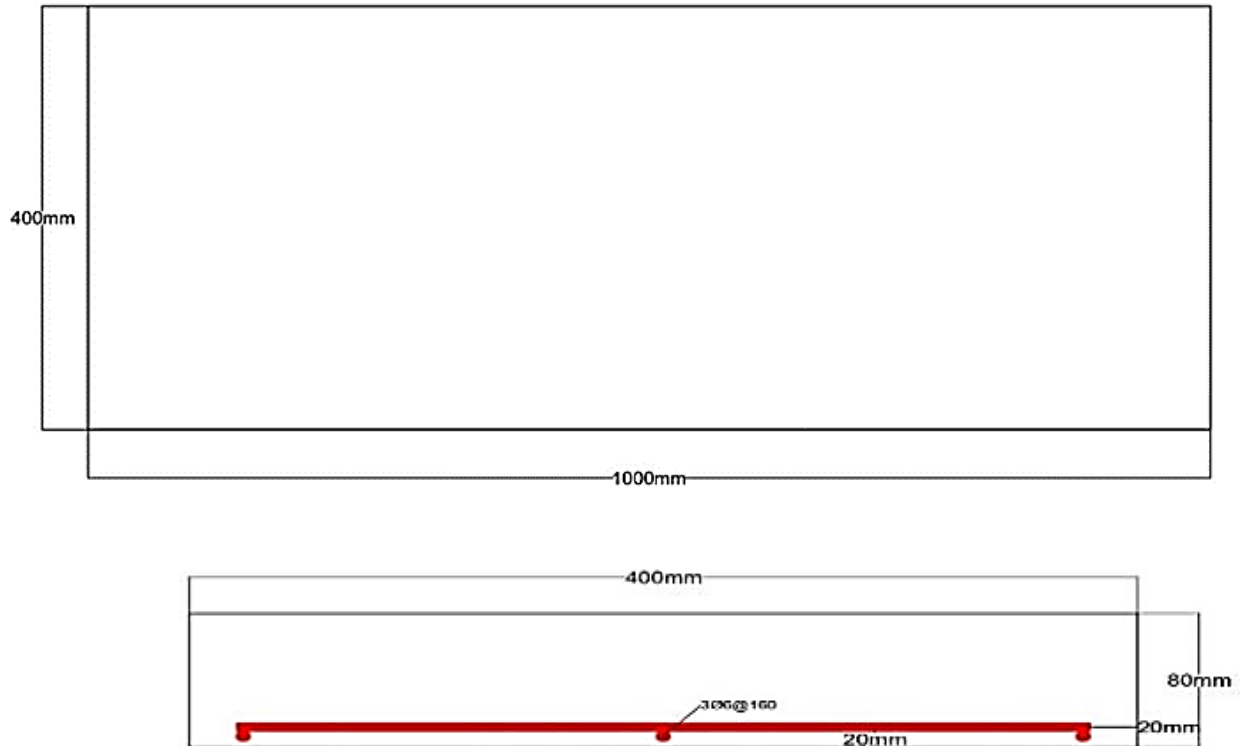


Figure 3.12: Slab Details.

### 3.9 Mould Preparation and Casting Procedure

Prior to the fabrication of moulds and casting the concrete, twenty moulds were used in this work.

### 3.10 Fabrication

The dimensions of these moulds are the same dimensions of the fabricated slabs. They were cleaned and oiled using a scraper and a steel brush to facilitate simple demoulding. The plastic moulds were first coated on the inside with oil prior to the casting process and before inserting the reinforcing steel cage. Spacers were then placed to ensure the correct positioning of the reinforcing steel cage and to maintain the desired concrete cover and diaper.

### 3.11 Process

- The concrete mixing process lasted approximately 10-12 minutes to achieve a uniform mixture.
- Using vibrators, the mixture was poured into the plastic moulds to consolidate the concrete around the cage rebar.
- Once the concrete was poured, the top surface was levelled and smoothed. Subsequently, the specimens were cured. Fig. 3.12 illustrates the preparation of the moulds, the fabrication process, and the casting procedure for the specimens.
- In the study, a 100 kg mixer was used to mix the concrete. Before inserting the reinforcement, cage, or casting control specimens, the forms and control moulds were oiled. This oiling process helps to ensure that the concrete does not stick to the forms, allowing for easy demoulding.
- To maintain the appropriate concrete cover, steel bars were placed inside the forms and securely positioned.
- These steel bars act as spacers and ensure that the reinforcement is properly embedded within the concrete at the specified depth. All ingredients of the concrete mixture, such as aggregates, cement, and water, were accurately weighed and carefully placed in a clean metal container before mixing. This process ensures the correct proportioning of the materials and helps maintain consistency in the mixture. Fig. 3.13 illustrates the casting process, which involved using plywood forms for the moulds and steel forms.
- The plywood forms were used to shape the main body of the concrete specimens, while steel forms may have been employed for specific areas or features requiring additional support or reinforcement.

- After the concrete was mixed and cast into the forms, the forms were left in place for 24 hours to allow the concrete to set. Subsequently, the forms were removed, and the specimens were immersed in water for a curing period of 28 days. Immersion in water is a common method of curing concrete, as it helps maintain proper moisture levels and promotes the development of strength and durability.
- Additionally, samples were taken from the cast concrete and poured into concrete cubes and cylinders. These samples were used to estimate the concrete properties, such as compressive strength, which is a fundamental characteristic for assessing the quality and performance of the concrete.
- For Group No. (1), the temperature sensor was put inside the model before the casting process started and during the distribution of the reinforcing steel. There were two versions linked: one to the bottom surface and the other to the reinforcing steel. The second sensor, a thermocouple, was connected to the first. The sensor has a head that can sense heat and is connected to the portion whose temperature has to be monitored. It also has a glass cable that can't catch fire and is connected to a device that sends and converts data to a computer so that the temperature may be recorded during the combustion time.



Figure 3.13: Fabrication, Moulds, and Casting of the Specimens for Group 1.



Figure 3.14 : Fabrication, Moulds, and Casting of the Specimens for Group 2.

### 3.12 Burning Methods and Fire Exposure

#### 3.12 .A Thermal and Loading Test of Specimens in Accordance with ASTM -E119 and ISO834(Group 1).

In this phase of the research, fire and load tests were conducted on reinforced concrete slab specimens to investigate their behavior under high temperatures and subsequent mechanical loading. The experiments were carried out using specialized test facilities designed according to ISO 834 and ASTM-E119 standards to simulate realistic fire conditions.

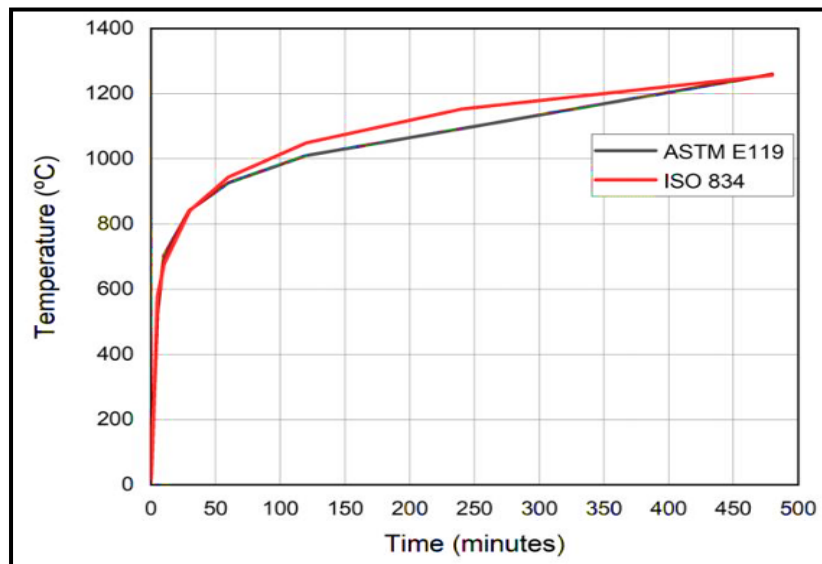


Figure 3.15: curve of ISO-834.

- The specimens were placed inside furnaces constructed from insulating refractory bricks, fireproof materials, and fiberglass layers, equipped with gas burners or nozzles to ensure uniform heat distribution show Figure 3.15 .



Figure 3.16: Firebricks for the oven, laser thermometer, and gas supply for the burners inside the oven.

- Steel frames and concrete bases supported the furnaces shown in figure 3.16, while protective roofs and insulation safeguarded the measurement and control equipment throughout the testing process.



Figure 3.17: The outer iron structure of the furnace

- Reinforced concrete slabs of dimensions (2250\*1000\*100) mm were prepared with embedded thermocouples to record internal temperatures continuously during the heating period. Prior to fire exposure, each specimen was gradually loaded up to its service load to replicate realistic in-service structural conditions. Once the service load was stabilized, the furnaces were ignited, following the standard fire temperature curve.
- For some tests, the top surface of the slabs was insulated with ceramic wool to maintain uniform heat distribution and minimize heat loss to the surroundings. The specimens were exposed to combined thermal and mechanical loading for 120 minutes, allowing continuous monitoring of temperature development, mid-span deflection, and structural response.
- Temperature measurements were recorded using infrared thermometers or thermocouples connected to multi-channel data loggers and dedicated computers for real-time monitoring and

automatic data storage. Simultaneously, LVDT at mid-span captured deformations and deflections, while hydraulic loading systems recorded applied loads continuously. This setup allowed synchronized measurement of thermal and mechanical responses throughout the heating and loading stages shows Fig. 3.17& Fig. 3.18.

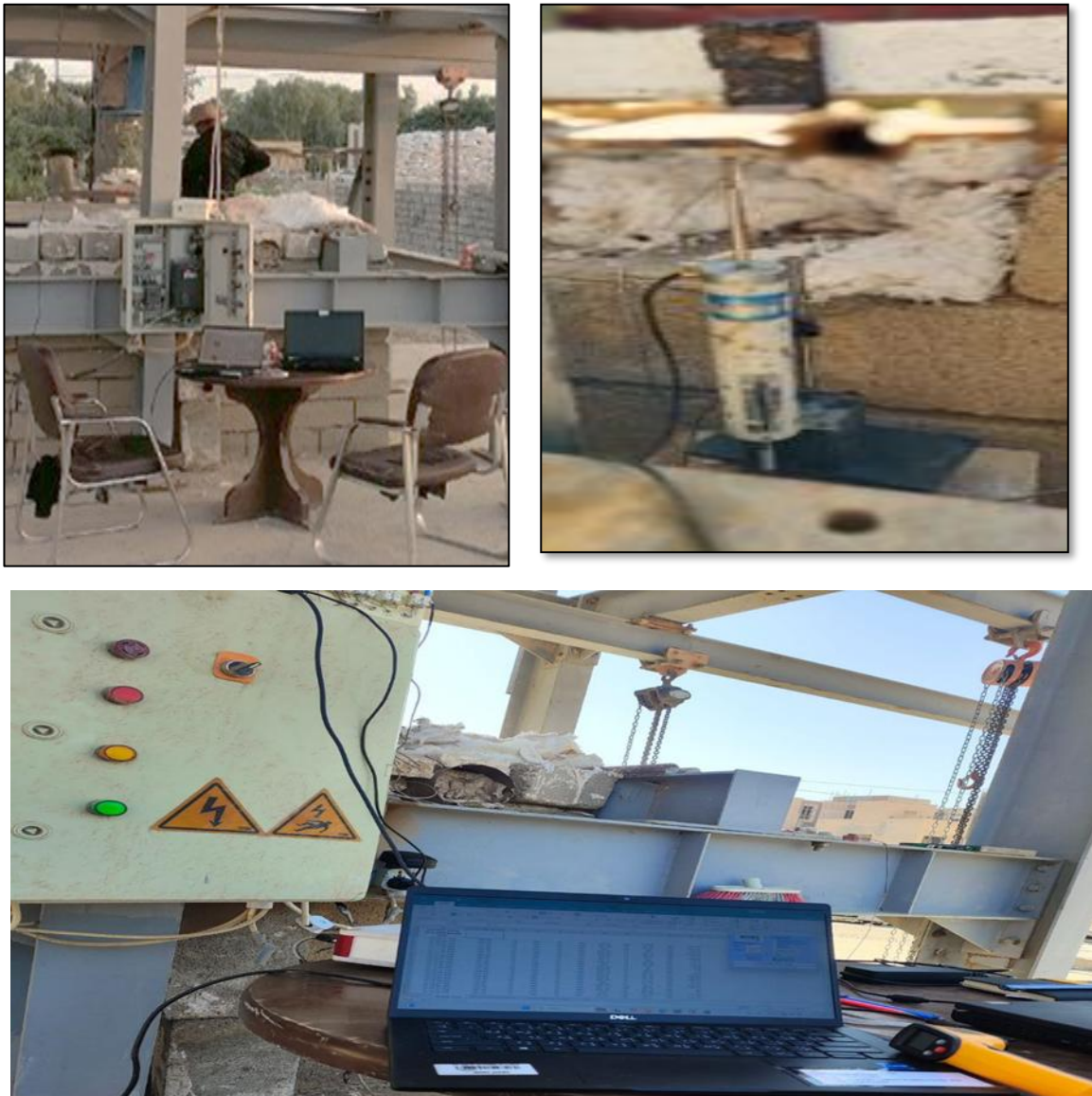
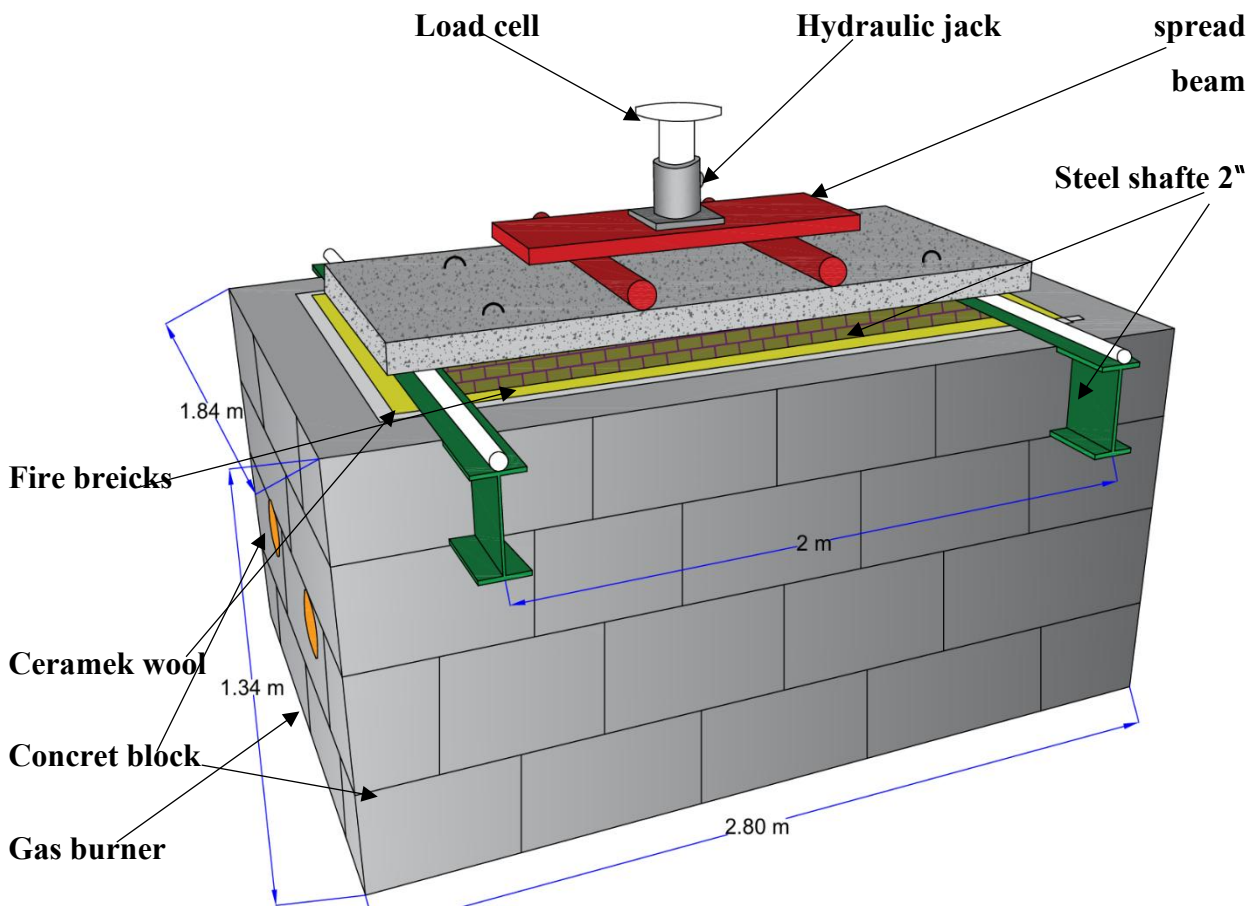


Figure 3.18: Computer and the device LVDT

- After completing the fire exposure, specimens were allowed to cool naturally in air to prevent thermal shock. once cooled to

safe temperatures, the slabs were transferred to hydraulic loading platforms, and central loading cylinders gradually applied increasing loads while the slab ends were supported on rigid steel supports simulating simple support conditions. Loading continued from service load up to the ultimate failure load in some tests to evaluate the residual strength and post-fire mechanical performance. Throughout the procedure, the development of cracks, deformations, and reductions in stiffness, compressive strength, and flexural capacity were carefully observed. The continuous and synchronized recording of all parameters provided a comprehensive evaluation of the reinforced concrete slabs' behavior under realistic fire and loading conditions.



(A) First Series Testing at University of Tikrit .



Figure 3.19: Testing and burning process.



Figure 3.20: Testing Process.

### 3.13. B Direct Flame Exposure Method

- The direct flame exposure test was conducted at the University of Misan using a simple furnace with internal dimensions of  $(1500 \times 2500 \times 1000)$  mm.
- The furnace was equipped with three gas-fired burners that served as the primary heat sources, providing direct and concentrated thermal exposure to the specimens. After igniting the burners, the temperature inside the furnace was gradually

increased until it reached the target level specified in the experimental program, either 300°C or 400°C. Once the desired temperature was achieved and stabilized, the exposure time was initiated.



Figure 3. 21:a-Gaseous Heat Source b-Laser Thermometer

- specimens were placed inside the furnace during each test cycle, positioned to ensure direct contact with the flame emitted from the three burners. The samples were subjected to continuous heating for a fixed duration of 75 minutes, while the temperature and flame stability were monitored to maintain consistent thermal conditions throughout the exposure period.
- At the end of the designated time, the specimens were left inside the closed furnace to cool gradually under natural cooling conditions before being removed.
- This procedure was repeated for all remaining samples until the entire burning sequence was completed, shows Fig. 3.21-3.22 .

- loading of the specimens was carried out after the completion of the fire exposure, during which the slabs were subjected to direct flame.



Figure 3.22 : Second Series Testing at University of Misan.

- The specimens were loaded using the hydraulic testing system illustrated in the following figure. A total load of 10,000 kg was gradually applied to the slabs until reaching their ultimate failure load. During the loading process, vertical deflection was carefully monitored using a mechanically installed LVDT. This device was positioned at the mid-span of each slab to accurately capture the deformation under the applied load shows Fig.3-23 and 3-24.
- The recorded deflection data allowed for a precise assessment of the slabs' structural performance following fire exposure



Figure 3.23: A Clip Illustrating the Loading and Mechanical LVDT Device.



Figure 3.24: Sample Inspection Device.

## CHAPTER FOUR: RESULTS AND DISCUSSIONS

### 4.1 Introduction.

This chapter talks about the results of an experiment that looked at reinforced concrete slabs made with one-way lightweight concrete and regular concrete. The main purpose of this effort is to find out how slabs act structurally when they are subjected to very high temperatures and stresses, up to the point of failure. A variety of comparisons were made to see how different elements, such as combustion temperature, concrete type (regular concrete and lightweight concrete), and heat exposure method (ASTM-E119, direct flame method), affected the results of this investigation.

### 4.2 Study of the Properties of Concrete Under the Influence of High Temperature Using the First Method

This methodology included studying the results of reinforced concrete slabs under the influence of different degradation temperatures according to American specifications and standards (ASTM-E119 and ISO-834). This method included studying the characteristics of ten specimens. The following variables were considered (Ambient-400-800) C°, the percentage of reinforcing steel ratio, and the type of concrete (normal concrete and lightweight concrete).

#### 4.2.1 Changes in Temperature During the Burning Stage Under Service Load.

As part of the thermal testing program for reinforced concrete slabs, the temperature variation with time was recorded during the burning stage while each specimen was subjected to its designated service load. The temperature was measured at four critical points representing the main zones of heat transfer within the slab: the unexposed top surface, chamber, the reinforcement bar at mid-depth, and the exposed bottom surface opposite to the fire. This monitoring

aimed to accurately capture the heat distribution and transfer through the specimen during fire exposure, providing a clearer understanding of the thermal and structural response of the concrete under simultaneous thermal and service load conditions Fig. 4.1 .

The service load can be roughly represented as a percentage of the ultimate load, which shows the loads that are not factored in that are acting on the structure when it is working normally. It usually falls between 50% of the ultimate load, depending on the type of loading and the load factors used in design [58].

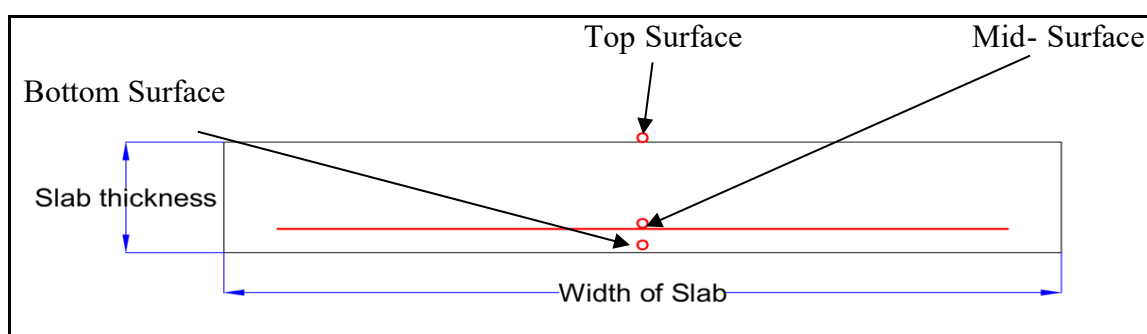


Figure 4.1 The Temperature Distribution on a Sample Slab Level.

From Fig. 4.2 illustrate the temperature distribution during the combustion phase at four points for the loaded concrete fired slabs. Figure indicates a slight fluctuation in the chamber temperature depending on the air currents on the test day. When the temperature in the combustion chamber was  $400^{\circ}\text{C}$ , the core (mid-depth) temperature of the slab specimen **SN2Ap-400** reached  $190^{\circ}\text{C}$ , as shown in the Fig. 4.2, the temperature distribution on a sample slab of normal reinforced concrete.

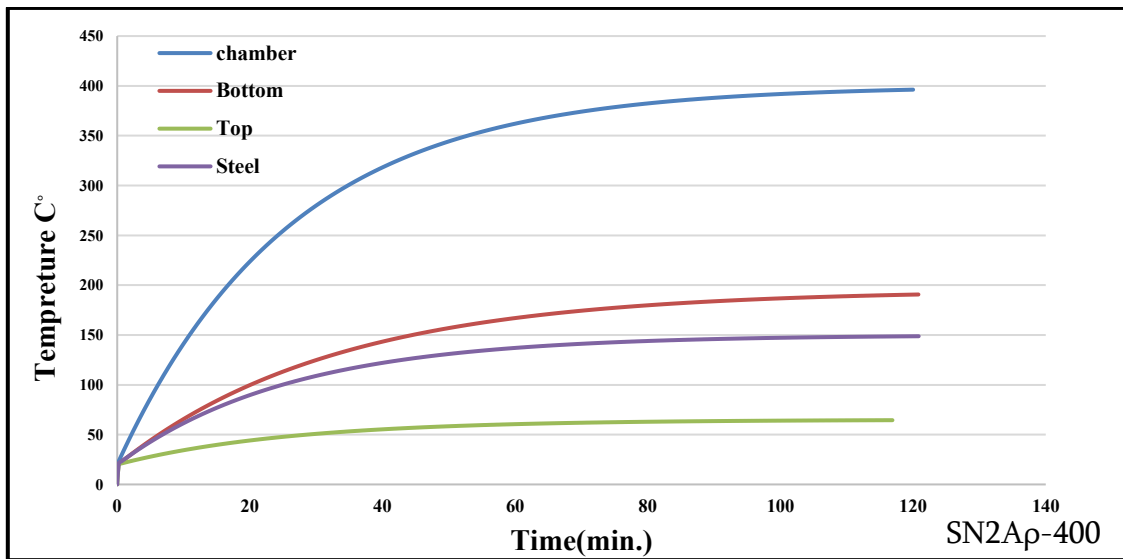


Figure 4.2 The Temperature Distribution on a Sample Slab of normal Reinforced Concrete.

Fig. 4.3 and Fig. 4.4 for specimens **SN3Ap-800** and **SN5Ap-800** illustrate the temperature distribution during the combustion phase at three points for the loaded concrete fired slabs. The temperature measurement of 800°C through the model using Thermocouples gave the impression of uniform heat transfer through normal concrete.

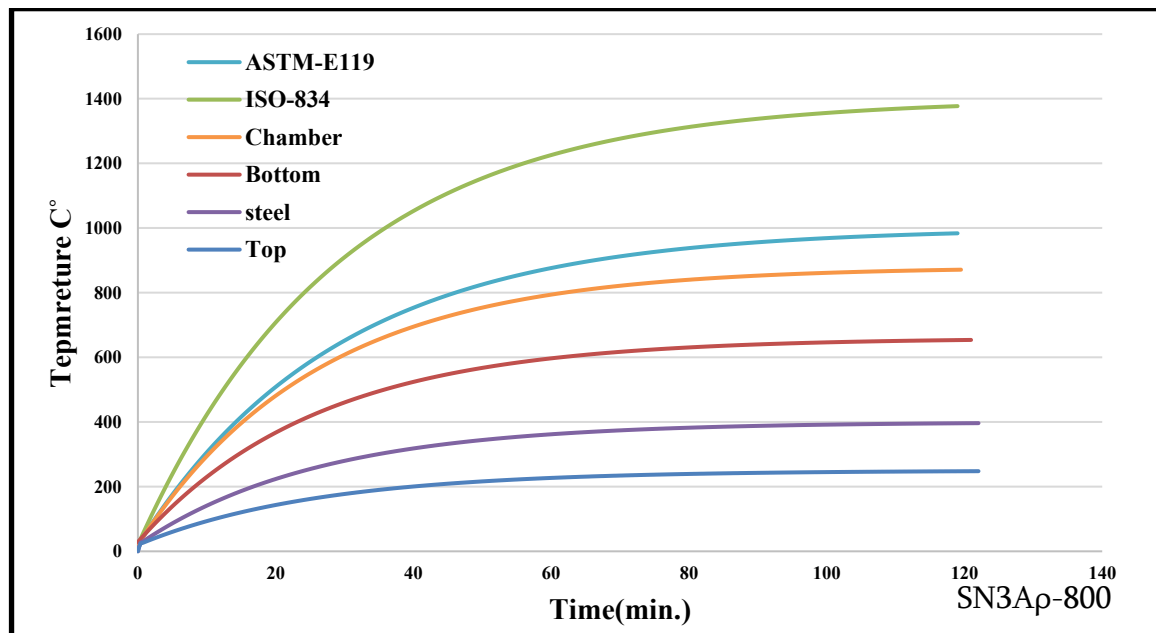


Figure 4.3 The Temperature Distribution on a Sample Slab (SNAp-800) of normal Reinforced Concrete.

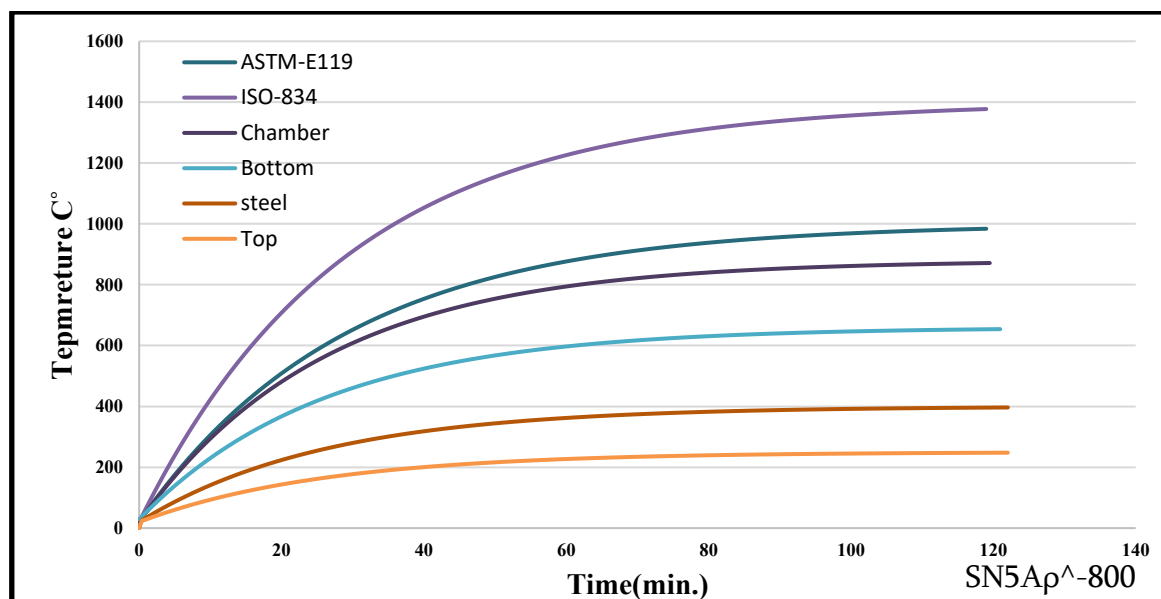


Figure 4.4 The Temperature Distribution on a Sample Slab (SN5Ap<sup>800</sup>) of normal Reinforced Concrete

From Fig. 4.5 and 4.6, at 400C° the temperature on the lower surface for the sample **SL2Ap-400** reached 200C°, while the temperature in the lightweight concrete samples was about 200 C° for the surface of the foam, while the temperature of the reinforcing steel was 110 C°, while the temperature of the upper surface far from the fire was 66 C°. This indicates that heat transfer is uneven throughout the section of the lightweight concrete, shows Fig. 4.5. While the slab **SL4Ap<sup>400</sup>** that was exposed to the same temperature of 400 °C was affected by heat transfer, but only slightly shows Fig. 4-6.

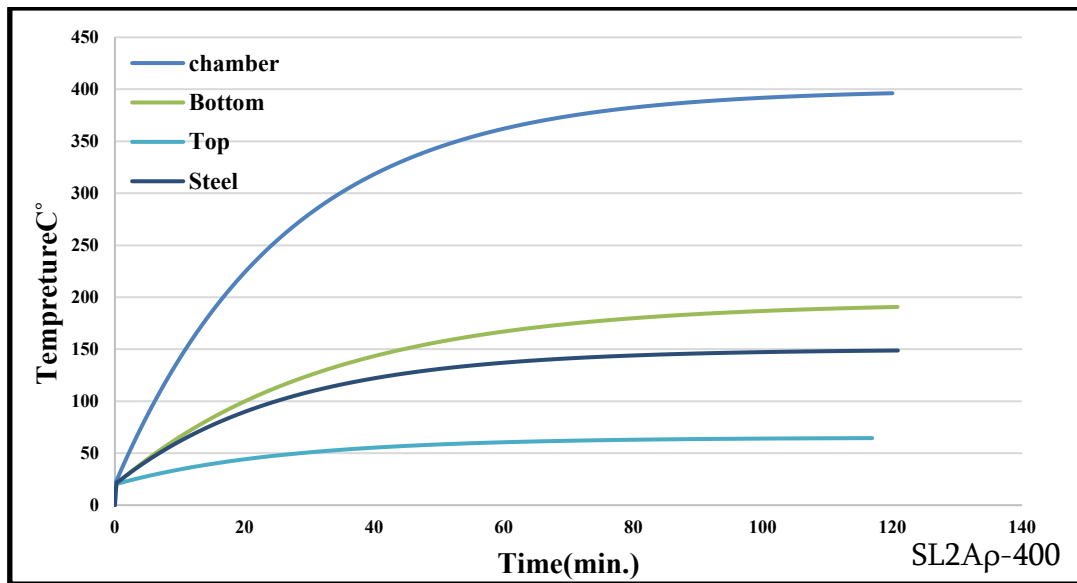


Figure 4.5 The Temperature Distribution on a Sample Slab (SL2Ap-400) of lightweight Reinforced Concrete.

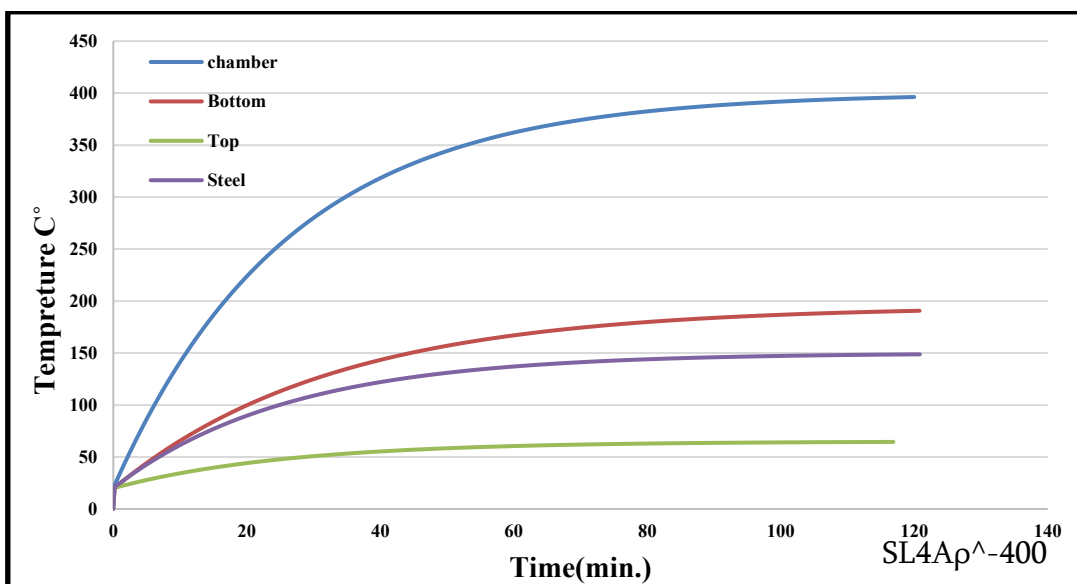


Figure 4.6 The Temperature Distribution on a Sample Slab (SLAp-400) of lightweight Reinforced Concrete.

During the combustion phase under loading at a furnace temperature of 800°C, the lightweight concrete slab( **SL3Ap-800**) recorded a bottom surface temperature directly exposed to fire of approximately 514°C, while the top surface, located away from the fire, remained significantly lower at only 60°C. This considerable thermal gradient indicates limited heat transfer through the slab

thickness despite the high furnace temperature, in comparison, the second specimen with a higher steel reinforcement ratio  $SL5A\rho^{-800}$ , subjected to the same temperature of  $800^{\circ}\text{C}$ , showed only a slight increase in the bottom surface temperature. This suggests that the denser reinforcement contributed to delaying heat propagation toward the internal core of the slab, thereby enhancing its thermal resistance under elevated temperatures, show Fig. 4-7 and 4-8.

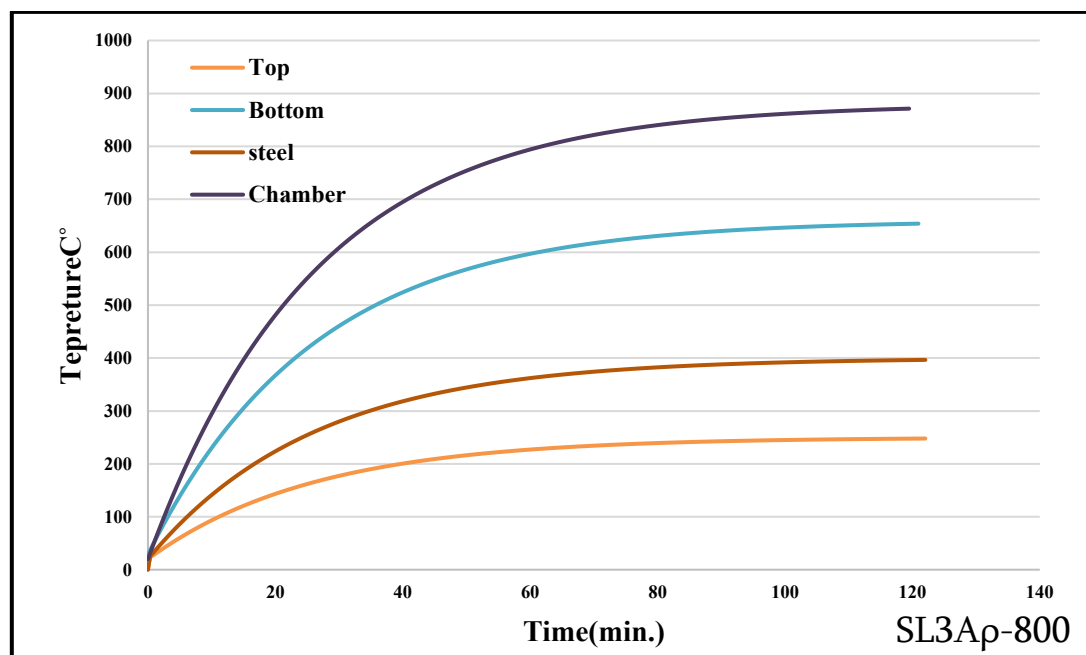


Figure 4.7 The Temperature Distribution on a Sample Slab ( $SL3A\rho-800$ ) of lightweight Reinforced Concrete.

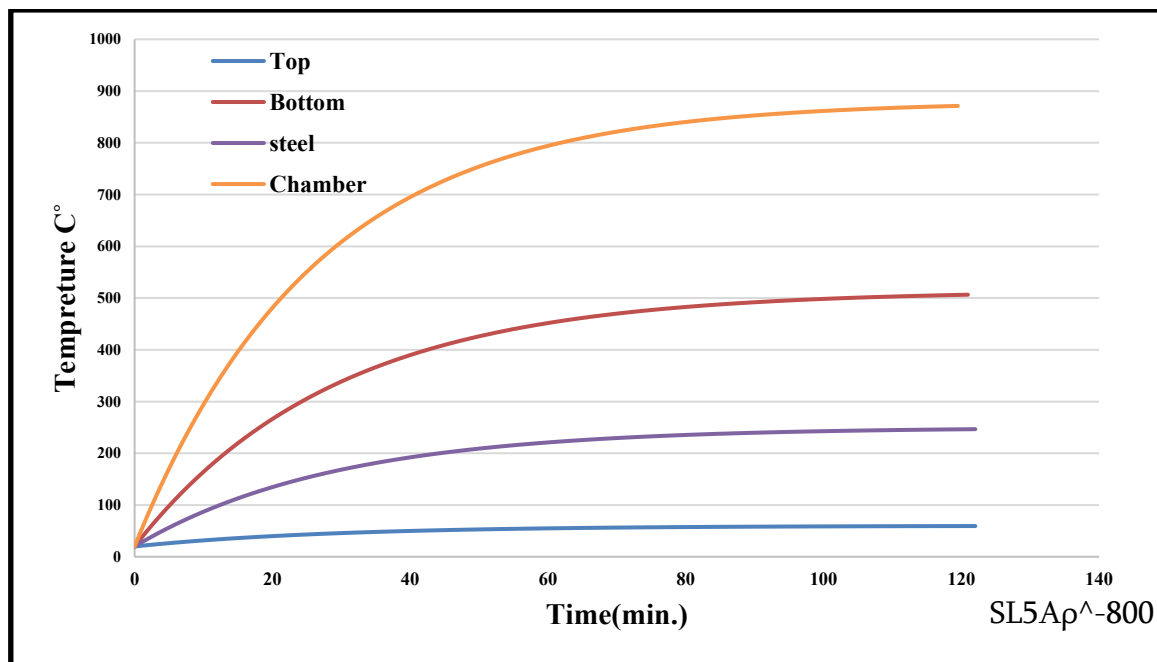


Figure 4.8 The Temperature Distribution on a Sample Slab (SL5Ap<sup>800</sup>) of lightweight Reinforced Concrete.

#### 4.2.2 Fire Load Test Results

Tested under concentrated fire load, two load lines were applied at the third center of the specimen using a hydraulic jack. The load was gradually increased until it reached 50% of the maximum load. The results are discussed in main sections, according to concrete type, to determine the behavior and performance of one-way slabs under high temperature conditions are:

A- Load Capacity and Failure Mode.

B-Load And Deflection Behavior.

D- Load Versus Steel Ratio.

E-Ductility.

F-Stiffness.

G- Flexural Toughness.

#### 4.2.2.1 Load Capacity and Failure Mode

All concrete slab specimens were loaded up to their service load while being exposed to elevated temperatures in order to simulate the combined effects of mechanical and thermal stresses. During this stage, the first visible cracks appeared on the bottom surface of the slabs, indicating the onset of interaction between thermal degradation and applied loading.

Following the firing phase, the specimens were allowed to cool gradually to ambient temperature and were then reloaded until failure. During the reloading stage, a distinct main failure crack developed at the mid-span of the slab, accompanied by a limited number of fine secondary cracks branching from it. The majority of these cracks were concentrated within the middle third of the slab span, where flexural moments reach their maximum and shear stresses are minimal. This crack distribution confirms that the failure mechanism was predominantly governed by flexural action. The experimental program comprised ten slab specimens divided into two main groups based on concrete type: normal-weight concrete and lightweight aggregate concrete. Within each group, the specimens were further categorized according to thermal exposure conditions and reinforcement ratio, as described below.

Reference specimens, one slab made of normal-weight concrete **SN1Ap-25** and one slab made of lightweight aggregate concrete **SL1Ap-25** were tested to failure without exposure to elevated temperatures. Both specimens exhibited a conventional flexural failure mode characterized by the initiation and gradual widening of flexural cracks at mid-span. Failure was accompanied by limited concrete crushing in the compression zone, with no significant spalling observed. Specimens exposed to 400°C, **SN2Ap-400**, **SL2Ap-400** this group included two specimens for each concrete type: one with conventional reinforcement and the other with dense reinforcement corresponding to a reinforcement ratio of 2%. Thermal exposure at 400°C resulted in a noticeable reduction in load-carrying

capacity compared to the reference specimens, along with accelerated crack development. specimens with dense reinforcement **SN4A $\rho$ <sup>-400</sup>**, **SL4A $\rho$ <sup>-400</sup>** demonstrated improved structural performance, including delayed crack propagation and higher residual load capacity, highlighting the beneficial role of increased reinforcement in mitigating thermal damage. Nevertheless, partial spalling of the bottom concrete cover was observed due to the deterioration of the bond between the cement paste and aggregate after heating.

Specimens subjected to 800°C **SN3A $\rho$ -800**, **SN5A $\rho$ <sup>-800</sup>**, **SL3A $\rho$ -800**, **SL5A $\rho$ <sup>-800</sup>** represented the most severe thermal condition and exhibited a substantial degradation in mechanical properties and ultimate load capacity. Failure in these specimens was characterized by a relatively brittle flexural mode accompanied by pronounced spalling of the concrete cover, particularly in the tensile zone. Although dense reinforcement contributed to an improvement in post-fire residual behavior, the detrimental effect of the high temperature was dominant, and flexural failure could not be prevented. Overall, all tested slabs regardless of concrete type, reinforcement ratio, or thermal exposure failed primarily in flexure. However, lightweight aggregate concrete slabs consistently exhibited wider cracks and lower ultimate loads than their normal-weight concrete counterparts. This behavior can be attributed to the high internal porosity and weaker interfacial bonding of lightweight aggregate particles, which facilitated crack propagation through the aggregate itself rather than around it, as commonly observed in normal-weight concrete, as illustrated in Fig. 4.9.

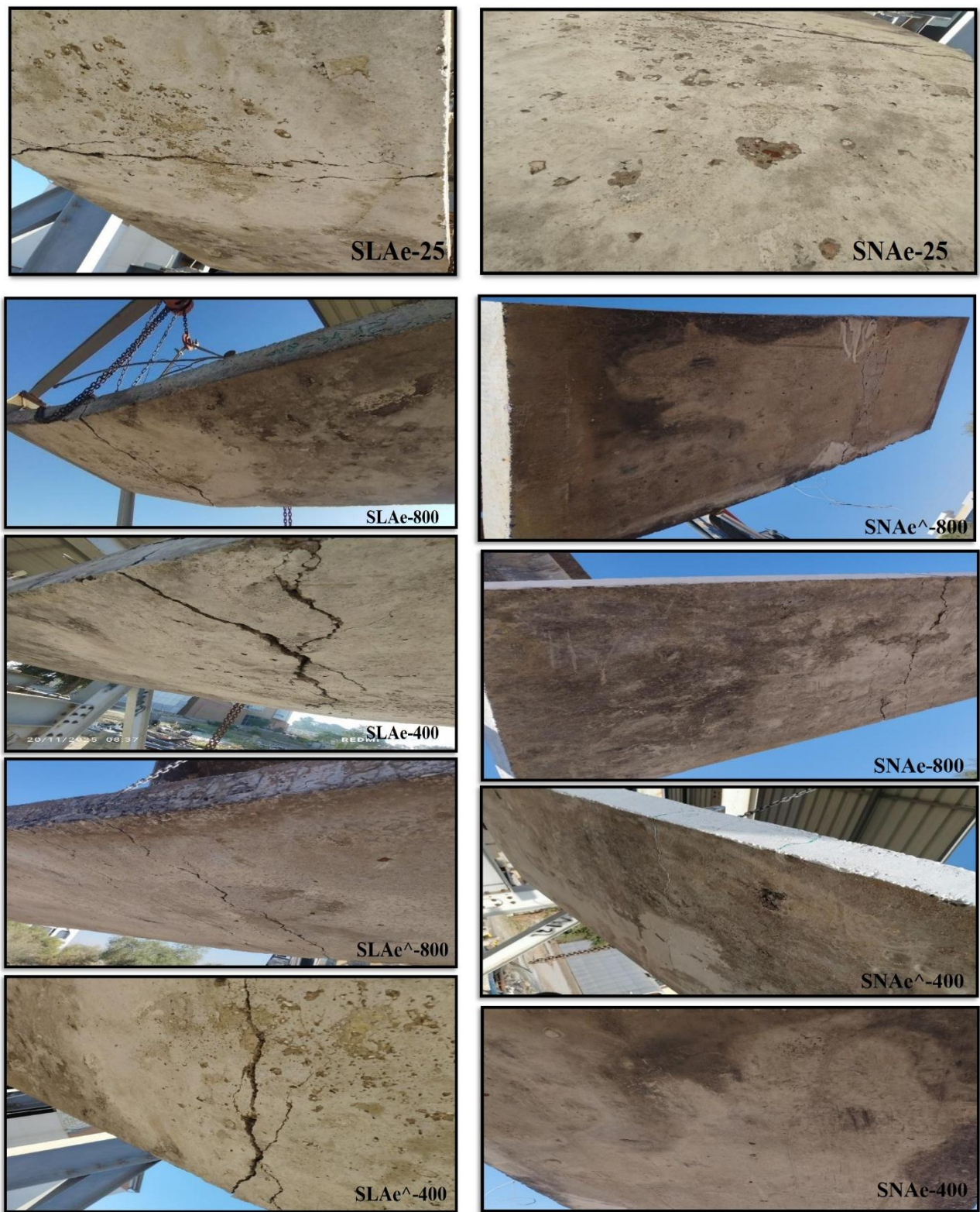


Figure 4-9 Models After Burning, Loading, and Failure Status.

#### 4.2.2.2 Load and Deflection Behavior

The vertical center to center deflection of all slab specimens was measured during fire exposure at each increment of the applied load. Fig. 4.10 illustrates the load deflection relationships for lightweight aggregate concrete slabs, while Fig. 4.11 presents the corresponding behavior for normal-weight concrete slabs. The failure load was defined as the maximum load recorded during testing, as summarized in Table 4-1, whereas the service load was taken as approximately 50% of the ultimate load. The lightweight aggregate concrete reference specimen **SL1Ap-25** exhibited relatively flexible behavior, with a service load of 23 kN and a corresponding deflection of 10.2 mm, while the ultimate load reached 46 kN with an ultimate deflection of 32.2 mm. As shown in Figure 4.10, this specimen exhibited lower stiffness compared to normal-weight concrete slabs. In contrast, the normal-weight concrete reference specimen **SN1Ap-25** sustained a higher service load of 26 kN with a smaller deflection of 9.5 mm, and an ultimate load of 52 kN with an ultimate deflection of 31 mm, as illustrated in Fig. 4.11. This behavior reflects the higher stiffness and load-carrying capacity of normal-weight concrete under ambient conditions. For lightweight aggregate concrete slabs, specimen **SL2Ap-400** exhibited a reduction in service load to 19.15 kN and an increase in service-load deflection to 10.6 mm, corresponding to a 3.7% increase relative to the reference specimen. The ultimate load decreased to 38.3 kN, accompanied by a slight increase in ultimate deflection of 2.1%. The load deflection curve in Fig. 4.10 shows an earlier deviation from linear behavior, indicating stiffness degradation due to thermal exposure. For normal-weight concrete, specimen **SN2Ap-400** showed a service load of 24.15 kN with a deflection of 10.4 mm, representing an 8.6% increase compared to the reference specimen. The ultimate load was reduced to 48.3 kN, while the ultimate deflection increased slightly by 3.1%. As illustrated in Fig. 4.11, normal-weight concrete slabs retained a greater portion of their stiffness compared to lightweight slabs at the

same temperature level. Lightweight aggregate concrete specimens exposed to 800°C, particularly **SL3Ap-800**, exhibited pronounced deterioration in structural behavior. The service load dropped to 12.5 kN, while the service-load deflection increased to 11.2 mm, representing an 8.9% increase. The ultimate load decreased significantly to 25.01 kN, with an ultimate deflection of 32.8 mm. Figure 4.10 clearly demonstrates a substantial reduction in curve slope, indicating severe stiffness loss. Conversely, the normal-weight concrete specimen **SN3Ap-800** exhibited a service load of 20.5 kN with a 7.7% increase in deflection, while the ultimate load decreased to 41.01 kN. The ultimate deflection increased by 21% compared to the reference specimen. Although notable degradation occurred, Fig. 4.11 indicates superior performance relative to lightweight concrete under the same thermal condition. For lightweight aggregate concrete specimens with dense reinforcement exposed to 400°C, such as **SL4Ap-400**, the increase in service-load deflection was limited to 2.8%, with only minor changes in ultimate deflection. This behavior highlights the beneficial role of increased reinforcement in controlling deformations, as evidenced by the load–deflection curves in Fig. 4.10. Similarly, normal-weight concrete specimens with dense reinforcement, including **SN4Ap-400**, exhibited smaller increases in deflection compared to specimens with conventional reinforcement, as shown in Fig. 4.11. At 800°C, dense reinforcement in specimens **SL5Ap-800** and **SN5Ap-800** contributed to improved deflection control; however, significant reductions in load capacity were still observed due to the severity of thermal damage. Overall, the load–deflection curves in Fig. 4.10 & 4.11 exhibit an initial linear response followed by nonlinear behavior after cracking initiation. Lightweight aggregate concrete slabs consistently displayed larger deflections and reduced curve slopes compared to normal-weight concrete slabs, indicating lower stiffness and higher sensitivity to thermal exposure.

The increase in deflection at service load remained relatively limited and did not exceed approximately 10% for all specimens, whereas the effect of temperature was more pronounced at ultimate load levels, particularly at 800°C. Dense reinforcement was effective in enhancing residual stiffness and limiting deformation, especially under moderate thermal exposure

**Table 4-1: Deflections of Specimens at Service and Ultimate Load.**

Specimens	Service Load PS (kN)	Deflection at service Load (mm)	% Increase in Deflection at service Load	Ultimate Load PU (kN)	Ultimate Deflection (mm)	% Increase in Deflection at the Ultimate Load of Reference Specimen
SN1A $\rho$ -25	26	9.5	Reference	52	31	Reference
SN2A $\rho$ -400	24.15	10.4	8.6	48.3	32	3.1
SN3A $\rho$ -800	20.5	10.3	7.7	41.01	32.3	21
SN4A $\rho$ -400	24.15	10.1	5.9	48.3	31.8	7
SN5A $\rho$ -800	20.3	10.2	6.8	40.6	32.1	21
SL1A $\rho$ -25	23	10.2	Reference	46	32.2	Reference
SL2A $\rho$ -400	19.15	10.6	3.7	38.3	32.9	2.1
SL3A $\rho$ -800	12.5	11.2	8.9	25.01	32.8	1.8
SL4A $\rho$ -400	19.5	10.5	2.8	39	32.4	0.6
SL5A $\rho$ -800	13.5	11.1	8.1	27.03	32.6	1.2

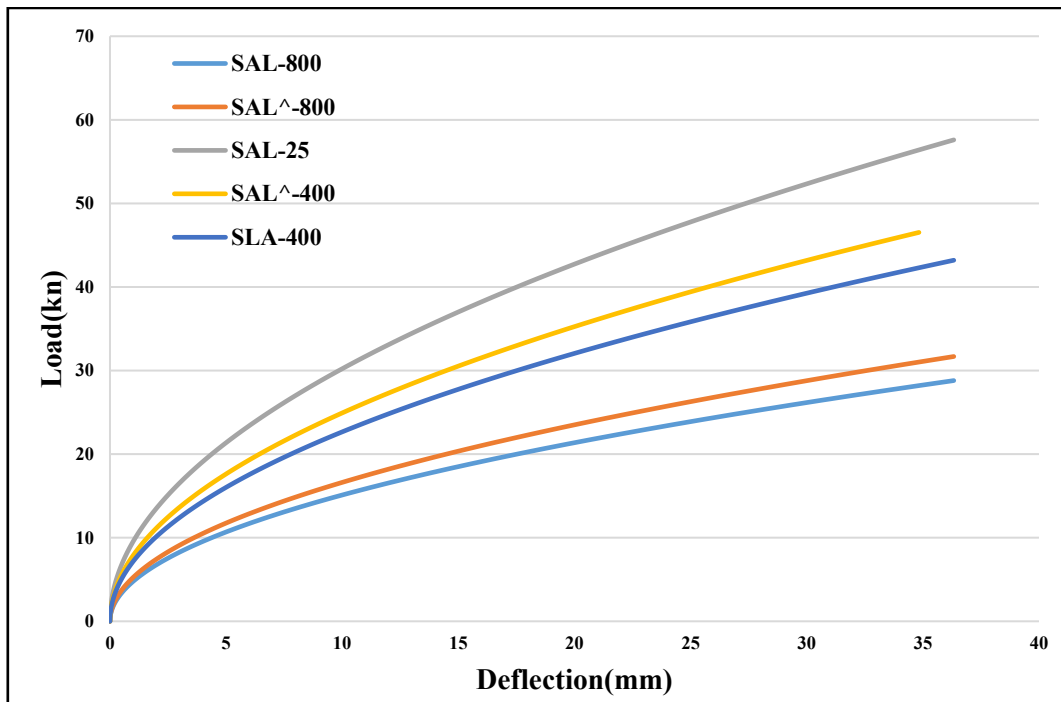


Figure 4.10 Load Deflection Curve for Lightweight Specimens.

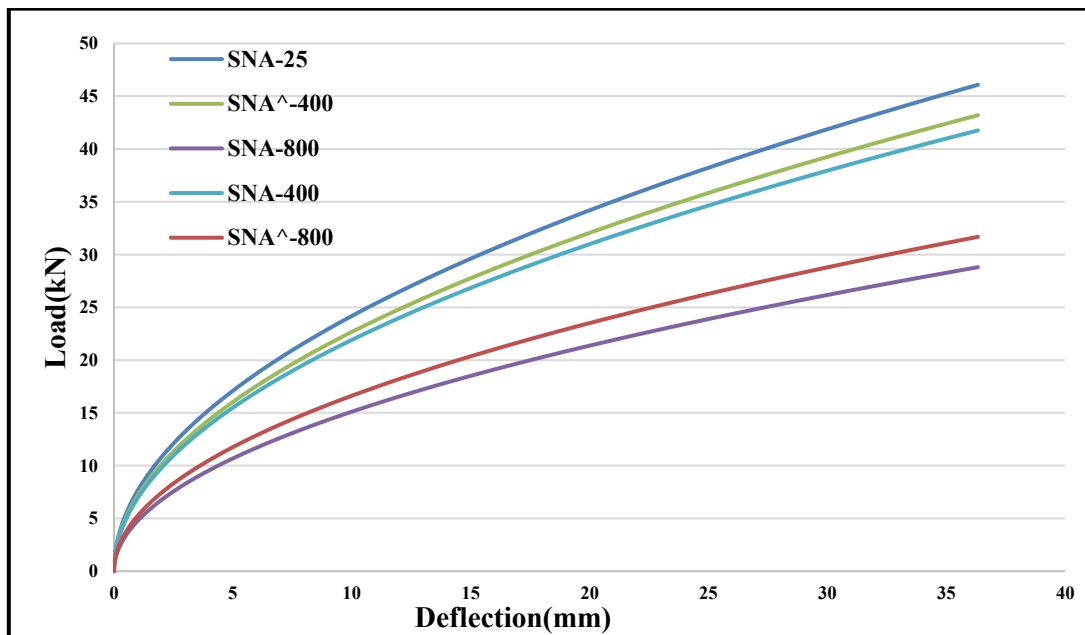


Figure 4.11 Load Deflection Curve for Normal Concrete Specimens.

Table 4.2 Percentage Decreasing in Ultimate Load.

Type concrete	Specimens	Service Load Ps (Kn)	%Decrease In Service Load	Ultimate Load Pu (Kn)	%Decrease In Ultimate Load
Normal	SN1A $\rho$ -25	26	Reference	52	Reference
	SN2A $\rho$ -400	24.15	7.1	48.3	7.1
	SN3A $\rho$ -800	20.5	21	40.6	21
	SN4A $\rho^{\wedge}$ -400	24.15	7.1	48.7	7.3
	SN5A $\rho^{\wedge}$ -800	20.3	21.9	41	21.9
Light Wight	SL1A $\rho$ -25	24	Reference	46	Reference
	SL2A $\rho$ -400	19.15	20	38.3	16.7
	SL3A $\rho$ -800	12.5	47	25	45
	SL4A $\rho^{\wedge}$ -400	19.5	18.7	39	15.2
	SL5A $\rho^{\wedge}$ -800	13.5	43	27	41

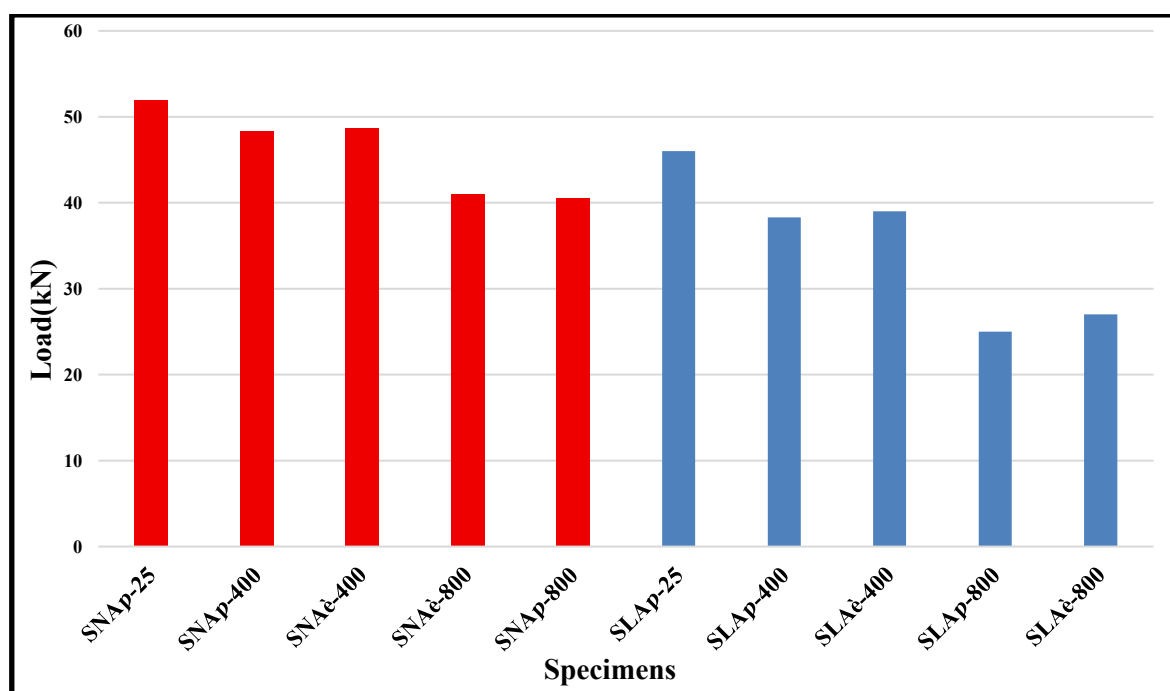


Figure 4.12 Different patterns and Load Conditions Resulting from Heat.

### 4.2.2.3 Load Versus Steel Ratio

The effect of reinforcement ratios on the ultimate load and deflection of reinforced concrete slabs after exposure to high temperatures was investigated, including both normal-weight and lightweight aggregate concrete, in comparison with reference specimens not exposed to heat. Reinforcement was designed according to code requirements with additional steel provided for shrinkage and thermal effects to ensure slab safety under elevated temperatures. For the reference specimens, **SN1Ap-25** for normal-weight concrete achieved an ultimate load of 52 kN with an ultimate deflection of 31 mm, while **SL1Ap-25** for lightweight concrete recorded an ultimate load of 46 kN with a deflection of 32.2 mm. These values serve as the baseline for evaluating the effects of thermal exposure and reinforcement variations. At 400°C, slabs with conventional reinforcement showed a limited reduction in ultimate load with **SN2Ap-400** and **SL2Ap-400** experiencing decreases of 7.1% and 16.7%, respectively, and minor increases in ultimate deflection of 3.1% and 2.1%. This indicates that conventional reinforcement is capable of maintaining most of the slab stiffness under moderate thermal exposure. Slabs with dense reinforcement, **SN4Ap-400** and **SL4Ap-400**, exhibited similar reductions in ultimate load of 7.1% and 15.2% with minimal increases in deflection of 2.5% and 0.6%, demonstrating that increased reinforcement within code limits enhances slab stiffness, improves crack distribution, and limits deformation under moderate heat. At 800°C, normal-weight concrete slabs, **SN3Ap-800** and **SN5Ap-800**, experienced significant reductions in ultimate load of 21–21.9% with minor increases in ultimate deflection of 3.4–4%. Lightweight aggregate concrete slabs, **SL3Ap-800** and **SL5Ap-800**, exhibited larger reductions of 41–45% while maintaining relatively stable ultimate deflection at 1.2–1.8%. These results indicate that high temperatures have a greater impact on lightweight concrete due to higher porosity and weaker bonding between aggregate and paste. Dense reinforcement in **SN5Ap-800** and **SL5Ap-800**

helped control deformations and prevented excessive deflection despite the substantial reduction in load-carrying capacity. Comparing the reinforcement cases shows that dense reinforcement reduces deflection at moderate temperatures and limits crack propagation, whereas conventional reinforcement results in slightly higher deflection and greater sensitivity to thermal effects, particularly in lightweight slabs at high temperatures. The results demonstrate that adopting reinforcement ratios in accordance with code requirements, including additional steel to accommodate shrinkage and thermal effects, significantly enhances the structural performance of slabs under elevated temperatures. This approach ensures that the reinforcement layout within the slab complies with the permissible increases specified by the code for heat and shrinkage considerations. As shown in Table 4-3, slabs with dense reinforcement exhibit improved residual behavior, maintain stiffness, and limit deformation compared to slabs with conventional reinforcement, confirming the effectiveness of this design strategy in preserving slab load-carrying capacity under high-temperature conditions.

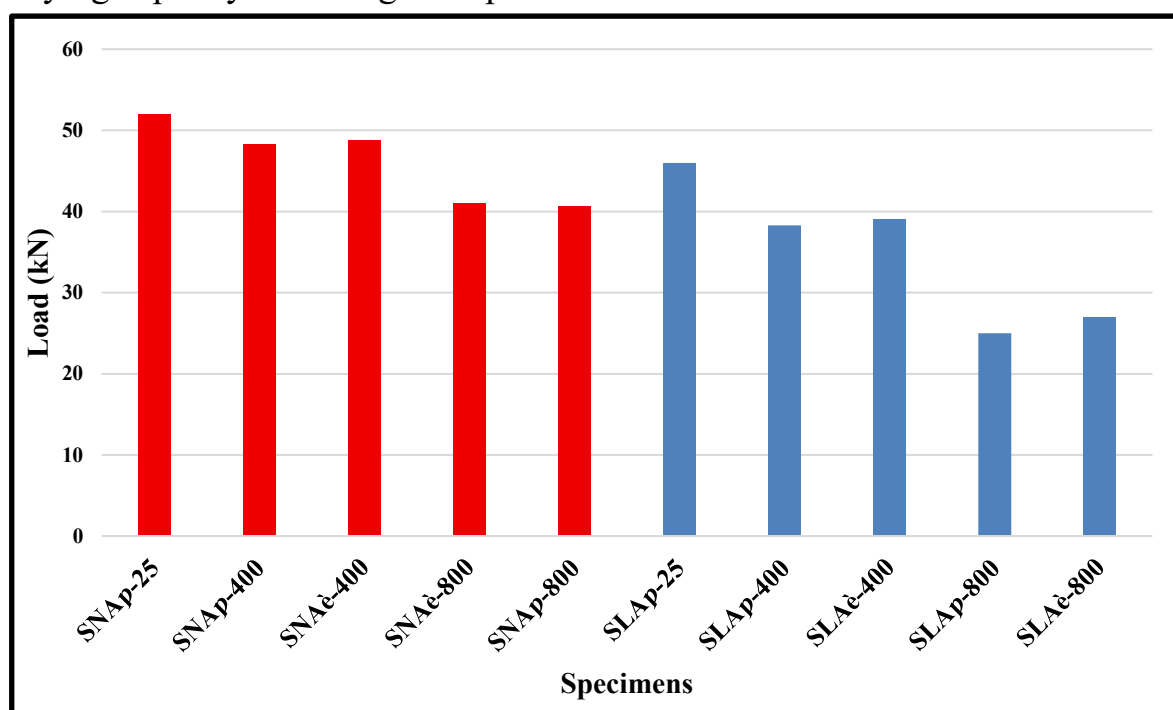


Figure 4.13 The Different Models and Load Conditions Resulting from Heat and the Ratio of Reinforcing Steel.

#### 4.2.2.4 Ductility Factor

The ductility factor, or the ratio of mid-span deflection at failure loads to the mid-span deflection at the initial yielding of tension main reinforcement bars, represents the structural member's capacity to withstand significant deformation [59]. Table 4.4 shows the ductility factors for each specimen. It is evident from Fig. 4.14 & Fig. 4.15 that the ductility factor decreases as the burning temperature rises, the results indicated that the ductility modulus diminished with rising temperature for both concrete types, with lightweight concrete demonstrating a more significant reduction than regular concrete. This is attributed to the porous nature of lightweight aggregates and their weak interfacial transition zone, making them more susceptible to thermal degradation and loss of plastic deformation capacity. Normal concrete, on the other hand, had a higher level of ductility because it had a larger aggregate density and stronger internal bonding. This meant that it could absorb more energy after curing.

**Table 4.4: Ductility Index for Specimens under load.**

Specimens	Yield Deflection (mm) ( $\Delta y$ )	Ultimate Deflection (mm) ( $\Delta u$ )	Ductility Factor ( $\Delta u / \Delta y$ )
SN1Ap-25	8.8	31	3.5
SN2Ap-400	10.1	32	3.16
SN3Ap-800	10.3	32.3	3.13
SN4Ap <sup>^</sup> -400	10	31.8	3.18
SN5Ap <sup>^</sup> -800	10.2	32.1	3.14
SL1Ap-25	10.2	32.2	3.15
SL2Ap-400	11.2	32.9	2.93
SL3Ap-800	11.7	32.8	2.8
SL4A <sup>^</sup> -400	11	32.4	2.95
SL5Ap <sup>^</sup> -800	11.5	32.6	2.83

**Note: Ductility Factor = Ultimate Deflection / Yield Deflection, Yield Deflection ( $\Delta y$ )**  
**Ultimate Deflection ( $\Delta u$ )**

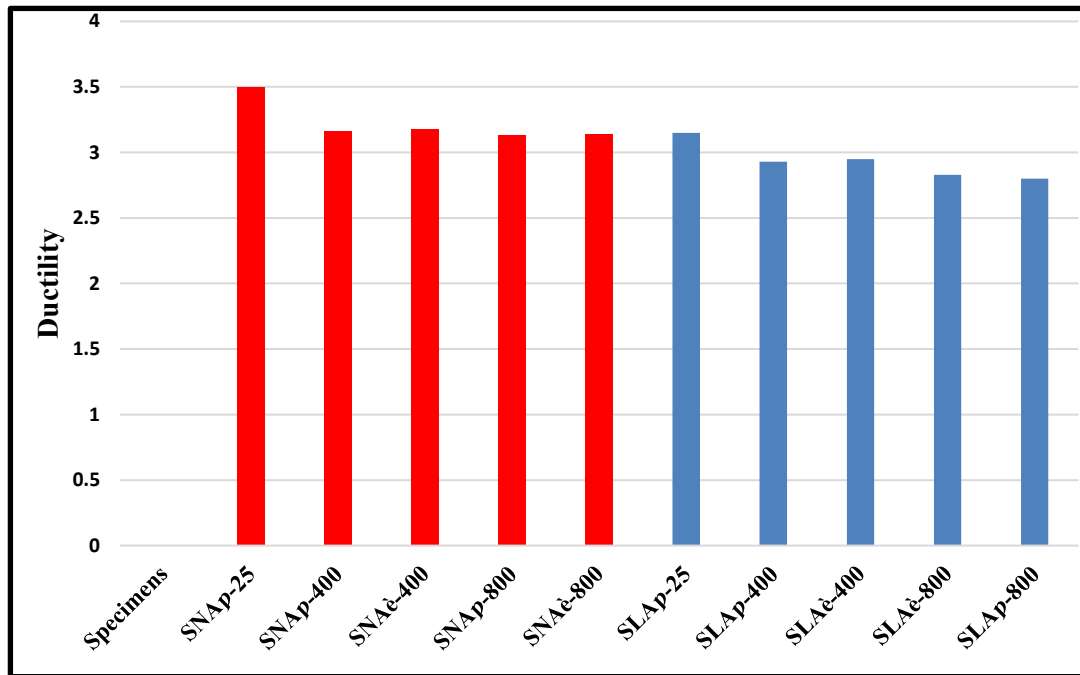


Figure 4-14 The Resulting Patterns and Ductility.

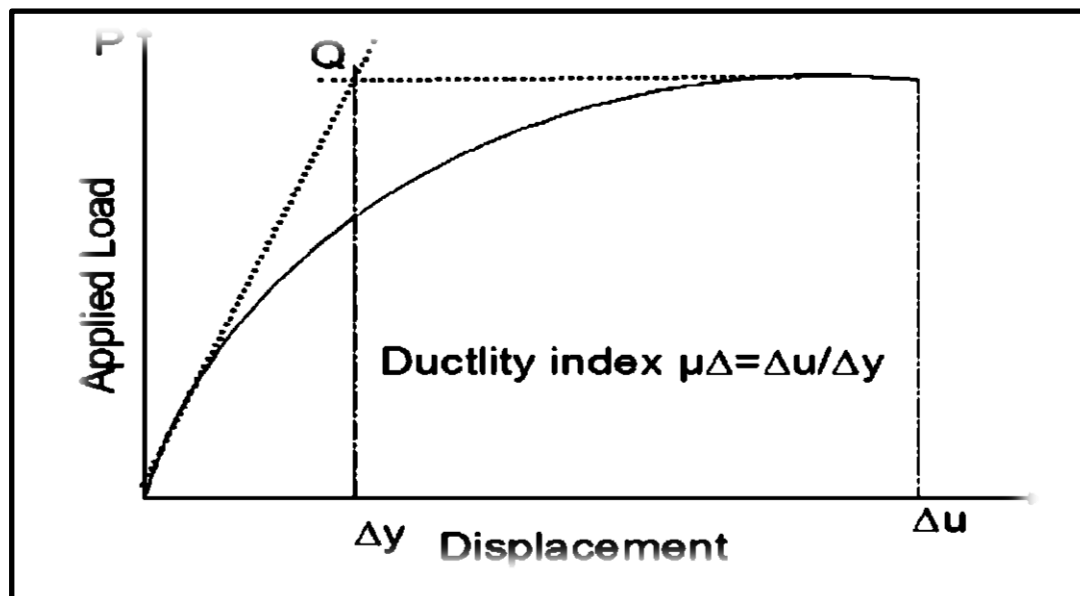


Figure 4-15: The Ductility Index.

#### 4.2.2.5 Stiffness

A body's stiffness  $K$  measures how resistant an elastic body is to. It is a function of Young's modulus  $E$ , the second moment of area  $I$  of the beam cross-section about the axis of interest, length of the beam, and beam boundary condition. The bending stiffness of a beam can analytically be derived from the equation of beam deflection when it is applied by a force [60]. See the Table 4-5 and Fig. 4.15 showing the details of the stiffness.

$$k = p/w \dots \dots \dots (4 - 1)$$

where  $p$  is the applied force and  $w$  is the deflection.

The results show that the stiffness ( $K$ ) decreased gradually with increasing temperature for all specimens due to the reduction in the modulus of elasticity and deterioration of the internal concrete structure. Normal weight concrete specimens exhibited a moderate and uniform reduction in stiffness, whereas lightweight concrete specimens showed a more pronounced decrease, particularly at 400°C, indicating higher sensitivity to elevated temperatures. Furthermore, the nearly constant or slightly reduced deflection observed in lightweight concrete at 800°C does not indicate an increase in stiffness, but rather premature failure at lower load levels, suggesting increased brittleness at higher temperatures.

**Table 4-5 Stiffness of the Specimens**

Specimens	0.7*Pu (kN)	Deflection (mm)	Stiffness K (kN/mm)
SNAp-25	36.4	31	1.17
SNAp-400	33.81	32	1.06
SNAp-800	28.707	32.3	0.89
SNAè-400	33.81	31.8	1.06
SNAè-800	28.42	32.1	0.89
SLAp-25	32.2	32.2	1.00
SLAp-400	26.81	32.9	0.81
SLAp-800	17.507	32.8	0.53
SLAè-400	27.3	32.4	0.84
SLAè-800	18.921	32.6	0.58

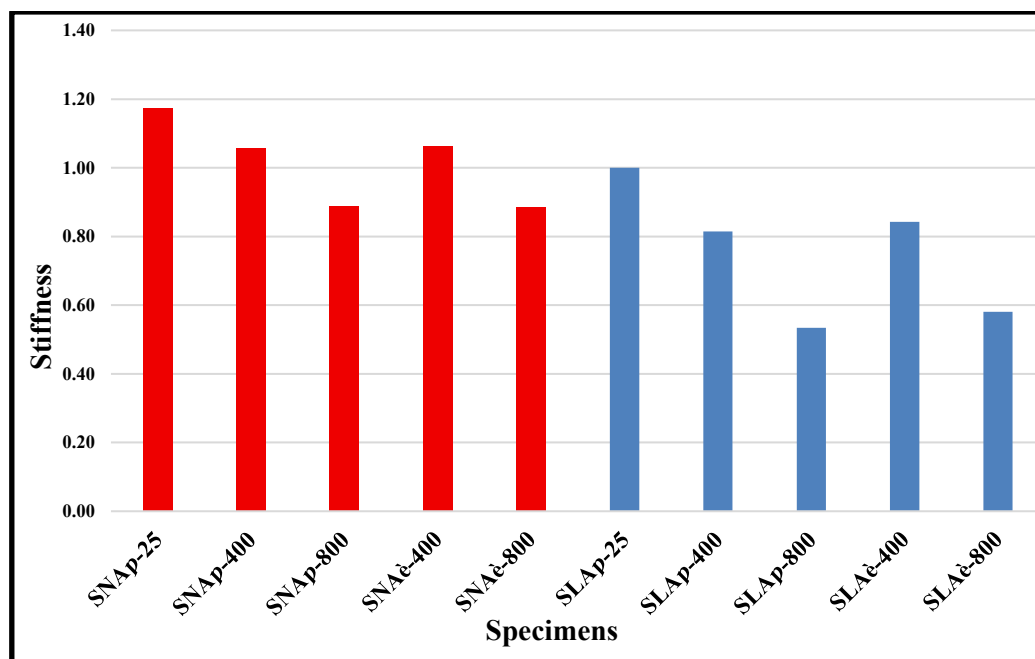


Figure 4.16 Specimen and Stiffness Resulting from Thermal Effect.

#### 4.2.2.6 Absorption Energy.

One definition of flexural strength is the ability to resist crack formation. Another interpretation is that flexural strength is a measure of a material's capacity to absorb energy [61]. The data in the Table 4-6 below represent the energy absorption of reinforced concrete slabs under high heat for both lightweight and normal concrete show Fig. 4-16.

Table (4-6) The Data in the Table Represent the Absorption Energy.

Specimens	The area under the curve (Absorption Energy) (kN.mm)	% Decrease of the Absorption Energy
SN12Ap-25	1420	Reference
SN2Ap-400	1310	7.7
SN3Ap-800	1210	14.7
SN4Ap-400	1320	7
SN5Ap-800	1250	12
SL1Ap-25	890	Reference
SL2Ap-400	805	9.5
SL3Ap-800	624	29.8
SL4Ap-400	801	10
SL5Ap-800	615	30

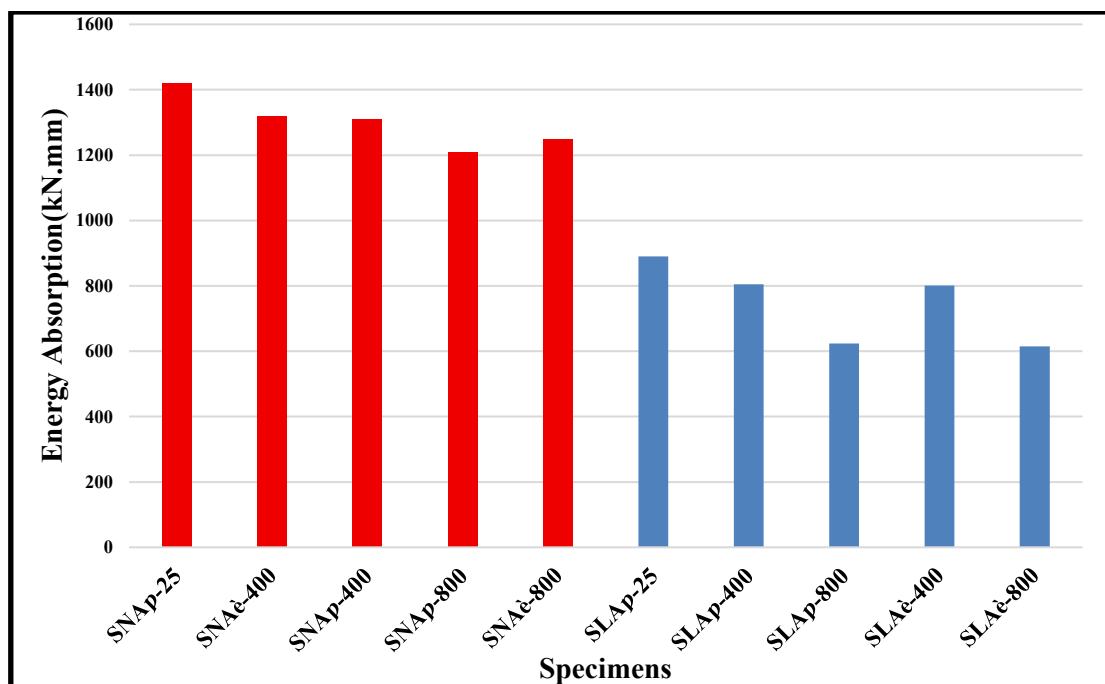


Figure 4.16 The Energy Absorption.

### 4.3 Study of the Properties of Concrete Under the Influence of High Temperature Using the second Method

This section included a study of the mechanical properties of reinforced concrete slabs under high temperatures, according to the standard of direct flame exposure for a period of 75 minutes. This methodology involved studying the properties of ten samples, taking into account the following variables: ambient temperature (25-300-400°C), the percentage of reinforcing steel, and the type of concrete (normal and lightweight).

#### 4.3.1 Changes in Temperature During the Burning Stage

As part of a thermal testing program for reinforced concrete slabs, models were exposed to direct flame under two temperature conditions (300°C-400°C). This procedure was designed to simulate real-world fire conditions in order to evaluate the thermal and structural behavior of the slabs under direct flame exposure. During the burning phase, temperature changes over time were continuously recorded to track heat transfer

across three main zones representing the heat transfer pathway in the model: the furnace zone combustion chamber, representing the fire environment, the lower surface of the slab directly exposed to the flame, and the upper surface of the slab on the side not exposed to the flame. This division helped to clarify the temperature difference across the depth of the slab and determine the rate of heat transfer from the exposed surface to the core of the section and then to the lower, unexposed surface. Fig. 4.17 and 4.18 and 4.19 ,4.20 illustrate the pattern of temperature change with slab depth during the heating period, showing the clear difference between the upper and lower surfaces.

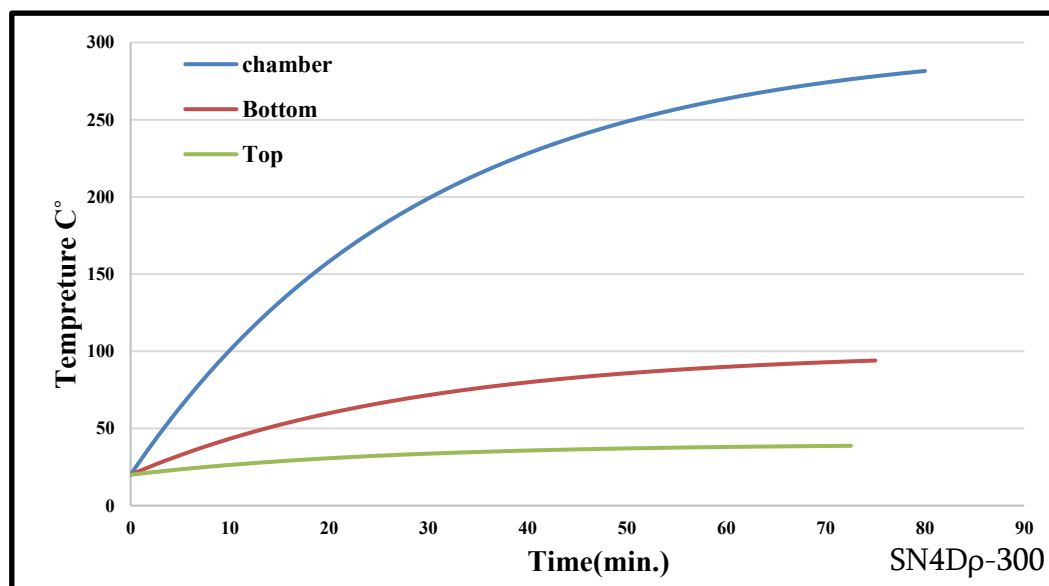


Figure 4-17 Show the Temperature Distribution at SN4Dp- 300C°.

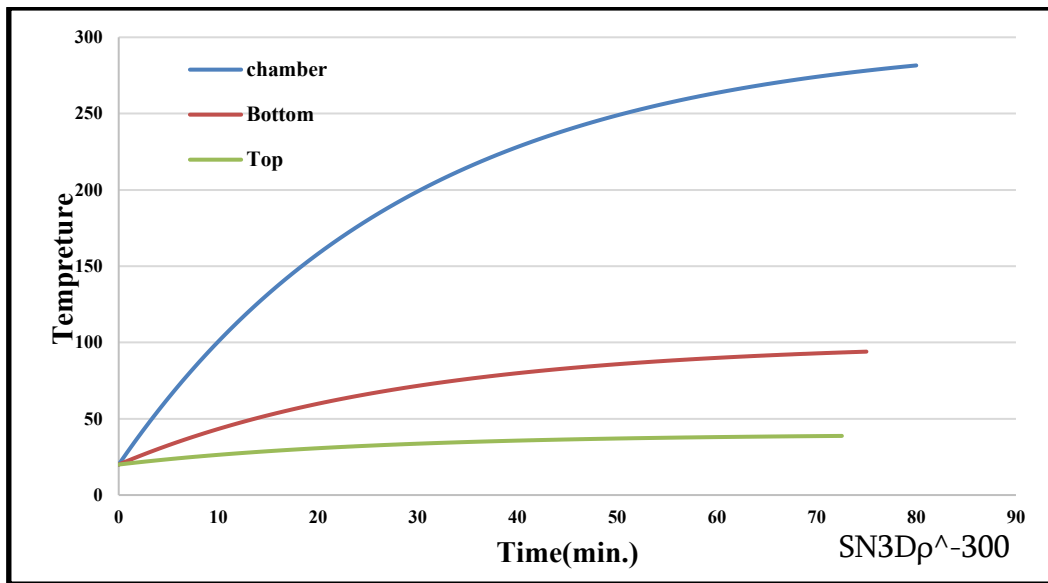


Figure 4-18 show the temperature distribution at SN3Dρ<sup>-300</sup>°C.

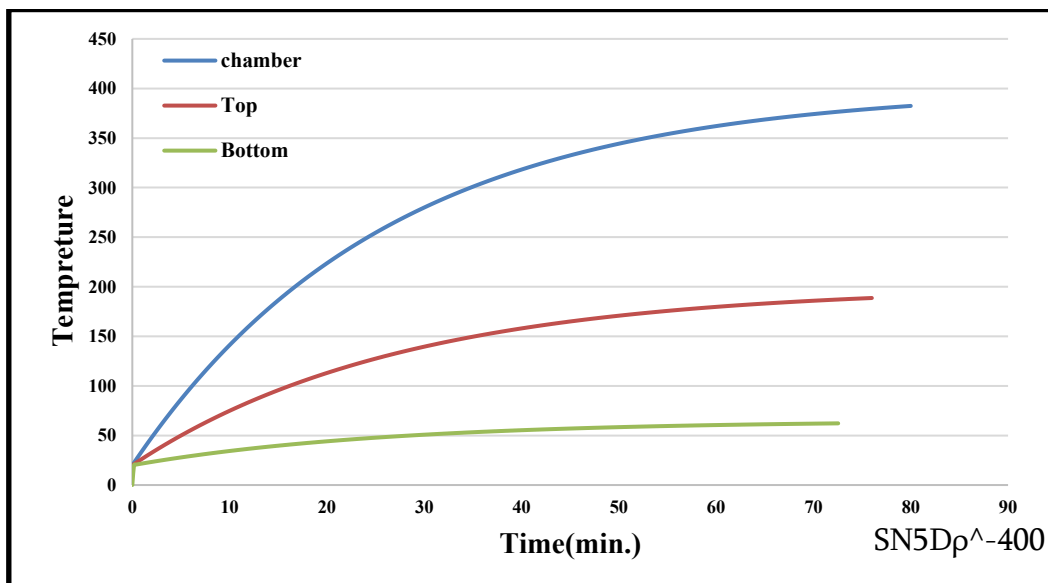


Figure 4-19 Show the Temperature Distribution at SN5Dρ<sup>-400</sup>°C.

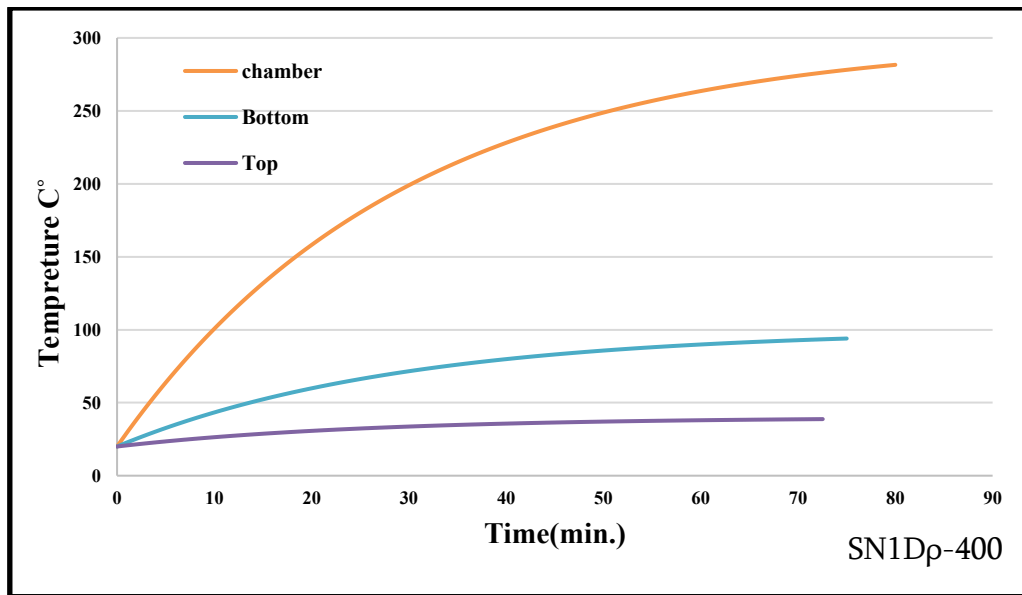


Figure 4-20 Show the Temperature Distribution at 400C°.

At the higher exposure of lightweight\_models, as shown in Fig. 4-21 and 4-22 and 4-23. a more pronounced thermal increase was recorded in all three regions. The top surface temperature approached the furnace temperature. The top surface remained at relatively low temperatures, confirming the insulating capacity of the concrete.

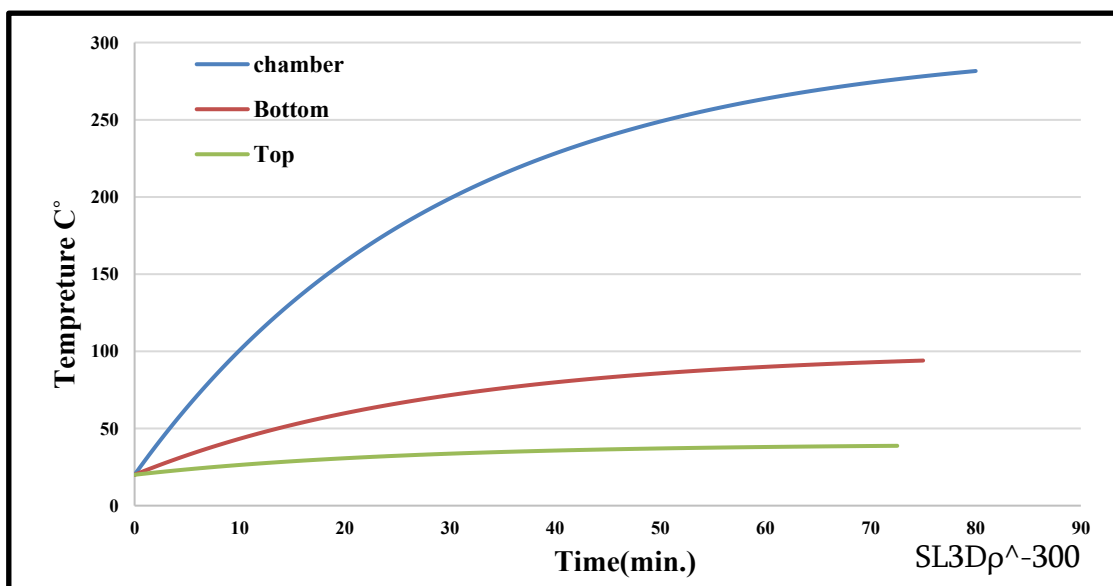


Figure 4-21 Show the Temperature Distribution at SL3Dp^300C°.

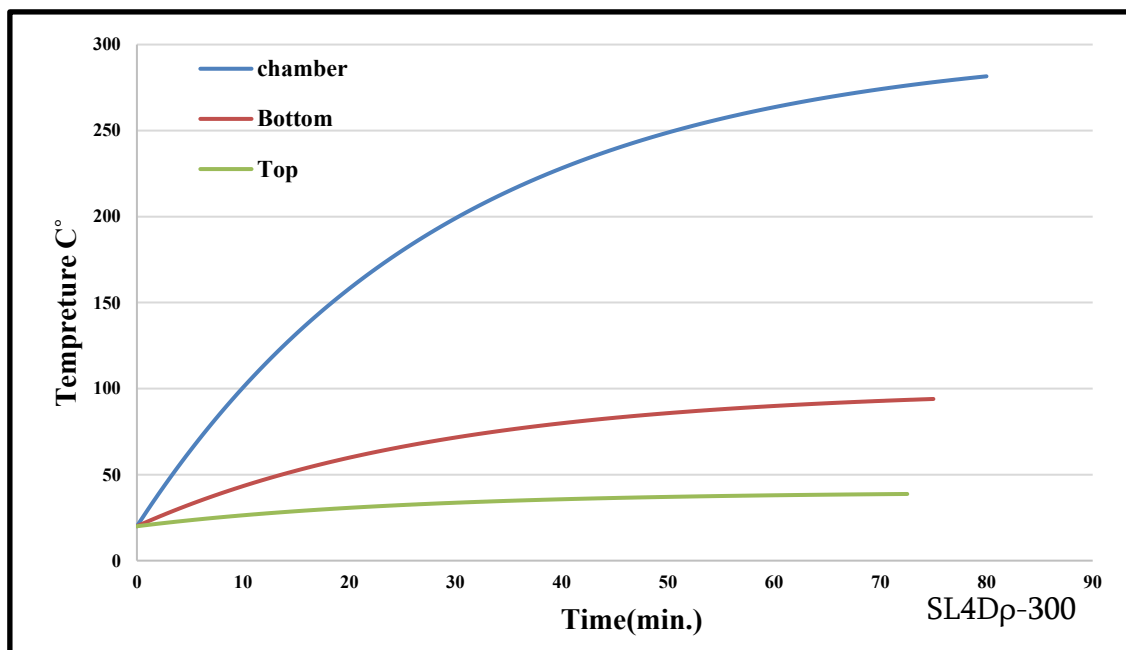


Figure 4-22 show the temperature distribution at SL4Dp-300C°.

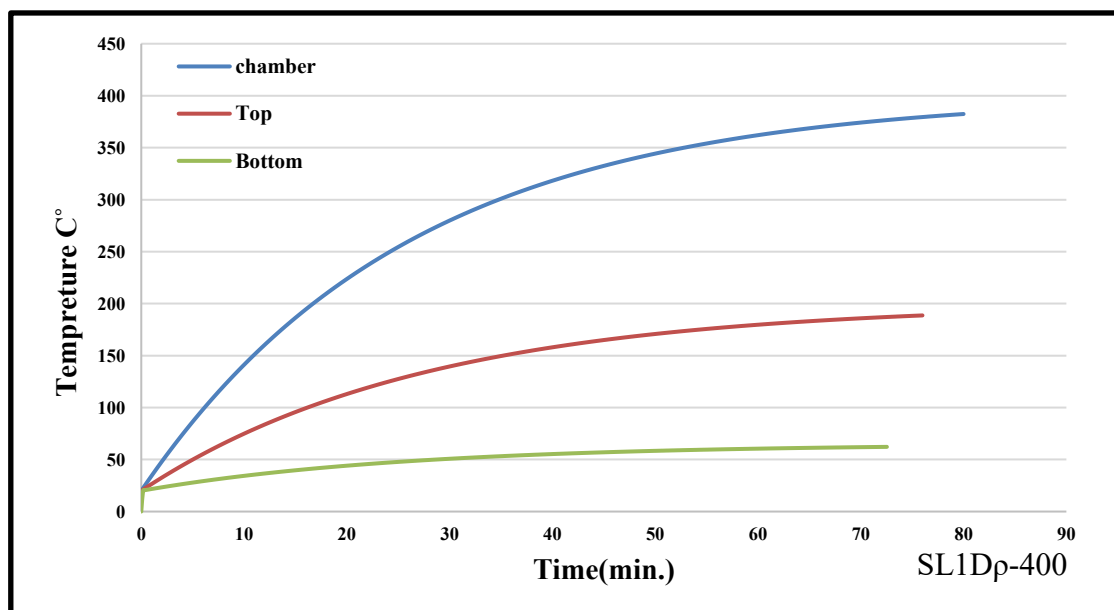


Figure 4-23 Show the Temperature Distribution at SL1Dp-400C°.

### 4.3.2 Post Fire Behavior

Specimens here were tested under a centrally concentrated load after being exposed to a direct flame, with a linear load placed in the third center of the specimen using a hydraulic jack. The results are discussed in several main sections according to the variables used: ambient temperature, ( $25^{\circ}\text{C}$ - $300^{\circ}\text{C}$ - $400^{\circ}\text{C}$ ), reinforcing steel ratio, and concrete type. The aim of this research is to determine the behavior and performance of one-way slabs at high temperatures:

A-Load Capacity and Failure Mode.

B-Load and Deflection Behavior.

D-Load-to-Steel Ratio.

E-Ductility.

F-Stiffness.

G-Flexural Strength.

#### 4.3.2.1 Load Capacity and Failure Mode.

The first set consists of five samples made exclusively from reinforced concrete slabs using normal concrete. These samples were prepared under standard conditions and to uniform dimensions to ensure the accuracy and reliability of the results. The main objective of this set is to establish a baseline for comparison and provide a reference for evaluating the mechanical response and failure behavior of normal concrete slabs under loading conditions applied with direct exposure to high temperatures. This group includes one control sample, and the other samples were recorded at ambient temperatures ( $25^{\circ}\text{C}$ - $400^{\circ}\text{C}$ - $300^{\circ}\text{C}$ ).

The applied load at the onset of the observed service response in the tensile zone of the tested slab is defined as the service load. Table 4.7 summarizes the experimental values for service and failure loads, experimental observations showed that the service load, visually recorded during testing, occurred at different load levels among the samples. The Decrease in service Load and ultimate load ratio

ranged from 26% to 46% indicating that the temperature increase resulting from fire exposure had only a minor effect on this ratio, despite the significant decrease in both individual loads (PS and Pu). These results suggest that increasing the temperature Exposure to high temperatures leads to a gradual deterioration in both the service and ultimate loads due to the loss of bond between the cement paste and the reinforcing steel, as well as a decrease in the mechanical strength of the concrete with increasing temperature.

**Table 4-7 Percentage Decrease in Ultimate Load.**

Specimens	Service Load (Ps) (kN)	Ultimate Load (Pu) (kN)	% Decrease in service Load concerning Reference	% Decrease in Ultimate Load concerning Reference
SN2DC $\rho$ -25	7.25	18.5	Reference	Reference
SN4DC $\rho$ -300	5.4	10.8	25	41.6
SN3D $\rho^{\wedge}$ -300	6	12	17	35
SN5D $\rho^{\wedge}$ -400	4.75	9.5	34	62
SN1D $\rho$ -400	4.4	8.8	39	52

Figures 4-24 illustrate the failure patterns of (SN3D $\rho$ -300) and (SN4DC $\rho$ -300) specimens, which were tested under 300°C. Both slabs exhibited a predominantly flexural failure pattern, characterized by the formation of a large vertical crack in the mid-span region extending from the tension face upwards towards the compression zone. The cracks gradually widened with increasing applied load until concrete crushing occurred in the upper compression zone, indicating the final failure stage.

Fig. 4-24 illustrate the failure patterns of SN1D $\rho^{\wedge}$ -400 and SN5D $\rho^{\wedge}$ -400 specimens. Minor secondary cracks appeared near the path of the main crack, indicating a gradual deterioration in stiffness and stress redistribution within the tension zone with increasing load. The absence of diagonal cracks near the supports confirmed that shear effects were minimal and that both specimens failed purely flexurally. Therefore, the overall failure pattern can be classified as flexural crush

failure, where reinforcement yielding was followed by concrete crushing at the compression face. The second group consisted of five samples of lightweight reinforced concrete slabs. These samples were prepared under standard conditions and to uniform dimensions to ensure the accuracy and reliability of the results. The main objective of this group was to establish a baseline for comparison and to study the changes in mechanical properties and failure behavior of lightweight concrete slabs under applied loading conditions resulting from direct exposure to high temperatures. This group included one control sample in addition to the other samples, whose temperatures were recorded between (25-300-400) °C. Table 4-8 shows the service and ultimate load results for the tested lightweight reinforced concrete slabs exposed to high temperatures. Each sample showed a distinct response depending on its reinforcement ratio and level of heat exposure.

**Table 4-8: Shows the service and Ultimate Load Results**

Specimens	Service Load (Ps) (kN)	Ultimate Load (Pu) (kN)	% Decrease In Service Load Concerning Reference	%Decrease In Ultimate Load Concerning Reference
SL5DC $\rho$ -25	8.9	17.8	Reference	Reference
SL4D $\rho$ -300	6	12	32	32
SL1D $\rho$ -400	3.75	7.5	57	57.8
SL2D $\rho$ <sup>^</sup> -400	5.4	10.8	39	39.3
SL3D $\rho$ <sup>^</sup> -300	8.4	16.8	5	5.6

Fig. 4-24 illustrate the failure pattern of lightweight concrete specimens (SL3D $\rho$ <sup>^</sup>-300) and (SL4D $\rho$ -300), tested at 300 °C under thermal stress. The specimens exhibited a rapid bending failure pattern, characterized by a dominant vertical crack in the mid-span extending upwards from the tension surface towards the compression zone. The main crack gradually widened with increasing applied load. These figures show that the bending cracks were nearly parallel, and

no cracks were observed near the support zones. The crack pattern in the slabs also exhibits similar behavior. Fig. 4-24 show the failure pattern of lightweight concrete specimens **SL1Dp-400** and **SL2Dp<sup>^</sup>-400** tested at 400C°. The specimens exhibited a flexural failure mode with a main vertical crack at mid-span extending from the tension face toward the compression zone. As the load increased, the main crack widened, and parallel bending cracks formed along the span, while no cracks appeared near the supports. The experimental results indicate that increasing the temperature has a significant effect on the failure behavior of normal-weight reinforced concrete slabs after fire exposure and loading to ultimate capacity. At moderate temperatures, such as 25°C to 400°C, failure initially appears as flexural bending with limited surface cracking. This form of failure is accompanied by a moderate reduction in service and ultimate loads due to partial deterioration of the bond between the cement paste and reinforcing steel, as well as a decrease in the mechanical stiffness of the concrete. at higher temperatures, such as 300°C and 400°C, the failure becomes more pronounced, characterized by severe flexural bending with branching cracks and noticeable spalling of the outer concrete cover. This behavior reflects the increasing impact of temperature on the load-carrying capacity of the slabs, as elevated heat weakens the bond between the aggregate and cement paste and increases the brittleness of the concrete, reducing stiffness and increasing deflections prior to reaching ultimate failure. Overall, it can be concluded that the mode of failure evolves from limited bending with minor cracking to severe bending with spalling of the concrete cover as the temperature rises. Furthermore, the results demonstrate that higher temperatures lead to a gradual decrease in both service and ultimate loads, highlighting the deterioration of the concrete's mechanical properties and the partial loss of interaction between the concrete and reinforcing steel under thermal exposure.

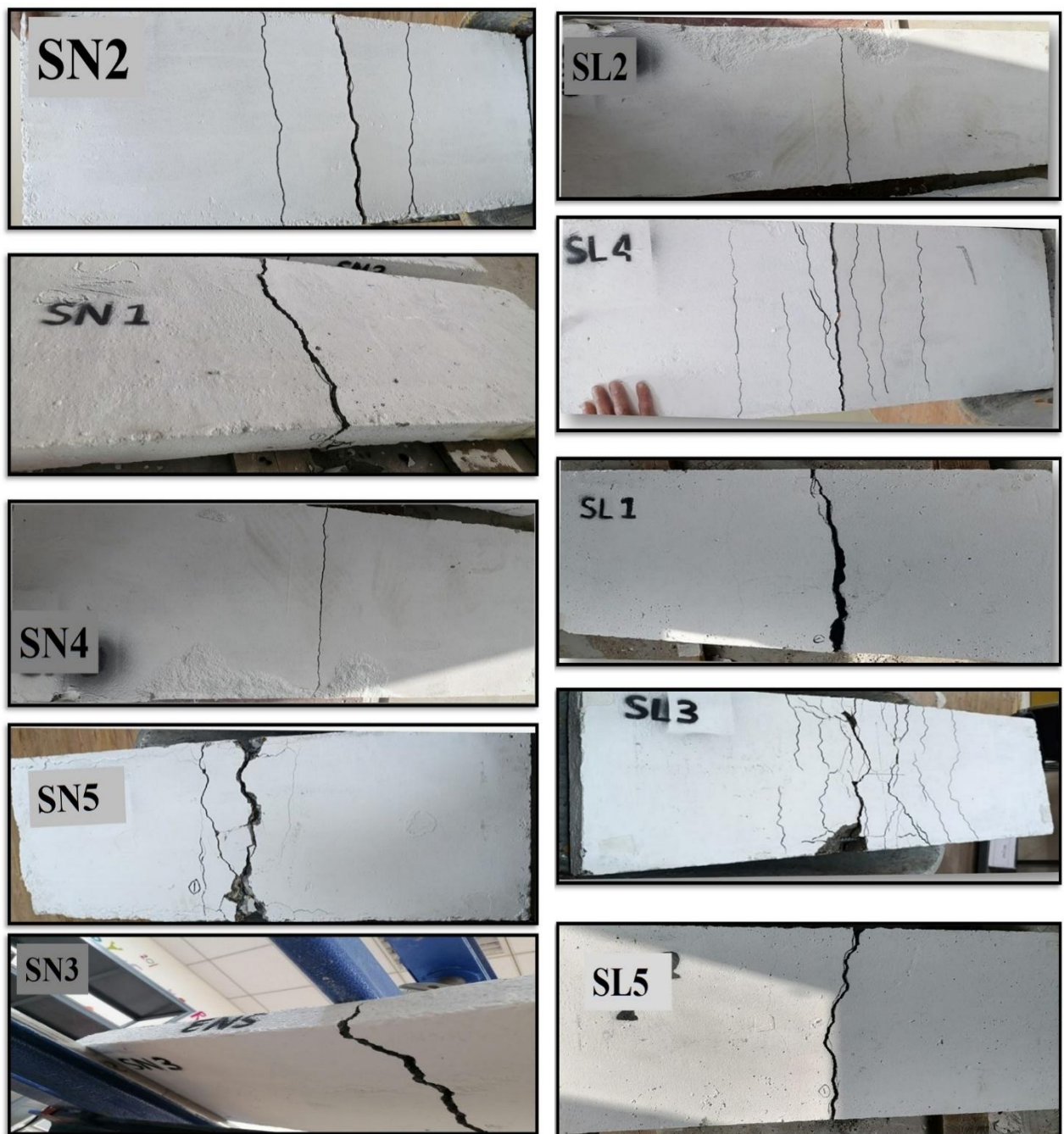


Figure 2-24 The Failure Pattern in Normal and Lightweight Concrete.

#### 4.3.2.2 Load and Deflection Behavior.

The load–deflection response of concrete slabs provides critical insight into their structural performance and deformation capacity under high thermal exposure. In this study, both normal-weight and lightweight concrete specimens exhibited noticeable changes in deflection with increasing temperature, reflecting the influence of thermal degradation on concrete stiffness and bond integrity

with reinforcing steel. For normal-weight concrete specimens, the reference sample **SN2DCp-25** exhibited a service deflection of 6 mm and ultimate deflection of 20 mm. Exposure to 300°C **SN4DCp-300** resulted in a moderate increase in service deflection to 7 mm (14%) and ultimate deflection to 21.5 mm (6.9%). At 400°C **SN5Dp'-400** and **SN1Dp-400**, deflections increased further to 7.01–7.2 mm at service load (14.4–16.6%) and 22.6–22.8 mm at ultimate load (11.5–12.2%). This increase in deflection is attributed to microcracking in the cement matrix, weakening of the concrete-steel bond, and partial loss of stiffness in the concrete, which becomes more pronounced as temperature rises. For lightweight concrete specimens, the reference **SL5DCp-25** exhibited higher baseline deflections of 8 mm at service load and 23 mm at ultimate load. After exposure to 300°C **SL4Dp-300** and **SL3Dp'-300**, service deflections increased to 9–8.3 mm (3.6–11.1%) and ultimate deflections to 24–24.5 mm (4.16–6.12%). At 400°C (**SL1Dp-400** and **SL2Dp'-400**), service deflections reached 10–10.5 mm (20–23.8%), while ultimate deflections remained in the range of 23.9–24.1 mm (3.7–4.5%). The higher deflection tolerance of lightweight concrete is mainly due to its greater internal porosity and lower modulus of elasticity, which allows more deformation under load without immediate failure. However, despite higher service deflections, the ultimate deflection increases were relatively moderate, suggesting that structural integrity is maintained under high temperatures, albeit with reduced stiffness. Overall, the data indicate that elevated temperatures lead to a gradual increase in service and ultimate deflections for all slabs, with the magnitude of deflection increase being more pronounced in lightweight concrete at service load, while normal-weight concrete shows a more consistent increase at ultimate load. The underlying mechanisms include thermal-induced microcracking, reduction in bond strength between reinforcement and concrete, and decreased concrete stiffness, which collectively explain the observed deflection behavior see Table 4-25 and Fig. 4-21 & Fig. 4-26.

**Table 4-9 Service Load and Ultimate Deflection.**

Specimens	Deflection at service Load (mm)	% Increase in Deflection at service Load	Ultimate Deflection (mm)	% Increase in Deflection at The Ultimate Load of Reference Specimen
SN2DC $\rho$ -25	6	Reference	20	Reference
SN4DC $\rho$ -300	7	14	21.5	6.9
SN3D $\rho'$ -300	6.5	7.6	21	5
SN5D $\rho'$ -400	7.01	14.4	22.6	11.5
SN1D $\rho$ -400	7.2	16.6	22.8	12.2
SL5DC $\rho$ -25	8	Reference	23	Reference
SL4D $\rho$ -300	9	11.1	24.5	6.12
SL1D $\rho$ -400	10.5	23.8	24.1	4.5
SL2D $\rho'$ -400	10	20	23.9	3.7
SL3D $\rho'$ -300	8.3	3.6	24	4.16

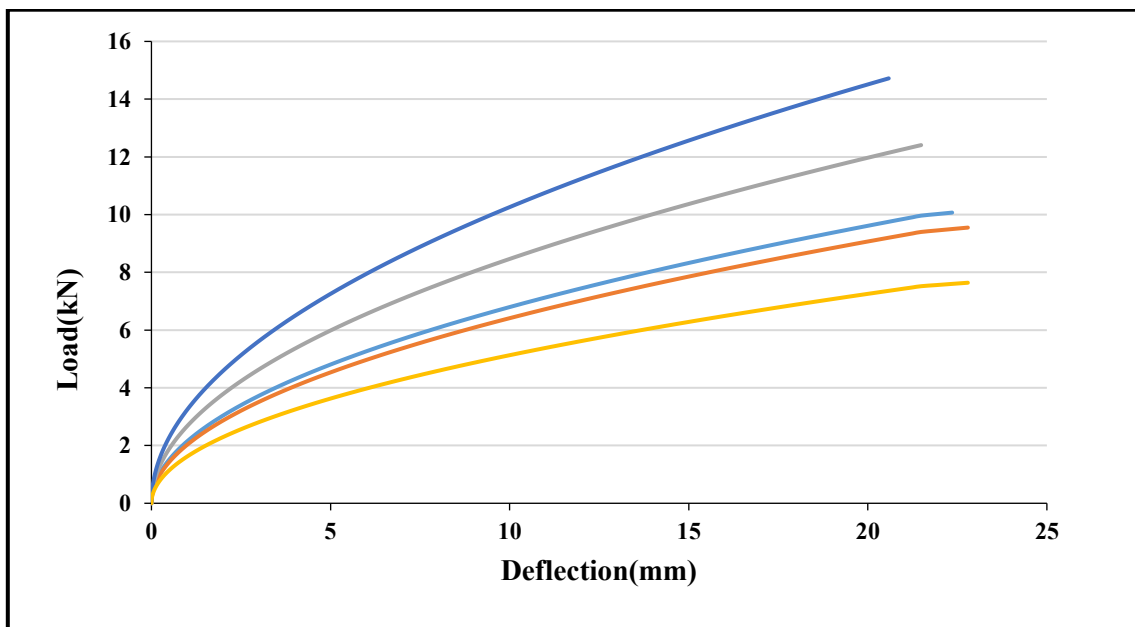


Figure 4-25 Load and Deflection Curve for normal Reinforced Concrete Slabs.

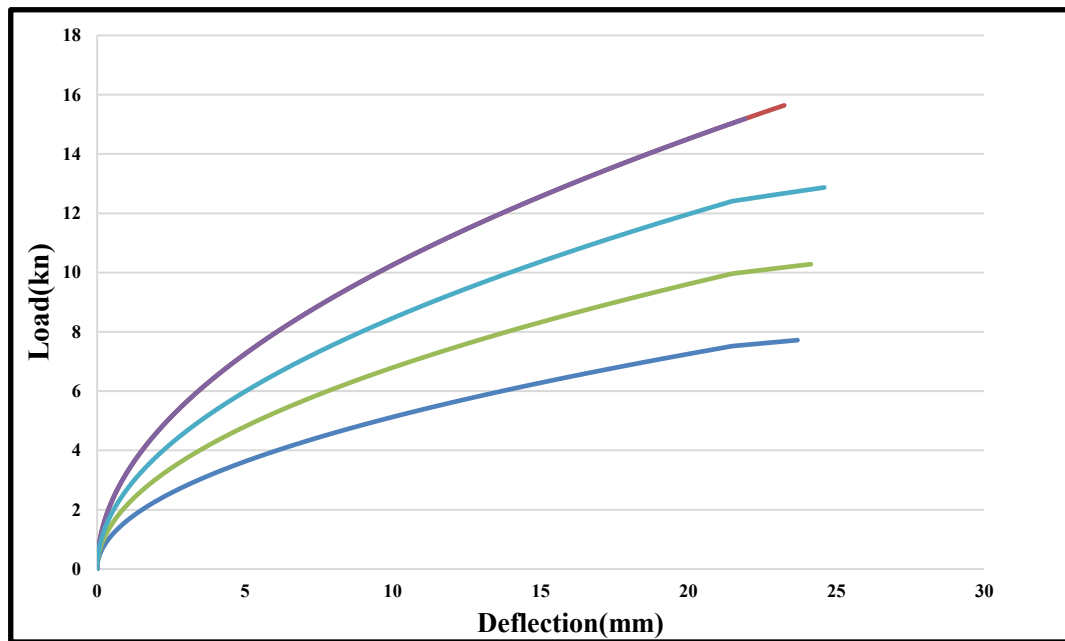


Figure 2-26 Load and Deflection Curve for Lightweight Reinforced Concrete Slabs.

Table 4-10 The Effect of Temperature on Load.

Type concrete	Specimens	Ultimate load Pu (kN)	Decreasing% in Pu
Lightweight Concrete	SL5DC $\rho$ -25	17.8	Reference
	SL4D $\rho$ -300	12	32
	SL1D $\rho$ -400	7.5	57
	SL2D $\rho^{\wedge}$ -400	10.8	39
	SL3D $\rho^{\wedge}$ -300	16.8	5.6
Normal Concrete	SN2DC $\rho$ -25	18.5	Reference
	SN4D $\rho$ -300	10.8	41
	SN3D $\rho^{\wedge}$ -300	12	35
	SN5D $\rho^{\wedge}$ -400	9.5	48
	SN1D $\rho$ -400	8.8	52

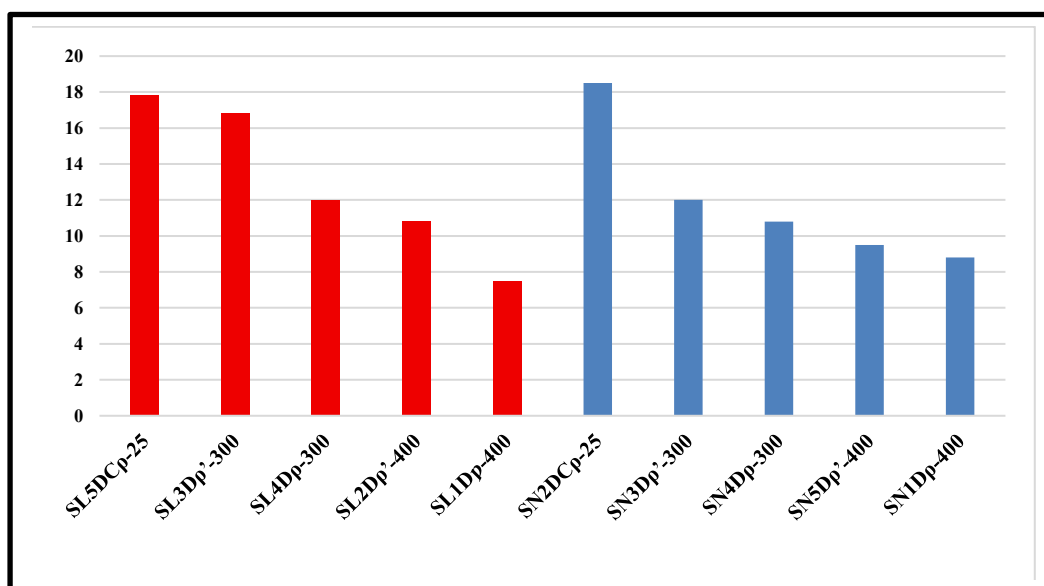


Figure 4-27 The Effect of Temperature on Load.

#### 4.3.3.3 Varying Reinforcement Ratios and Loading Conditions.

Table 4-11 summarizes the experimental results of reinforced concrete slab specimens subjected to elevated temperatures of 25°C, 300°C, and 400°C, considering different reinforcement ratios and loading conditions. The results clearly demonstrate that increasing the exposure temperature leads to a progressive reduction in the ultimate load capacity of all specimens. This degradation is primarily attributed to the deterioration of concrete stiffness, thermal damage to the cement matrix, and weakening of the bond between concrete and reinforcing steel under high-temperature conditions. For the lightweight concrete slabs, the reference specimen **SL5DCp-25**, tested at ambient temperature, achieved an ultimate load of **17.8 kN**. Upon exposure to 300°C, specimen **SL4Dp-300** exhibited a significant reduction in ultimate load to 12 kN, corresponding to a decrease of 32.5%. In contrast, specimen **SL3Dp-300**, which incorporated a higher reinforcement ratio, showed a markedly lower reduction of only 5.6%, sustaining an ultimate load of 16.8 kN. This behavior highlights the beneficial role of increased reinforcement in enhancing flexural resistance and mitigating heat-induced strength degradation. At a higher temperature of 400°C, the influence of

reinforcement ratio became more pronounced. Specimen **SL1Dp-400**, characterized by a lower reinforcement content, recorded the lowest ultimate load of 7.5 kN, with a substantial reduction of 57.8%. Meanwhile, specimen **SL2Dp<sup>^</sup>-400**, containing a higher reinforcement ratio, maintained a comparatively higher ultimate load of 10.8 kN, limiting the reduction to 39.3%. These results indicate that adequate reinforcement contributes to improved load redistribution, enhanced internal cohesion, and restraint of thermally induced cracking in lightweight concrete slabs. A similar trend was observed for the normal-weight concrete slabs. The reference specimen **SN2DCp-25** achieved an ultimate load of 18.5 kN at room temperature. When exposed to 300°C, specimen **SN4Dp-300** experienced a reduction in ultimate load to 10.8 kN, representing a 41.6% decrease, whereas specimen **SN3Dp<sup>^</sup>-300**, with a higher reinforcement ratio, sustained a higher ultimate load of 12 kN, with a lower reduction of 35.1%. This confirms the positive influence of increased reinforcement in preserving flexural capacity under moderate thermal exposure. Under 400°C exposure, specimen **SN1Dp-400** showed a pronounced decrease in ultimate load to 8.8 kN, corresponding to a reduction of 52.4%, while specimen **SN5Dp<sup>^</sup>-400** maintained a slightly higher capacity of 9.5 kN, with a reduced loss of 48.6%. The improved performance of specimens with higher reinforcement ratios can be attributed to the ability of steel reinforcement to bridge cracks, delay stiffness degradation, and maintain structural integrity despite the reduction in concrete strength at elevated temperatures. Overall, the experimental results presented in Table 4-11 and illustrated in Fig. 4-28 confirm that while elevated temperature adversely affects the ultimate load capacity of reinforced concrete slabs, increasing the reinforcement ratio significantly mitigates this effect. Higher reinforcement ratios enhance internal cohesion, limit the propagation of thermal cracks, and improve the residual load-carrying capacity, particularly under severe thermal exposure.

**Table 4-11 Steel Reinforcement Ratio and Ultimate Load.**

Specimens	Ultimate load Pu (kN)	%Decreasing In (Pu)
SL5DC $\rho$ -25	17.8	Reference
SL4D $\rho$ -300	12	32.5
SL1D $\rho$ -400	7.5	57.8
SL2D $\rho$ -400	10.8	39.3
SL3D $\rho$ -300	16.8	5.6
SN2DC $\rho$ -25	18.5	Reference
SN4D $\rho$ -300	10.8	41.6
SN3D $\rho$ -300	12	35.1
SN5D $\rho$ -400	9.5	48.6
SN1D $\rho$ -400	8.8	52.4

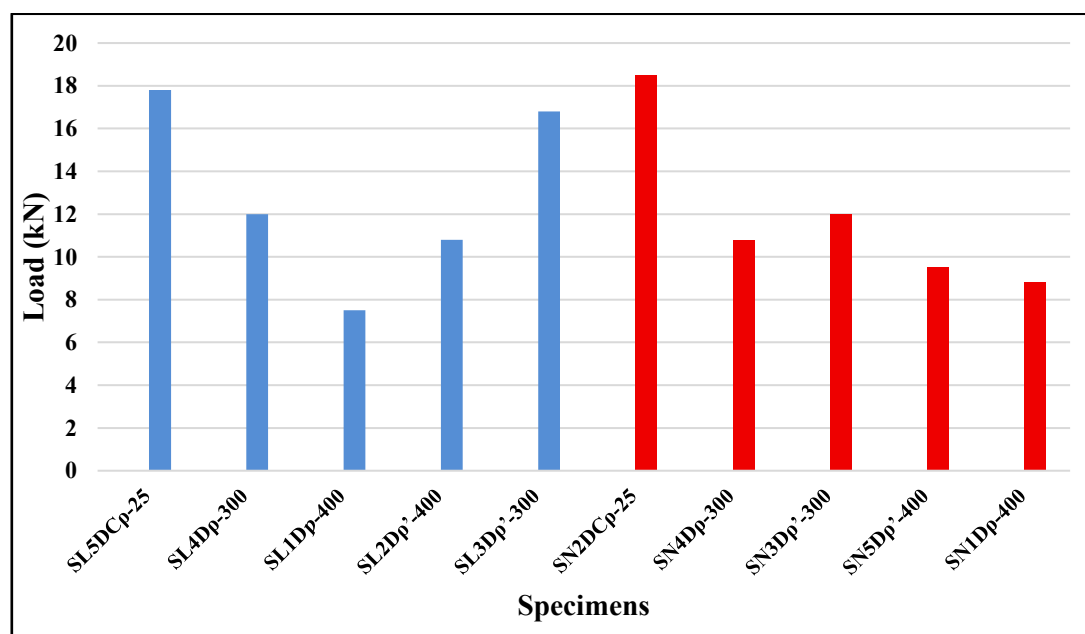


Figure 4-28 The Effect of Temperature on Load When Controlling the Reinforcement Ratio.

#### 4.3.3.4 Ductility

The term "ductility" describes the ability of reinforced concrete components to withstand a large displacement before failure show Fig. 4-29 & 4-30. The ratio of the maximum deflection ( $\Delta_u$ ) to the yield deflection ( $\Delta_y$ ) is known as the ductility index (D.I) The results reveal that all of the models that were exposed to direct flame heat kept their ductility, with ductility index values ranging from

2.23 to 2.85. This means that the elements could absorb strain before breaking. It was noted that (SN) models attained much greater ductility index values than (SL) models, indicating enhanced elasticity when subjected to heat. Additionally, the higher slump at the yield point was accompanied by a slight increase in the ultimate slump; however, for certain models, the ductility index decreased. This phenomenon is because high temperatures make concrete and steel less rigid, which is what causes the characteristics to break down. The results show that direct flame exposure lowers ductile efficiency, although the behaviour stays within structurally acceptable limits, which is derived from the load-deflection curve show Table 4-12.

**Table 4-12 Ductility Index.**

Specimens	Deflection at yield Load (mm)	Ultimate Deflection (mm)	%Ductility Index
SL5DC $\rho$ -25	8.9	23	2.58
SL4D $\rho$ -300	9	24.5	2.72
SL1D $\rho$ -400	9.67	24.1	2.49
SL2D $\rho^{\wedge}$ -400	10.7	23.9	2.23
SL3D $\rho^{\wedge}$ -300	10.66	24	2.25
SN2DC $\rho$ -25	7	20	2.85
SN4D $\rho$ -300	8	21.5	2.68
SN3D $\rho^{\wedge}$ -300	7.8	21	2.69
SN5D $\rho^{\wedge}$ -400	9.2	22.6	2.45
SN1D $\rho$ -400	9.4	22.8	2.42

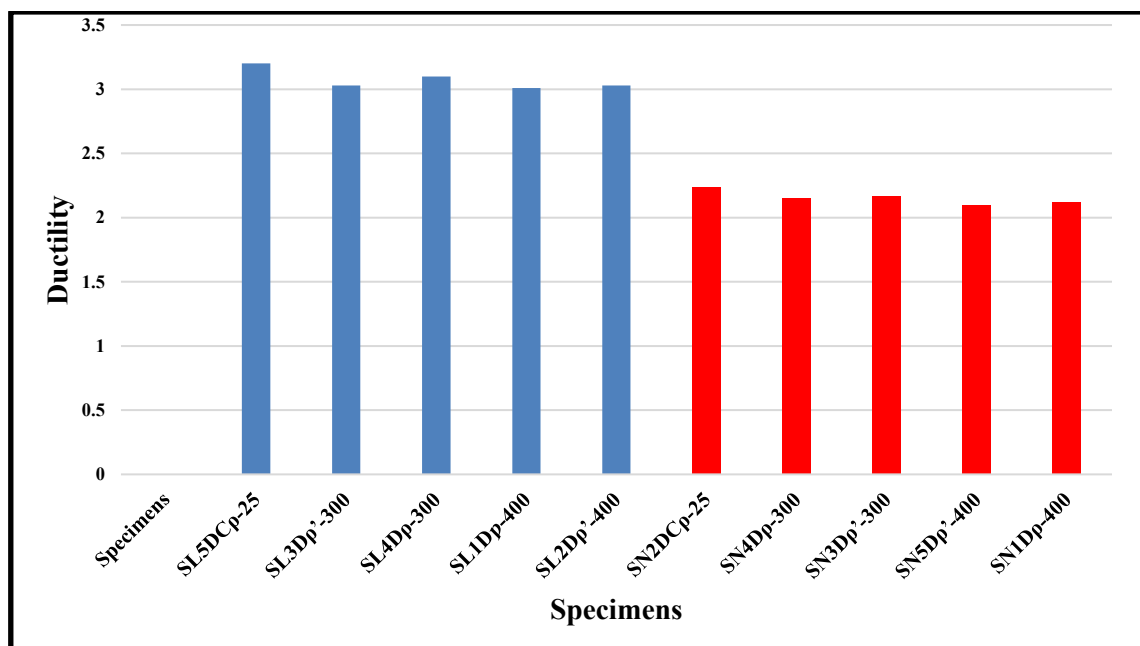


Figure 4-29 Ductility for Specimen.

#### 4.3.3.5 Stiffness

The stiffness of a structural element is calculated using the formula  $k = 0.7P_u / w$ , where  $P_u$  is the ultimate load (kN) and  $w$  is the deflection (mm). Stiffness represents the ability of a slab to resist deformation under loading. The table's results demonstrate that the samples that were directly exposed to flame were much softer than the control samples. This shows how high temperatures can change the properties of materials. The results indicate that specimen (**SL1Dp-400**) exhibited the greatest reduction in stiffness, with a decrease of approximately 60% compared to the reference specimen. This reduction can be attributed to the deterioration of the modulus of elasticity of both concrete and reinforcing steel at elevated temperatures. In contrast, specimen (**SL3Dp-300**) showed only a minor reduction of about 9%, indicating that it retained a significant portion of its stiffness after heating. Furthermore, it was observed that normal-weight concrete (SN) specimens consistently exhibited higher stiffness values than lightweight concrete (SL) specimens after exposure to elevated temperatures, Table 4.13

shows the stiffness values of the tested slabs, while Fig. 4.32 illustrates their behaviour under load.

**Table 4.13 The Stiffness Values**

Specimens	0.7*Pu (Kn)	Deflection (mm)	Stiffness $K=0.7Pu/w$
SL5DC $\rho$ -25	12.46	23	0.542
SL4D $\rho$ -300	8.4	24.5	0.343
SL1D $\rho$ -400	5.25	24.1	0.218
SL2D $\rho$ -400	7.56	23.9	0.316
SL3D $\rho$ -300	11.76	24	0.490
SN2DC $\rho$ -25	12.95	20	0.648
SN4D $\rho$ -300	7.56	21.5	0.352
SN3D $\rho$ -300	8.4	21	0.400
SN5D $\rho$ -400	6.65	22.6	0.294
SN1D $\rho$ -400	6.16	22.8	0.270

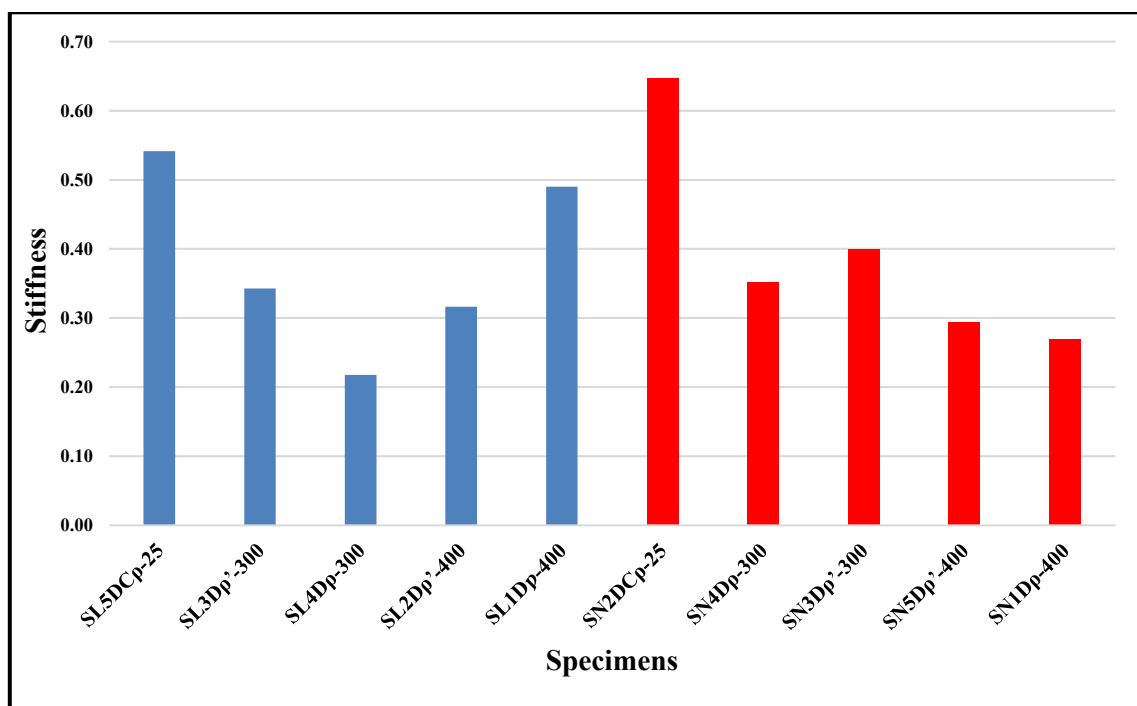


Figure 4-30 The Stiffness of the Working Models Using Direct Flame Exposure.

### 4.3.3.6 Energy Absorption.

The area under the load-deflection curve is used to calculate the energy absorption of concrete slabs. Data presented in Table 4.14 indicate that energy absorption increases significantly with higher applied loads. Additionally, elevated temperatures affect the slab properties, The table results indicate that the models' capacity to absorb energy significantly diminished when subjected to direct fire. This reduction is attributed to the high temperatures, which caused both the concrete and reinforcing steel to lose their structural integrity. Model (SL1Dp-400) experienced the most substantial decrease in energy absorption, plummeting by 53%. This demonstrates that the element's ability to dissipate energy prior to failure was severely compromised. Conversely, model (SL3Dp<sup>^</sup>-300) exhibited the smallest decline at 12.8%, suggesting that it retained a greater level of energy absorption capacity at lower temperatures. Additionally, it was observed that the (SN) models generally displayed an average reduction of 25% to 45%, outperforming some (SL) models. These variations can be attributed to differences in temperature and the extent of thermal damage sustained by the concrete component. Overall, the data clearly illustrate that direct exposure to fire considerably diminishes the ability to absorb energy, resulting in noticeable changes in their ability to absorb energy shows Fig. 4-33.

**Table 4.14 Energy Absorption Data.**

Specimens	The Area Under the Curve (Energy Absorption.), (kN. mm)	% of The Decrease in Energy Absorption.
SN2DCp-25	200	Reference
SN4Dp-300	110	45
SN3Dp <sup>^</sup> -300	150	25
SN5Dp <sup>^</sup> -400	130	35
SN1Dp-400	118	41
SL5DCp-25	195	Reference
SL4Dp-300	140	28
SL1Dp-400	90	53
SL2Dp <sup>^</sup> -400	112	42
SL3Dp <sup>^</sup> -300	170	12.8

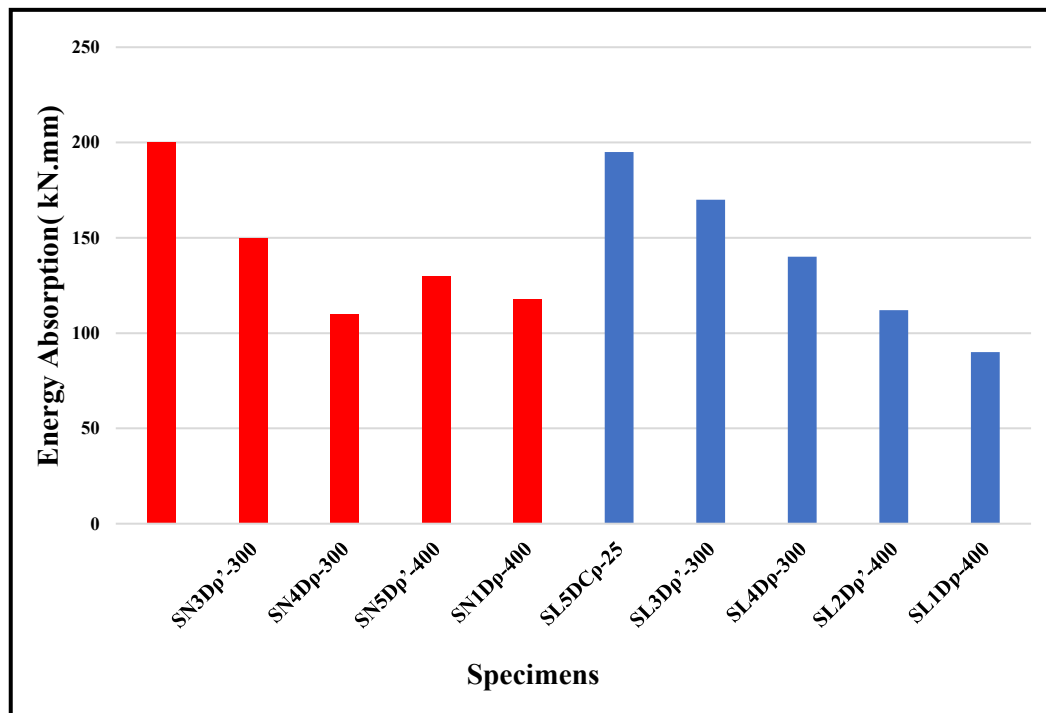


Figure 4.31 Energy Absorption.

## CHAPTER FIVE: CONCLUSIONS AND RECOMMENDATION

### 5.1 Introduction

This chapter presents the discussion and analysis of the experimental results of reinforced concrete slabs made from both ordinary and lightweight concrete after exposure to elevated temperatures. The experimental program included ten specimens for each heating method, in which two different heating procedures were applied:(direct flame heating)and (gradual heating according to the ISO-834 standard fire curve and the American standard ASTM- E119) .

After 28 days of curing, the specimens were heated according to their designated method and then tested under flexural loading until failure. The results were analyzed in terms of ultimate load, mid-span deflection, stiffness, ductility, energy absorption, and failure modes, to evaluate the structural behavior of the slabs under high-temperature conditions.

### 5.2 Conclusions

This research aimed to evaluate the structural behavior of normal and lightweight concrete slabs under high temperatures using two different heating methods:

1. Direct flame heating.
2. Gradual heating according to the ISO-834 standard curve and ASTM-E119.

The results were analyzed based on the ultimate load, deflection, stiffness, ductility, energy absorption, and failure modes.

### 5.3 Flexural Behavior of Concrete Slabs at Exposed Fire

#### 1. Ultimate Load:

- a. Slabs exposed to direct flame at 300–400 °C showed a significant reduction in load capacity (41-62) % for normal concrete and (32-57) % for lightweight concrete compared with the reference slabs.
- b. Slabs subjected to ISO-834 gradual heating at 400–800 °C (7-21) % for normal concrete and (16-40) % for lightweight concrete.

#### 2. Deflection:

- a. Direct flame specimens exhibited larger deflections due to rapid thermal gradients (8-4) % for normal and lightweight.
- b. According curve ISO834-ASTM-E119: Gradually heated slabs maintained lower deflections, reflecting slower stiffness degradation (2.5-1.2) % for normal and lightweight concrete.

#### 3. Stiffness:

- a. Both heating methods reduced initial stiffness, more pronounced in direct flame specimens (32-42) % for normal and lightweight.
- b. ISO-834 exposure preserved a higher portion of the stiffness (15-25) % for normal and lightweight concrete.

#### 4. Ductility:

- a. The direct-flame-heated specimens recorded higher ductility ratios, ranging between (2.55–2.5)% for both normal-weight and lightweight concrete slabs.
- b. Specimens heated under the ISO-834 curve showed comparatively lower ductility ratios, within the range of (3.14–2.8)% for normal-weight and lightweight concrete.

#### 5. Energy Absorption:

- a. The direct-flame-heated specimens recorded decrease (36.5-33.9) % to the energy for both normal-weight and lightweight concrete slabs.
  - b. Specimens exposed to the ISO-834 heating curve to the energy decrease (10-20) % for normal-weight and lightweight slabs.
6. Failure Mode:
- a. The direct flame exposure produced non-uniform surface damage, accompanied by, localized and irregular cracking patterns, indicating uneven thermal distribution across the slabs.
  - b. In contrast, the ISO-834 heating method resulted in a clear flexural failure pattern due to the more uniform temperature distribution, while surface spalling was observed in both heating methods.
7. Effect of Increased Reinforcement
- a. Direct Flame Exposure: Moderate reinforcement resulted in a slight increase in ultimate load and reduced deflection at elevated temperatures.
  - b. A significant deterioration in stiffness, ductility, and energy absorption was observed, along with a decrease in cracking and a widening of gaps, upon rapid heat exposure.
  - c. Heating According to ISO-834:
    - a- The slabs exhibited higher ultimate load-bearing capacity with less deflection compared to the reference samples when subjected to high heat using this method and according to the established study variables.
    - b- A deterioration and failure in stiffness and ductility, as well as an increase in energy absorption, were observed when the studied

working samples were heated according to this specification, but to a lesser extent than with the first method, direct flame exposure heating.

#### **5.4 Recommendations**

1. It is recommended to adopt gradual heating according to the ISO-834 standard and the ASTM-E119 standard for evaluating the performance of concrete slabs, as the ISO temperature curve provides a more accurate and realistic assessment of slab behavior compared to direct flame exposure.
2. The complete replacement of LECA aggregate is not advised, as it causes significant deterioration in concrete under high temperatures; partial replacement is preferred to maintain good thermal and mechanical performance.
3. Lightweight concrete is recommended for applications requiring higher fire resistance, as it demonstrated better ductility, higher energy absorption, and improved resistance to thermal deformation compared to ordinary concrete.
4. Reinforcement ratio should be increased only within reasonable limits, as moderate increases improve ultimate load, reduce deflection, and enhance stiffness, ductility, and energy absorption under high temperatures without causing other structural issues.
5. The ISO-834 method is recommended for future studies involving large structural elements such as columns or bridges, as it provides a better representation of the actual mechanical deterioration of concrete properties under high temperatures, enabling a more accurate and realistic evaluation of structural performance.

6. Alternative aggregates, such as recycled aggregates, are recommended for future studies, with reliance on the ISO-834 temperature curve and ASTM standards, as they provide the most reliable and accurate results for evaluating concrete performance under elevated temperatures.
7. Improvement the lightweight R.C. slab with smart martial [Reactive powder ,Fiber ,Recycle Matreal], Improve the hardened properties of concrete .

## REFERENCES

- [1] Heiza, K. M., Eid, F. M., & Masoud, T. (2017). *Light Weight Self Compacting Concrete With Light Expanded Clay Aggregate (LECA)*. *ERJ. Engineering Research Journal*, 40(1), 65-71.
- [2] Wang, J., Xiao, Z., Zhu, C., Feng, C., & Liu, J. (2021). Experiment on the bonding performance of the lightweight aggregate and normal weight concrete composite beams. *Case Studies in Construction Materials*, 15, <https://doi.org/10.1016/j.cscm.2021.e00565>.
- [3] Wang, Y., & Lee, S. (2007). Fire resistance of concrete structures. *Fire Safety Journal*, 42(6), 459–469.
- [4] Pacheco-Torgal, F., & Jalali, S. (2011). Fire performance of concrete. *Construction and Building Materials*, 25(5), 1666–1673.
- [5] Neville, A. M. (2011). *Properties of Concrete*, 4th. London Pearson Education Limited, 443(846), 444.
- [6] Levon, A., & Sako, Z. (1983). *Building Construction [In Arabic]*. Mosul, Iraq: University of Mosul Press.
- [7] Longarini, N., Crespi, P., Zucca, M., & Scamardo, M. (2025). Numerical evaluation of the equivalent damping ratio due to dissipative roof structure in the retrofit of historical churches. *Applied Sciences*, 15(6), 3286.
- [8] Buchanan, A. H., & Abu, A. (2001). *Structural design for fire safety (Vol. 273)*. New York: Wiley.
- [9] Ojaimi, M. F., Altaee, M. K. E., & Aljabbri, N. S. (2021). Structural behavior of two-way slabs cast with different fiber types and contents. *Periodicals of Engineering and Natural Sciences*, 9(3), 831-843.
- [10] VUT Brno Faculty of Civil Engineering. (2025). Two-Way Slab (Lecture Notes). Al-Mustansiriyah University. (2025). *Reinforced Concrete Design II: Two-Way Slab Behaviour*. <https://www.scribd.com/document/495254213/RC-chptr-1>

- [11] Cavill, R., & Rodd, R. (2004). Effects of fire on concrete in building structures. *Journal of Fire Protection Engineering*, 14(4), 235–249.
- [12] Bush, A. L., Bryan, D. P., & Hack, D. R. (2006). Lightweight aggregates. *Industrial Minerals and Rocks*, 181-194.
- [13] umkham, B., Shijagurumayum, C., & Suresh, T. (2022). Fire Resistance of Concrete Structure – A Review. *SAMRIDDHI: A Journal of Physical Sciences, Engineering and Technology*, 14(01 SPL), 63–67
- [14] Zhang, M., & Fu, J. (2015). Fire resistance of reinforced concrete: The impact of fire on concrete strength and performance. *Fire Science Reviews*, 4(1), 23–35.
- [15] ISSA, A. S., & Al-ASADI, A. K. (2022). Mechanical properties of lightweight expanded clay aggregate (LECA) concrete. *Scientific Review Engineering and Environmental Sciences (SREES)*, 31(3), 161–175. <https://doi.org/10.22630/srees.3150>.
- [16] Darwin, D., Dolan, C. W., & Nilson, A. H. (2016). *Design of concrete structures* (Vol. 2). New York, NY, USA: McGraw-Hill Education.
- [17] Neville, A. M. (1981). *Properties of Concrete*, Pitman Publishing Ltd, p. 779.
- [18] Li, J. (1992). *Elastic behaviors and microstructure infcc-fct premartensitic transformations*. University of Maryland, College Park..
- [19] Ellingwood, B. R., & Shaver, J. R. (1979). *Fire effects on reinforced concrete members* (Vol. 985). Department of Commerce, Office of the Assistant Secretary of Commerce for Science and Technology, National Bureau of Standards.
- [20] Costa, C. N., & Silva, V. P. (2003). Dimensionamento de estruturas de concreto armado em situação de incêndio. Métodos tabulares apresentados em normas internacionais. *V Simpósio Epusp sobre estruturas de concreto*, 5, 2003.

- [21] Khoury, G. A. (2000). Effect of fire on concrete and concrete structures. *Progress in structural engineering and materials*, 2(4), 429-447.
- [22] Hameed, Y. M., & Ismael, M. A. (2022). Structural behavior of reinforced lightweight concrete slabs. *Diyala Journal of Engineering Sciences*, 122–132.
- [23] del Coz-Díaz, J. J., Martínez-Martínez, J. E., Alonso-Martínez, M., & Rabanal, F. P. Á. (2020). Comparative study of lightweight and normal concrete composite slabs behaviour under fire conditions. *Engineering Structures*, 207, 110196.
- [24] Allam, S. M., Elbakry, H. M., & Rabeai, A. G. (2013). Behavior of one-way reinforced concrete slabs subjected to fire. *Alexandria Engineering Journal*, 52(4), 749–761.
- [25] Johnson, R. P., & Wang, Y. C. (2018). *Fire resistance* (Chapter 6). In *Composite Structures of Steel and Concrete: Beams, Slabs, Columns and Frames for Buildings* (4th ed., pp. 223–245). John Wiley & Sons Ltd.
- [26] Shyamala, G., Mahesh, V., Kumar, K. R., & Reddy, I. R. (2020). Thermal behavior of concrete subjected to elevated temperature: Case studies. *IOP Conference Series: Materials Science and Engineering*, 981(3), 032068.
- [27] Wang, Y., Wu, J., Huang, Z., Jiang, J., Yuan, G., Zhang, Y., ... & Zhou, M. (2020). Experimental studies on continuous reinforced concrete slabs under single and multi-compartment fires with cooling phase. *Fire Safety Journal*, 111, 102915.
- [28] Wang, Y., Jiang, Y., Huang, Z., Li, L., Huang, Y., Zhang, Y., ... & Duan, Y. (2021). Post-fire behaviour of continuous reinforced concrete slabs under different fire conditions. *Engineering Structures*, 226, 111342.
- [29] Ali, H. S. M., Albayati, N. A.-M., Mohammed, B. R., & Jabbar, A. M. (2023). *Effect of fire flame on some mechanical properties of*

*self-compacting concrete. Al-Esraa University College Journal for Engineering Sciences*, 5(7), Article 9

[30] Wróblewska, J., & Kowalski, R. (2020). Assessing concrete strength in fire-damaged structures. *Construction and Building Materials*, 254, 119122.

[31] Abbood, A. A., & Kharnoob, M. M. (2024). Influence of fire-flame temperature and duration on the behavior of reinforced concrete beams with construction joints. *Journal of Engineering*, 30(05), 132–150.

[32] Shbeeb, N. I., Al-Akhras, N. M., Shannag, M. J., & Alfendi, H. R. (2012). Strengthening of lightweight reinforced concrete slabs using different techniques. *The IES Journal Part A: Civil & Structural Engineering*, 5(1), 16–27.

[33] Abdulah, M. D. (2015). Behavior of reinforced lightweight concrete two-way slabs strengthened with CFRP sheets. *Engineering and Technology Journal*, 33(8), 1813.

[34] Fall, D., Shu, J., Rempling, R., Lundgren, K., & Zandi, K. (2014). Two-way slabs: Experimental investigation of load redistributions in steel fibre reinforced concrete. *Engineering Structures*, 80, 61–74.

[35] Mashshay, A. F., Hashemi, S. K., & Tavakoli, H. (2023). *Post-Fire Mechanical Degradation of Lightweight Concretes and Maintenance Strategies with Steel Fibers and Nano-Silica. Sustainability*, 15(9).

[36] Jean, & Eat. (2020). Comparative study of lightweight and normal concrete composite slabs behaviour under fire conditions. *Engineering Structures*, 207, 1–12.

[37] Huang, Z. (2010). Modelling the bond between concrete and reinforcing steel in a fire. *Engineering Structures*, 32(11), 3660–3669.

[38] Muna (2024). *The behavior of self-compacting concrete slabs under elevated temperatures* (Experimental study). Unpublished manuscript / Conference paper / Journal submission

- [39] klak, F.S., & Jomaa'h, M.M. (2023). *Structural response of reinforced LECA aggregate concrete slabs subjected to high temperatures. Insight – Civil Engineering*, 6(1), Article 617
- [40] ASTM C191-19. (2019). *Standard Test Methods for Time of Setting of Hydraulic Cement by Vicat Needle*. ASTM International.
- [41] Central Organization for Standardization and Quality Control. (1984). *IQS 5/1984: Portland cement* (in Arabic).
- [42] ASTM C136 / C136M-14. (2014). *Standard Test Method for Sieve Analysis of Fine and Coarse Aggregates*. ASTM International.
- [43] Ministry of Construction and Housing, Iraq. (1984). *Iraqi Standard Specification No. 45/1984 for Concrete and Aggregates*. Baghdad: Ministry of Construction and Housing.
- [44] Central Organization for Standardization and Quality Control. (1980). *IQS 45/1980: Aggregates from natural sources for concrete and building construction* (in Arabic).
- [45] Ministry of Construction and Housing, Iraq. (1984). *Iraqi Standard Specification No. 45/1984 for Concrete and Aggregates*. Baghdad: Ministry of Construction and Housing.
- [46] Leca International, 2018. *LECA Lightweight Expanded Clay Aggregate – Product Data Sheet*. Leca International
- [47] Central Organization for Standardization and Quality Control. (1992). *Iraqi Standard Specification (IQS) No.1703/1992: Water used in concrete*. Baghdad, Iraq.
- [48] Neville, A. M. (2012). *Properties of Concrete* (5th ed.). Pearson Education Limited.
- [49] ASTM C494-99. (1999). *Standard Specification for Chemical Admixtures for Concrete*. ASTM International.

- [50] ASTM A615/A615M-22. (2022). *Standard Specification for Deformed and Plain Carbon-Steel Bars for Concrete Reinforcement*. ASTM International. [https://doi.org/10.1520/A0615\\_A0615M-22](https://doi.org/10.1520/A0615_A0615M-22)
- [51] ASTM A496-02. (2002). *Standard Specification for Steel Wire, Deformed, for Concrete Reinforcement*. ASTM International.
- [52] STM C143 / C143M-20. (2020). *Standard Test Method for Slump of Hydraulic-Cement Concrete*. ASTM International
- [53] British Standards Institution. (1983). *BS 1881-116: Testing concrete—Method for determination of compressive strength of concrete*.
- [54] ASTM C496/C496M-18. (2018). *Standard test method for splitting tensile strength of cylindrical concrete specimens*.
- [55] ASTM C78/C78M. (2015). *Standard test method for flexural strength of concrete (using simple beam with third-point loading)*.
- [57] Thamrin, R., Zaidir, & Zakiyyah, A. (2021). *Effect of reinforcement ratio on flexural behavior of reinforced concrete beams strengthened with CFRP plates*. IOP Conference Series: Earth and Environmental Science, 708, 012015.
- [58] Al-Attar et al., 2020)
- [59] Husain, M., Eisa, A. S., & Roshdy, R. (2017). Alternatives to enhance flat slab ductility. *International Journal of Concrete Structures and Materials*, 11(1), 161–169.
- [60] Sullivan, T., Calvi, G., & Priestley, M. (2004). Initial stiffness versus secant stiffness in displacement-based design. In *13th World Conference on Earthquake Engineering (WCEE)*.
- [61] Abdel-Karim, M., et al. (2024). *Flexural improvement of RC slabs by FRP or steel using different strengthening systems and novel anchoring techniques*. *International Journal of Concrete Structures and Materials*.

## APPENDIX (A)

### Flexural strength of reference slab according to ACI-318-18

All slabs were designed according to ACI-318-18 Code. The steps of analysis of the reference slab as follows.

Date :

$$f_y = 445.5 \text{ MPa} , f_c' = 24 \text{ MPa} \quad L = 850 , b = 400 \text{ mm}$$

$$t_s = 80 \text{ mm} , \phi = 8 \text{ mm} \quad A_{bar} = 50.24 \text{ mm}^2$$

Concrete cover=25 mm

$$d = h - \text{cover} - \frac{d_b}{2} = 80 - 25 - 4 = 50 \text{ mm}$$

$$f_c' < 28 \text{ MPa} \rightarrow \beta_1 = 0.85$$

$$\rho_b = 0.85 \times \beta_1 \times \frac{f_c'}{f_y} \times \left( \frac{600}{600 + f_y} \right) =$$

$$\rho_{max} = 0.85 \beta_1 \frac{f_c'}{f_y} \frac{0.003}{0.003 + 0.004} = 0.0167$$

$$A_{smax} = \rho_{max} \times b \times d = 334 \text{ mm}^2$$

$$\text{No. of bar} = \frac{A_{smax}}{A_{sbar}} = 6,6 \approx 7$$

$$A_{smin} \geq (0.0014 \times 400 \times 80) = 44,8 \text{ mm}^2$$

$$A_{smin} \geq 0.0018 \times \frac{420}{445,5} \times 400 \times 80 = 54,3 \text{ mm}^2 (\text{use the max. value})$$

$$\text{NO. of bar} = \frac{A_{smax}}{A_{sbar}} = \frac{54,3}{50,24} = 2 \text{ bar}$$

Use NO.of bar =4 bar

$$A_s = 4 \times 50,24 = 200,96 \text{ mm}^2$$

$$A_{smin} = 54,3 \text{ mm}^2 \leq A_s = 200,96 \text{ mm}^2 \leq A_{smax} = 334 \text{ mm}^2$$

Date :

$$f_y = 512 \text{ MPa}, f_c' = 24 \text{ MPa}$$

slab dimension =  $1000 \times 2250$  mm,  $t(h)=100$  mm,  $\Phi=10$ mm

$$f_y = 512 \text{ MPa}, f_c' = 24 \text{ MPa}$$

$$L = 2000 \text{ mm}, b = 1000 \text{ mm}$$

$$t_s = 100 \text{ mm}, \Phi = 10 \text{ mm}, A_{bar} = 79 \text{ mm}^2$$

Concrete cover=25 mm

$$d = h - \text{cover} - \frac{d_b}{2} = 100 - 30 = 70 \text{ mm}$$

$$f_c' < 28 \text{ MPa} \rightarrow \beta_1 = 0.85$$

$$\rho_b = 0.85 \times \beta_1 \times \frac{f_c'}{f_y} \times \left( \frac{600}{600 + f_y} \right) = 0.0183$$

$$\rho_{max} = 0.85 \beta_1 \frac{f_c'}{f_y} \frac{0.003}{0.003 + 0.004} = 0.0145$$

$$A_{smax} = \rho_{max} * b * d = 1016 \text{ mm}^2$$

$$\text{No. of bar} = \frac{A_{smax}}{A_{sbar}} = 12,8 \approx 13$$

$$A_{smin} \geq (0.0014 * 1000 * 100) = 140 \text{ mm}^2$$

$$A_{smin} \geq 0.0018 * \frac{420}{512} * 1000 * 100 = 147.6 \text{ mm}^2 (\text{use the max. value})$$

$$\text{NO. of bar} = \frac{A_{smax}}{A_{sbar}} = \frac{147.6}{79} = 2 \text{ bar}$$

Use NO.of bar =5 bar

$$A_s = 5 * 79 = 395 \text{ mm}^2$$

$$A_{smin} = 147.6 \text{ mm}^2 \leq A_s = 395 \text{ mm}^2 \leq A_{smax} = 1016 \text{ mm}^2$$

# APPENDIX (B)

BUILDING TRUST



## PRODUCT DATA SHEET

# Sika® ViscoCrete®-180 G

High range water reducing & superplasticizing admixture

### DESCRIPTION

Sika® ViscoCrete®-180 G is a High range water reducing & superplasticizing admixture for Concrete & Mortar utilizing Sika's ViscoCrete® polycarboxylate polymer technology (3rd Generation).

### USES

1. High-performance Concrete (HPC).
2. Flowing Concrete.
3. Durable Concrete.
4. Pumped Concrete.

### CHARACTERISTICS / ADVANTAGES

1. High water reduction, resulting in higher density, higher strength and reduced permeability.
2. Easier and faster pumping of concrete.
3. Increased workability and easier placeability.
4. Allows contractors to finish the concrete early.
5. Increased concrete durability and uniformity.
6. Reduced shrinkage and cracking.
7. Reduced rate of carbonation of the Concrete.

### PRODUCT INFORMATION

<b>Composition</b>	Aqueous solution of modified <b>polycarboxylates</b>
<b>Packaging</b>	1000 LTRs IBC 20 kg Pail
<b>Shelf life</b>	12 months from date of production if stored properly in undamaged unopened, original sealed packaging.
<b>Storage conditions</b>	In dry conditions at temperatures between +5°C and +35°C. Protect from direct sunlight. It requires recirculation when held in storage for extended periods.
<b>Appearance and colour</b>	Light brownish
<b>Specific gravity</b>	1.065 ± ( 0.02 ) g/cm <sup>3</sup>
<b>pH-Value</b>	4 - 6

## الملخص

تُعدّ المنشآت الخرسانية المسلحة عرضةً للحريق، الذي قد يُلحق أضرارًا بالعناصر الخرسانية تتراوح بين الطفيفة والكارثية. لذا، من الضروري تحديد نوع ومدى الضرر الذي يُمكن أن يُسببه الحريق. تهدف هذه الدراسة إلى بحث سلوك وخصائص ألواح الخرسانة خفيفة الوزن عند تعرضها المباشر للهب أو وفقًا لمعياري ASTM-E119 والمواصفة ISO-834. يتضمن البرنامج التجريبي دراسة تأثير درجة حرارة الحرق، ونوع الخرسانة، ونسبة التسليح، وطريقة الحرق ASTM-E119، أو ISO-834، أو التعرض المباشر للهب (على بعض الخصائص الميكانيكية الهامة للخرسانة خفيفة الوزن مقارنةً بالخرسانة غير المتضررة (غير المعرضة للحريق)، مثل مقاومة الضغط، والصلابة، والمطيلية، وتخزين الطاقة. تضمنت الاختبارات العمل على ألواح خرسانية خفيفة الوزن وعادية باستخدام طريقتين: الأولى وفقًا لمعيار ASTM-E119، ISO-834 بأبعاد 1000 × 400 × 80 ملم، مسنده باسناد بسيط، تحت حمل مركز مطبق على سطحها العلوي. شمل العمل التجريبي صب 20 لوحًا لتقييم تأثير درجة حرارة الحرق وطريقة الحرق على نوع الخرسانة ونسبة التسليح، والتي تعتمد على الخواص الميكانيكية للخرسانة والسلوك الإنشائي للألواح الخرسانية الخفيفة والعادية تحت الحمل، بما في ذلك إزاحات منتصف الإزاحة وأنماط التشققات. أظهرت النتائج أن حرق الخرسانة وفقًا للطريقة الأولى، ASTM-E119، ISO 834، عند درجات حرارة تتراوح بين 400 و800 درجة مئوية، أدى إلى انخفاض بنسبة 14% في مقاومة الضغط للخرسانة العادية مقارنةً بانخفاض بنسبة 28% للخرسانة الخفيفة المحروقة عند نفس درجات الحرارة. وبالمثل، أظهرت الطريقة الثانية، وهي التعرض المباشر للهب، أن التسخين عند درجات حرارة تتراوح بين 300 و400 درجة مئوية أدى إلى انخفاض مقاومة الضغط للخرسانة العادية بنسبة 51%، مقارنةً بانخفاض قدره 44% للخرسانة الخفيفة عند نفس درجات الحرارة. وبناءً على نتائج اختبارات ألواح الخرسانة، أدت طريقة التسخين المستخدمة إلى زيادة الانحراف إلى ما بين 1.2 و4 ملم للخرسانة الخفيفة تحت تأثير الحمل والحرارة، وذلك باستخدام كلٍ من طريقة ISO-834 وطريقة التعرض المباشر للهب. وتراوح تأثير ذلك على الصلابة بين 25 و42%، وعلى المطيلية بين 2.5 و2.8، وعلى فقد الطاقة بين 20 و33.9%.

وختامًا، يمكن استنتاج أن تعريض العناصر الإنشائية لدرجات حرارة عالية يؤدي إلى تكوّن وانتشار الشقوق داخل البنية الداخلية للخرسانة، مصحوبًا بتغيرات ميكانيكية وكيميائية تُسهم في تدهور كبير في الخواص الميكانيكية لمواد العنصر الإنشائي. أظهرت النتائج أيضًا أن التعرض المباشر للهب يُسبب فقدانًا جزئيًا للطاقة الحرارية، على عكس ما يتحقق عند الالتزام بالموصفات القياسية المعتمدة ASTM-119 وISO-834، مما يؤثر على طبيعة الضرر الناتج. ولا يقتصر هذا التدهور على انخفاض مقاومة الخرسانة فحسب، بل يؤثر أيضًا بشكل كبير على مقاومتها للإجهاد وآلية تشكل الشقوق وانتشارها، وذلك تبعًا لنوع الخرسانة المستخدمة في هذا البحث.



جمهورية العراق  
وزارة التعليم العالي والبحث العلمي  
جامعة ميسان / كلية الهندسة  
قسم الهندسة المدنية

## سلوك البلاطة الخرسانية المسلحة خفيفة الوزن المعرضة للحريق

رسالة مقدمة

إلى  
مجلس كلية الهندسة بجامعة ميسان  
استكمالاً لمتطلبات الحصول على درجة  
ماجستير العلوم في الهندسة المدنية  
بواسطة

نور كاظم حمود  
(بكالوريوس هندسة مدنية، 2009)  
الإنشاءات

المشرف

الأستاذ. الدكتور. سامر محمد جاسب  
2026م